DETAILED DESIGN REPORT FOR DANMAX

In situ materials studies in the 15-35 keV range using powder X-ray diffraction and full field imaging at MAX IV.

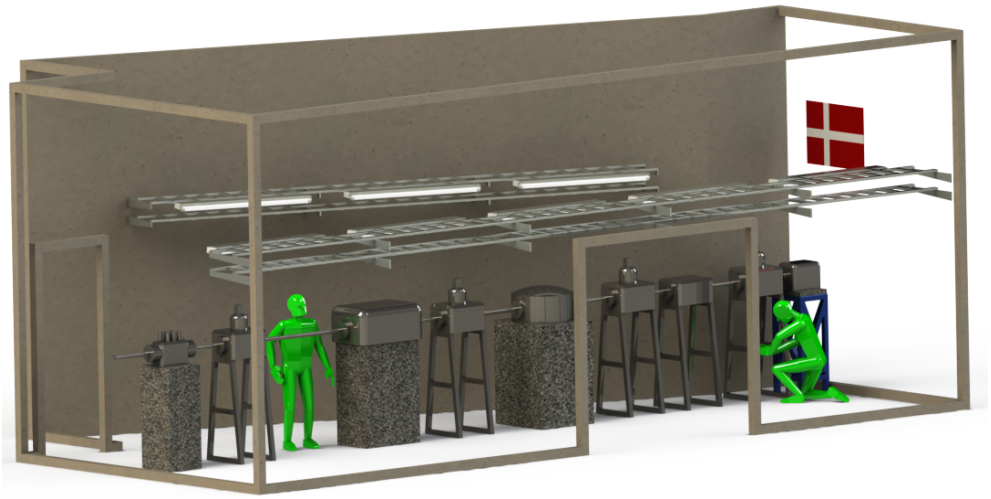

Version 2.0
December 2017

Innokenty Kantor, Erik Bergbäck Knudsen
Department of Physics, Technical University of Denmark.
Mads Ry Vogel Jørgensen
Department of Chemistry & iNANO, Aarhus University.

1. Summary

DanMAX will be a world-leading materials science beamline dedicated to in situ and operando experiments on real materials. The beamline will operate in the 15 - 35 keV range and have two end stations: one for full field imaging and one for powder X-ray diffraction. With a large and diverse user community there will be a focus on high throughput and extended provision of data analysis tools. The combination of two related techniques will ensure cross talk between communities and seed new collaborations and science taking advantage of the high complementarity of the techniques.

The beamline will be built at achromat 4 at the MAX IV 3 GeV storage ring. The project is funded by grants from 'Nationalt Udvalg for Forskningstruktur' under the Danish Ministry of Higher Education and Science, the Capital Region, and the Central Denmark Region. In addition to these grants the MAX IV laboratory, Technical University of Denmark, Aarhus University, and University of Copenhagen are also contributing financially to the project.

Figure 1.1 Aerial view of the MAX IV Laboratory. Foto: Perry Nordeng.

The *imaging end station* will enable multi-modal, multi-scale analysis of the internal structures of bulk materials and objects. It will combine absorption/phase contrast, diffraction contrast, and grating-based imaging on medium sized (0.1 - 3 mm) samples. It will be explicitly designed to enable acquisition of time-resolved 3D movies of structural evolution with a 3D spatial resolution in the range 50 nm - 5 µm. As such it will allow direct observation and quantification of material responses to external loads, e.g. during mechanical, thermal, electrical or chemical loading.

The *powder X-ray diffraction end station* will use the latest generation of curved pixel strip detector and the latest generation of large 2D detectors for high-speed *in situ* experiments. The curved pixel strip detector will have a large angular coverage, which will facilitate e.g. pair distribution function (PDF) measurements. The 2D detector will be movable and can be positioned at different distances

from the sample. Placed close to the sample the 2D detector allows high *Q* range coverage at moderate reciprocal space resolution. Alternatively, the 2D detector can be moved further away from the sample to increase peak resolution at the expense of *Q* range coverage, or to enhance the low *Q* region. Both configurations are compatible with very fast data collection. Texture analysis, and diffraction tomographic experiments will benefit from the very small and high brilliance of the beam at MAX IV.

This document summarizes the optical design of the DanMAX beamline and the project management during the procurement and construction. The main part of the document contains summarized descriptions of the optical components while detailed descriptions can be found in the appendices. Separate documents will contain the descriptions of the experimental station, the instruments and the infrastructure.

Contents

1. Summary 2
2. Project Background 5
3. Scientific Background 6
4. Beamline Design 8
5. Insertion Device 12
6. Front End 14
7. Beamline Optics 15
   7.1. High-pass filter 15
   7.2. High resolution monochromator 15
   7.3. High intensity monochromator 16
   7.4. Higher harmonic rejection 20
   7.5. Beam transport 20
   7.6. Diagnostics 20
   7.7. Radiation Safety 21
   7.8. Commissioning plan and beamline development 22
8. Experimental Station 22
   8.1. Imaging instrument 23
   8.2. PXRD instruments 23
9. Virtual Experiments with McXtrace 24
10. Hutches and Infrastructure 25
11. Beamline Control 27
12. Timeline 27
13. Roles and Responsibilities 27
14. Budget 30
15. References 30
Appendix A. Insertion Device A-1
Appendix B. Beamline Optics B-1

2. Project Background

DanMAX is a beamline that combines two powerful techniques to create a unique instrumental platform to do experiments on *real materials*, under *real conditions* in *real time* at MAX IV. It is a beamline for chemistry, materials science and engineering.

Denmark has a strong expertise in these fields and a well-developed synchrotron users community in both, academia and industry. There is a strong interest in building a world class instrument to serve these communities. The DanMAX user consortium, which combines 48 staff members from five major Danish universities and 17 industrial companies, have been created to organize these efforts. The university partners of the DanMAX consortium are Aarhus University (AU), Technical University of Denmark (DTU), University of Copenhagen (KU), University of Southen Denmark (SDU), Roskilde University (RUC) and Aalborg University (AAU). The science case for DanMAX was compiled in the Conceptual Design Report in November 2014 (Gundlach *et al.*, 2014). The full list of the DanMAX consortium partners can be found in the Appendix A of the CDR.

The new beamline will distribute its activities and resources equally between the two major experimental techniques – powder diffraction and full field imaging. In addition to a general open access beam time, a priority access will be granted to Danish users, both academic and industrial. 5% of the beam time will be used for a joint educational program for Danish and Swedish scientists and students. As Sweden has a strong tradition in spectroscopy, and the Danish X-ray community has its main strengths in diffraction and imaging, both Danish and Swedish parties will benefit from this project. The unique properties of the source and the proximity of the site have from the onset attracted strong interest in MAX IV within these Danish communities.

The project was initiated in with the submission of the DanMAX proposal for the National Danish Infrastructure Roadmap in 2010. During prioritization, the proposal was postponed with the argument that an upper level Danish-Swedish understanding was not in place. Later discussions between the Danish and Swedish ministries had the outcome that Danish participation in the funding of MAX IV indeed would have to take place at the university level and most likely in terms of co-funding of a beamline.

During 2014, the DanMAX consortium had secured grants of approximately 100 million Swedish kroner from the “Nationale Udvalg for ForskningsInfrastruktur (NUFI)” under the Danish Agency for Science, Technology and Innovation, from the Danish regions, and from the universities themselves. The beamline proposal was presented at the “MAX IV User Meeting” in September 2014, and presented to the MAX IV board on October 2nd, 2014. The board gave a favorable feedback and the CDR describing the scientific case for DanMAX was submitted to the MAX IV management in November 2014.

A Memorandum of Understanding between MAX IV, the Technical University of Denmark (DTU), Aarhus University (AU) and University of Copenhagen (KU) was signed on December 16th, 2014 outlining their principal commitment to cooperate regarding the financing, construction and

operation of DanMAX. The collaboration contract between MAX IV, DTU, AU and KU specifying the project terms was signed in May 2016.

The first version of this DDR (November 2016) was submitted for external review in December 2016. The review panel consisted of Ingolf Lindau (Stanford University and LU, Chair), Raymond Barret (ESRF), Andrew Fitch (ESRF), Horst Schulte-Schrepping (DESY), Ivan Vartaniants (DESY, not able to attend, SAC representative), and Timm Weitkamp (SOLEIL, not able to attend, but provided written input). The committee recommended the optical solution presented in the DDR, but suggested some minor changes to the DDR and missing data that should be added before the optics procurement could be initiated. The DanMAX team are grateful for the discussions with the panel members during the review and the suggestions presented in the review report.

This second version of the DDR incorporates the changes suggested by the review committee. In addition, all McXtrace* simulations have been redone and updated with a new and more precise source model. Finally, the design and layout of the radiation safety hutches and control rooms etc. have been finalized and a description has been added here.

3. Scientific Background

X-ray tomography allows 3D mapping of internal structures of materials without destructive sample treatment. Study of internal structure of materials, such as porosity, grain shape and growth, cracks formation, etc. during operation conditions provides invaluable information about the material properties. A more general area of application is 3D characterization of material microstructures over representative volumes. Examples are the characterization of pore structure and connectivity for fluid flow modeling in porous media or understanding the morphology and juxtaposition of material microstructures that control macroscopic deformation. The ability to observe materials under the correct environmental conditions, and as a function of time, is often essential. Furthermore, when studying paleontological, archaeological and cultural artifacts X-ray imaging techniques often are the only option for non-destructive study of their internal structures.

DanMAX will provide a number of unique or improved options for imaging:

- *Improved contrast and resolution*. Setting new records with respect to time or spatial resolution is not an aim in itself. However, the increased number of photons on the sample, and the increased coherent fraction, implies that for *a given acquisition time* the spatial resolution and in particular the contrast of phase contrast images will be superior.
- *4D materials science*. This field has emerged within the last decade. Here the synchrotron is used to generate 3D movies of materials behavior. The initial map is used as input for 3D modeling. In this way two movies – an experimental and a simulated one – can be compared point by point and time-step by time-step. This is seen as a much-improved route towards establishing and validating materials models. The increased number of photons on the sample and the improved contrast will facilitate 3D movies acquired at a much reduced acquisition time.

* http://www.mcxtrace.org/

- *Multiscale imaging*. It is characteristic that materials and components are organized hierarchically. Hence, the option to "zoom in and out" in the material is a major asset. DanMAX will first of all provide absorption and phase contrast imaging with high spatial resolution, permitting fine scale studies of bulk material microstructures. Combinations of these techniques with local tomography or grid-based dark-field imaging will enable multiscale analyses of structures and processes from 50 nm to several mm.
- *Multimodal imaging*. Another key focus of DanMAX will be multimodal imaging and, in particular, exploitation of full-field diffraction contrast imaging. A large group of materials are polycrystalline, e.g. most metals, ceramics, rocks, ice, sand and soil. Using diffraction based methods such as 3D X-Ray Diffraction (3DXRD) and Diffraction Contrast Tomography (DCT) the evolution of the individual grains and domains can be followed, as well as their orientation and stress state. On the sub-micron scale point beam methods allow distinguishing and mapping nano crystalline and amorphous constituents as well as following their response to e.g. external load. In a similar way to phase-contrast imaging this can also provide enhanced contrasts in low attenuation matter. In all cases it is a major science driver that the improved brilliance allows the acquisition time for diffraction based maps to be much lower, such that the gathering of multimodal data can become routine operation.

Powder X-ray diffraction (PXRD) is one of the most powerful ways to study the atomic structure of microcrystalline materials. The immense intensity of synchrotron radiation combined with the low divergence of the beams allows for more complex materials to be studied while using minimal sample volumes, which minimize systematic error effects such as extinction and absorption. The extremely low divergence of the MAX IV source will further enhance the peak resolution by reducing the instrumental broadening.

The goal of DanMAX is to do experiments on *real* material studied under *realistic* conditions at *realistic* time scales. This means that fast and efficient detectors are needed in addition to advanced sample environments e.g. electrochemical cells, furnaces, cryostats, gas flow and high pressure cells etc. Another requirement is a large angular detector coverage to capture the full diffraction pattern at once. A high angular detector coverage will also facilitate PDF reconstruction, which is particular advantageous in case of amorphous phases forming during e.g. the formation of nanoparticles, during chemical reaction, and during phase transitions.

In addition to conventional PXRD another interesting development is diffraction tomography. This technique is similar to both X-ray tomography and 3D X-ray diffraction. It yields a complete 3D picture of the distribution of nano/micro-crystal phases in the sample and can e.g. also be used to map out stress/strain as a function of position in the sample.

The available energy range for the beamline is wide and facilitates both fluorescent elemental mapping in the low energy range and collection of accurate diffraction data or PDF using high energy X-rays. Element specific fluorescence using an energy dispersive detector combined with position resolved diffraction is a powerful technique to study chemically/structurally graded materials.

The beam time at DanMAX is divided equally between the two techniques. Since the target scientific cases require hard X-rays, the insertion device of DanMAX should be optimized for the maximum flux around highest energy (35 keV).

4. Beamline Design

DanMAX will be a highly versatile beamline and thus the optics needs to be able to tailor the beam properties to the individual experiments. It is also important to design the optics to preserve the high coherence of the beam for phase-contrast imaging, and maximizing photon flux is required for ultrafast time-resolved studies. The total length of the beamline must be below 55 m in order to fit within the existing experimental hall of the MAX IV 3 GeV storage ring. Extending the beamline outside the experimental hall would dramatically increase its cost and would be incompatible with the available budget. At the same time, it is of utmost importance that the delivered beam is stable, both in intensity, energy, and position over time. Finally, it is a requirement that the users are able to tune the beam properties including the energy and the size of the beam at the sample.

The requirements above have led us to propose the optical scheme illustrated in Figure 4.1. Overall the beamline will have two modes of operation: high energy resolution or high intensity. This is possible by using two monochromators; first a cryo-cooled Si (111) double crystal monochromator (DCM) followed by a water-cooled multilayer mirror monochromator (MLM). To decrease vibrations both monochromators are horizontally deflecting, thus, ensuring a more stable beam.

By combining the two monochromators the beamline can run in three modes:

- *DCM only*: Monochromatic mode without harmonic rejection. This option ensures the highest monochromatic flux and preserved coherence. This mode is good for phase contrast imaging, diffraction contrast imaging and PXRD in the range 20-35 keV.

- *DCM and MLM*: Monochromatic mode with harmonic rejection. The DCM determines the band pass and higher harmonics are rejected by the MLM. This option is necessary for PXRD and diffraction contrast imaging at lower photon energies (15-20 keV), see Appendix B.5.

- *MLM only*: Quasi-monochromatic mode. The band pass of the MLM is determined by the multilayer coating and can be matched to the width of the undulator peaks ($\Delta E/E$ ~ 1% or 0.3% depending on the coating), thus leading to a quasi-monochromatic beam with very high intensity. This operational mode is perfect for e.g. fast absorption contrast imaging and fast (low resolution) diffraction.

Finally, the beam size/divergence can be adjusted by inserting Be compound refractive lenses (CRL) into the beam. The beam size can be adjusted from approx. 40 x 5 μm^2 to 1.3 x 1.2 mm^2 (FWHM) using the CRLs in the optical hutch. Additional optical elements will be added in the experimental hutch to focus the beam even tighter or to create large beams.

To ensure a fast change between the two modes, with minimal time spend adjusting optics, fixed exit operation of the monochromators ensures that the beam position is not changed when

changing between modes nor when changing energy. Additionally, several beam monitors will be installed in the optical path to aid in efficient alignment, see section 7.6.

An overview of the finite element analysis (FEA) and ray-tracing analysis used to study the performance of the optics scheme is given below. Detailed descriptions of the optics, including a description of the individual components, and details from the FEA and ray-tracing analysis, can be found in Appendix B.

The ray-tracing analysis was performed in a complete DanMAX model using McXtrace (Knudsen *et al.*, 2013, see section 9) with input from other computer codes as appropriate. E.g. SPECTRA[†] (Tanaka & Kitamura, 2001) for undulator radiation, IMD (Windt, 1998) for multilayer reflectivity, XOP/Shadow[‡] (Sánchez del Rio & Dejus, 2011) and Comsol[§] for monochromators under heat load.

The coordinate system used throughout this report is compliant with the MAX IV and McXtrace convention, as illustrated in Figure 4.2.

Other design options were considered, e.g. using a beam splitter to build two beamline branches, thus effectively doubling the available beam time. After careful discussions we have decided against such a solution, see Appendix B.9. Instead we will prepare the beamline to be easily upgradable with a parallel beamline. The beam for this instrument will be diffracted from a diamond 111 Laue monochromator which will replace the second high-pass diamond filter. The beam will subsequently be diffracted by a Ge 220 monochromator to be nearly parallel with the primary beam. The photon energy will be limited to narrow interval matching only the 5^{th} or 7^{th} harmonic at various undulator gaps (see appendix B.2).

The use of the beamline will be decided by the DanMAX consortium and the DanMAX steering group. The beamline could support the existing DanMAX instruments, e.g. sample testing for PXRD and imaging, or alternatively it could be another technique e.g. single crystal diffraction. Since the use of the side station has not been decided and the funding has not been secured, the detailed design of the optics has not been performed.

[†] http://radiant.harima.riken.go.jp/spectra/index.html

[‡] https://www1.aps.anl.gov/Science/Scientific-Software/XOP

[§] www.comsol.com

Table 1 Main characteristics of the DanMAX beamline.

	Proposed scheme	Requirements from the science case in the CDR / DanMAX Consortium
X-ray source	3m long in vacuum undulator, 16 mm period length, 4.0 mm minimum gap. K_{max} = 1.66 Source size 53.9 x 6.4 μm^2 (h x v, RMS) Source divergence 11.3 x 9.8 μrad^2 (h x v, RMS)	Highest possible flux at 35 keV. Significant dips/holes in the spectrum is acceptable
Energy range	15 – 35 keV (0.83 – 0.35 Å)	10 – 35 keV*
Filter	1 mm diamond @ 24.0 m	
Beam splitter†	Diamond (111) Laue monochromator @ 24.3 m narrow energy range, ~15 keV	
High resolution monochromator (hDCM)	Liquid nitrogen cooled horizontally deflecting double crystal (Si (111)) monochromator @ 26.6 m.	
Energy bandwidth, (monochromatic) ΔE/E (FWHM)	1.7 x 10^{-4} (@15 keV) – 3.2 x 10^{-4} (@ 35 keV)	2-3 x 10^{-4}
High intensity monochromator (hMLM)	Water-cooled horizontally deflecting double W/B_4C or $Ni_{0.93}V_{0.07}/B_4C$ multilayer monochromator @ 29.4 m.	
Energy bandwidth, (high intensity) ΔE/E (FWHM)	0.3% – 1% (depending on ML coating and energy)	Transmission of the whole undulator harmonic peak
Focusing optics	Transfocator with Be CRLs @ 32.1 m	Stable and convenient spot size variation
Sample position	Imaging: 42.4 m, PXRD: 45.0 and 47.3 m	
Beam size at sample position (FWHM)	~5 x 40 μm^2 to 0.8 x 0.8 mm^2 (hDCM) ~10 x 100 μm^2 to 1.2 x 1.3 mm^2 (MLM)	~10 µm to 10 mm 50 nm for direct projection high-resolution tomography
RMS divergence at sample position (unfocused)	~8 x 7 μrad^2 (h x v) with the hDCM (15-35 keV) ~16 x 10 μrad^2 (h x v) with the MLM (15-35 keV)	
RMS divergence at sample position (collimated)	~1.5 x < 1 μrad^2 (h x v) with the hDCM (15-35 keV) ~5 x < 0.5 μrad^2 (h x v) with the MLM (15-35 keV)	<50 µrad
Flux at sample position (MLM)	~6 x 10^{14} ph/s (15 keV), ~5 x 10^{13} ph/s (35 keV)	Highest possible
Flux at sample position (hDCM)	~4 x 10^{13} ph/s (15keV), ~5 x 10^{12} ph/s (35keV)	Highest possible

*The CDR specifies 10-35 keV, however, at the1st DanMAX Users Meeting it was agreed that 15-35 keV was a better design criterion. However, the optical component could reach ~12 keV if necessarily. †The beam splitter is a potential upgrade of the beamline, for more details Appendix B.2. §Smaller or larger beam sized would be obtained using additional optics in the experimental hutch (Details have not yet been decided).

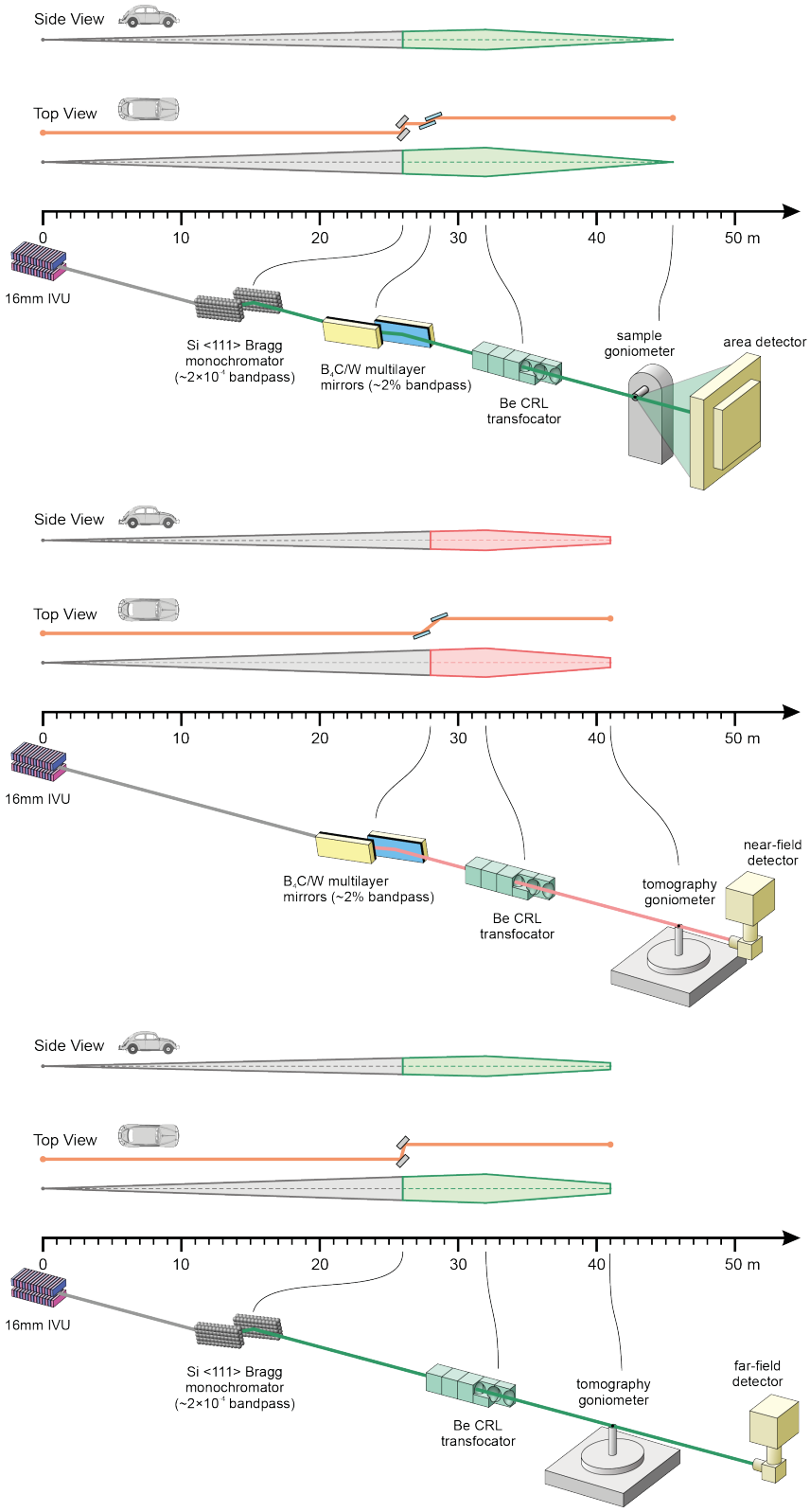

Figure 4.1 Proposed optics scheme for DanMAX. Top: Narrow bandwidth with harmonic rejection using both Si (111) hDCM and multilayer mirrors. Middle: High intensity mode using only multilayer mirrors. Bottom: Narrow bandwidth without harmonic rejection using only Si (111) hDCM.

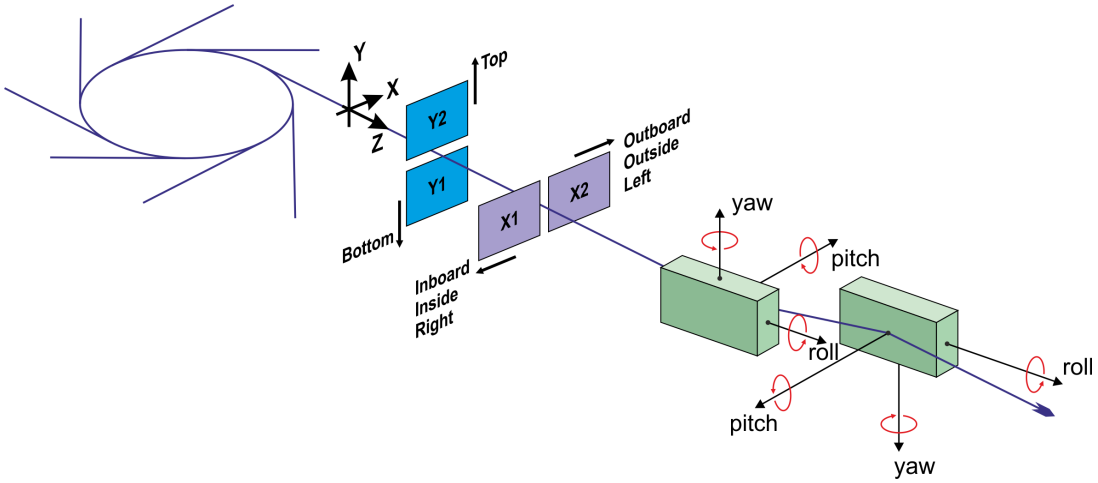

Figure 4.2 Coordinate system used in this report. Not shown: 'Downstream' = +Z, 'Upstream' = -Z. Figure adapted from original by Peter Sjöblom and Antonio Bartalesi (MAX IV).

5. Insertion Device

The design of the insertion device (ID) has been finalized and a vendor has been chosen after an open tender call. The contract with the vendor, Hitachi, was signed in July 2016 with expected delivery in January 2018. Here, the choice of technology and the main parameters are presented for reference. Further details about the DanMAX ID and a comparison of different technologies can be found in Appendix A

According to the scientific goals of DanMAX, the ID should provide the highest possible photon flux in hard X-ray range, i.e. the aim has been to optimize the ID in order to have maximum flux around 35 keV (the highest operation energy). The DanMAX beamline will utilize the achromat 4 straight section at the MAX IV 3 GeV storage ring, which has a length of 4.3 m. Significant dips in the spectrum are acceptable, since the beamline will not be used for spectroscopy. A monochromatic beam of ~0.01%-2% bandwidth is required. Additionally, preference was given to a choice of technology that pose a low risk and operational costs were considered.

Table 2 Parameters of the DanMAX IVU16 reference design.

DanMAX 3 m IVU16	
Period length (mm)	16
# Periods	187
Magnetic gap range (mm)	4.0 – 50.0
Peak field at min. gap (T)	1.181
Effective field at min. gap (T)	1.114
Effective K at min. gap	1.66
Photon energy range (keV)	9.5 - 40
Magnet pole material	NdFeB
Pole material	Vanadium Permendur
Electron beam size RMS (μm)	53.9 x 6.3 (h x v)

To maximize the flux most of the straight section should be used, leaving room only for essential infrastructure at each end. The maximal feasible magnetic length is approximately 3 m. With a magnetic array length of 3 meters the minimal physical gap is 3.8 mm and minimal magnetic gap is 4.0 mm. To increase the peak field, it is necessary to use a small gap, thus, the device needs to be in vacuum.

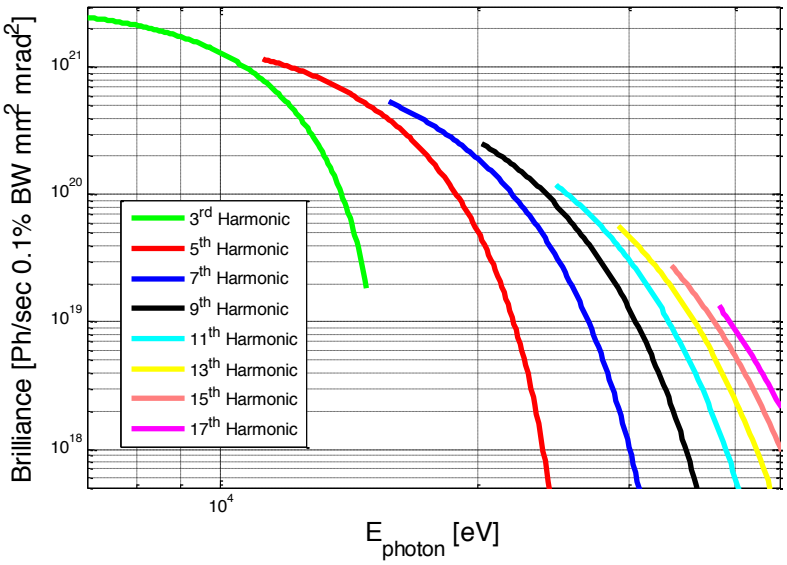

Figure 5.1 Predicted brilliance of the IVU16 reference design.

The electron energy of MAX IV is 3 GeV and thus 35 keV radiation is only available from the higher harmonics from the undulator (~11th-19th depending on design). For these high harmonic numbers the phase errors reduce the peak brilliance significantly (see Table A.1.1) e.g. for the 11th harmonic the brilliance can be doubled by decreasing the phase error from 5 degrees to 2.5 degrees. Therefore, the phase errors need careful consideration.

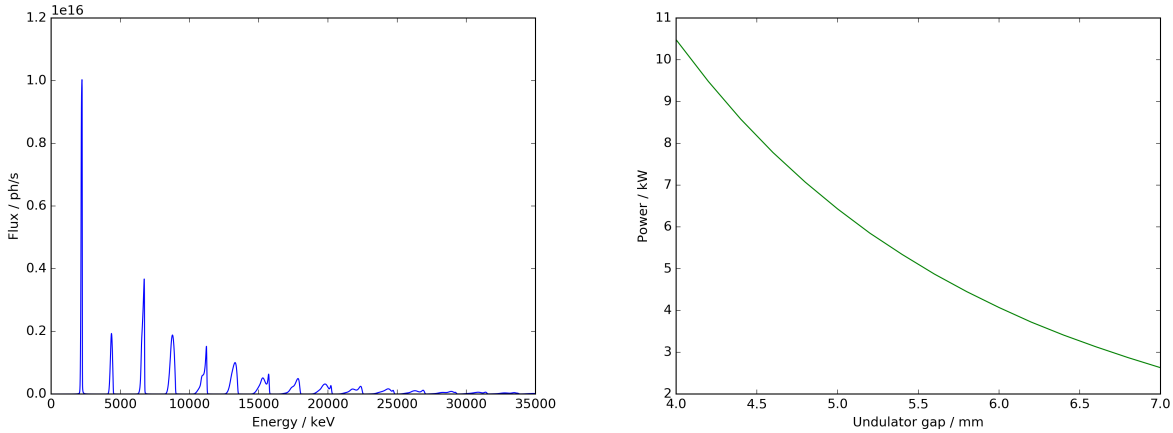

Figure 5.2 Left: Spectral flux from the DanMAX IVU16 through the fixed FE mask (100 x 100 µrad^2) 4 mm undulator gap. Right: Total power (no mask) emitted as a function of undulator gap.

Based on these criteria it was decided to use a 3 m long in-vacuum permanent magnet undulator operating at room temperature (IVU). The undulator period was chosen to be 16 mm. Figure 5.1 and Figure 5.2 shows the performance characteristics of the IVU16.

6. Front End

The front end (FE) is designed to protect both users and equipment on the beamline but also the machine in case of any vacuum failures on the beamline itself. DanMAX will be equipped with a front end from Toyama. The FE is essentially an upgraded version of the FEs used on the first MAX IV 3 GeV beamlines. The technical description of the FE reference design used in the call for tender can be found in a separate document.

The FE will have two fixed apertures followed by movable apertures for defining the beam. The first fixed mask has an aperture of 1 x 1 mrad^2 and will only absorb approximately 70 W. The wide opening is, however, necessary for the functionality of the two downstream X-ray Beam Position Monitors. The second fixed mask has an aperture of 100 x 100 µrad^2 and will absorb up to 9.5 KW. This aperture, situated approximately 16 m from the source, define the maximum possible opening of the front end. Up to 850 W could be transmitted through this aperture but this can be further reduced in movable apertures situated downstream. With these apertures, we will define an acceptance cone of 35 x 35 µrad^2 and thus further decrease the maximum power transmitted through the front end to 125 W in order to ensure that the downstream components will not be damaged. The 35 x 35 µrad^2 aperture matches the extent of the central cone and thus the total flux at the energy of interest through the 35 x 35 µrad^2 front end aperture is almost the same as the flux through the maximum allowed 100 x 100 µrad^2 mask (Figure 6.1).

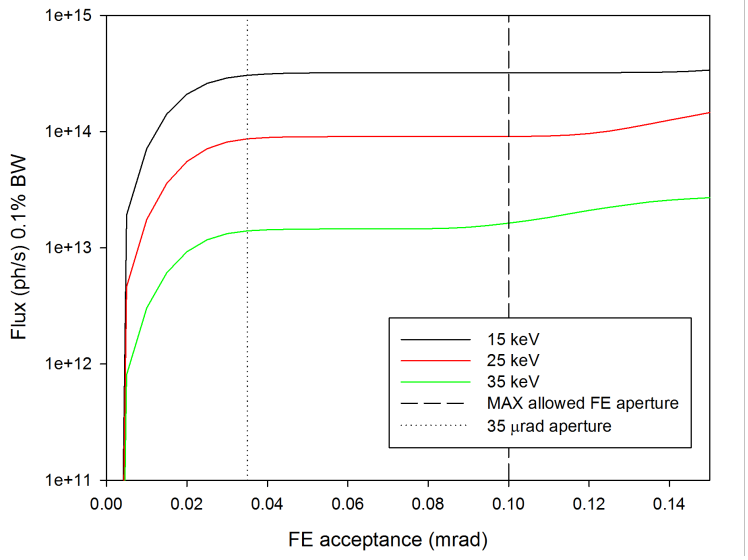

Figure 6.1 The total flux through a front end as a function of aperture size. Dashed line shows maximum allowed acceptance (0.1 mrad) and a proposed 35 µrad aperture is a dotted line.

The opening of the mask will be secured via the PLC system and redundant encoders to ensure that the mask position can be scanned but the mask opening cannot exceed 35 x 35 µrad^2 if the undulator is closed and the current in the storage ring is high.

7. Beamline Optics

The DanMAX beamline, as described in the conceptual design report, has a strong focus on in-situ experiments. To suite the requirements of the community the photon energy should be tunable in the range from 15 to 35 keV and the energy resolution needs to be on the order of $\Delta E/E \sim 10^{-2}$ (FWHM) for some experiments and $\Delta E/E \sim 10^{-4}$ (FWHM) for others. Ideally the energy resolution should be continuously tunable, however, we are not aware of any existing technology capable of this. The beam size must be adjustable ranging from 50 nm to 10 mm (FWHM). The optics should also preserve the coherence and keep the length of the beamline below approximately 50 m. In addition to these physical requirements it has been an overall design goal to design a user-friendly beamline where users can change beam properties without, or with only little, help from the beamline staff.

A present, the DDR describes the components of the optical hutch which are capable of only preliminary beam shaping in the range of ~1.3 x 1.2 mm^2 to ~40 x 10 μm^2 (FWHM). Smaller and larger beams will be created with the additional downstream components.

The proposed optical scheme is shown in Figure 4.1, Table 1 and a summary of the most import aspects if the components are given below.

Table 3 lists and Figure 7.1 shows the components and their approximate location. Detailed descriptions of the individual components can be found in Appendix B. Table 4 gives a summary of heat load at each of the optical components as obtained from the raytracing calculations, see below for the McXtrace model used in the simulations.

7.1. High-pass filter

The fundamental harmonic of the IVU16 is located at approximately 2.2 keV, thus much lower than the working energy range of DanMAX. To decrease the heat load on the optical elements a set of single crystal diamonds with a total thickness of 1.0 mm will be placed at the upstream end of the optical hutch. The diamond crystals will absorb approximately 75 W and transmit approximately 55 W. The transmission at 15 keV is approx. 75% and increases to 92% at 35 keV.

7.2. High resolution monochromator

DanMAX will utilize a Si (111) double crystal monochromator with horizontal beam deflection (hDCM), see Figure 4.1. At conventional synchrotron sources monochromators are typically employing a vertical scattering geometry. The primary reason for this is the higher energy resolution in this direction caused by the lower divergence in vertical direction compared to horizontal direction. The horizontal divergence of the MAX IV source is greatly reduced and thus the energy resolution using a horizontal geometry is nearly as high as a vertically deflecting geometry. A horizontally deflecting geometry is especially attractive as it can be made more rigid, thus less prone to vibrations. Additionally, there are no gravitational forces working on the rotation of the crystals. A drawback to this geometry is the loss of reflected intensity due to the P-polarization of the undulator radiation. However, this effect is small at the working energy of DanMAX and will only cause a loss of 13% at 15 keV and decreasing to only a 2.5% loss at 35 keV. Horizontally

deflecting monochromators are also employed at BioMAX, NanoMAX (Kristensen, *et al.*, 2016) and CoSAXS.

The monochromator will be operated in fixed exit mode. When used without the multilayer monochromator (MLM) the horizontal offset will be 10 mm, and when used in combination with the MLM the offset will be 4 mm.

Automated scripts will be developed to facilitate safe switching between the various monochromator modes, i.e. DCM only, DCM + MLM and MLM only. This will also facilitate that users potentially can switch between modes with little or no intervention from the beamline staff.

The monochromator will be placed at 25.7 m from the source. The power on the first crystal is 71 W with a peak power density on the surface less than 20 W/mm^2. This heat load is manageable; however, the crystals will need to be cooled with liquid nitrogen. The incident power will cause a thermal dent (due to the negative thermal expansion of Si at low temperature) which causes a slight focusing of the beam. This is most pronounced in the meridional (horizontal) direction. Overall the meridional divergence varies from 5 to 6 µrad (RMS) and the sagittal (vertical) divergence decreases from approx. 4 µrad at low energy to 3 µrad (RMS) at the higher energies. The energy resolution of the monochromator will be <1x10^{-4} (ΔE/E, RMS). Further details about the hDCM can be found in Appendix B.3.

7.3. High intensity monochromator

For experiments that do not need the high energy resolution of the hDCM but would benefit from a higher flux, there will be the possibility to use a double bounce multilayer monochromator (MLM) see Figure 4.1. The reflectance from a multilayer mirror shows a sequence of relatively narrow bands caused by the periodic structure. The energy resolution of these reflectance bands can be matched to the energy resolution of the undulator peaks to maximize the transmitted intensity.

The multilayers consisting of B_4C/W layers will be deposited on a Si substrate. The layer period will be 25 Å with a thickness ratio of Γ = 0.8. A total of 200 bilayers will be deposited. The expected final roughness is better than 3 Å (RMS) for a substrate roughness of ~1 Å (RMS). The second coating of alternating $B_4C/Ni_{0.95}V_{0.06}$ layers with a 20 Å period and Γ = 0.65 will be deposited on the same substrate next to the first one. This additional coating will provide an intermediate spectral resolution ($\Delta E/E$ ~ 3.5×10^{-3}) at the cost of a reduced flux. This narrower bandwidth could of an interest for some time-resolved X-ray diffraction experiments, as well as high-resolution imaging with CRL objective due to the lower chromatic aberrations of the beam.

The monochromator will be operated in fixed exit mode with a 10 mm offset when used without the hDCM and with a 6 mm offset when used together with the hDCM. The incident angles range from 0.41 to 0.97 degrees.

The MLM will be located at 27.3 m from the source. The maximum total power absorbed by the first ML, if used without the hDCM, is 65 W. The power density on the surface is reduced to approximately 2.5 W/mm^2, due to the larger footprint of the beam compared to the hDCM. Due to the lower power density it is feasible to water cool the first mirror and cool the second mirror using e.g. flexible copper braids or preferably solid copper heat conductors immersed in cooled a EGaIn

bath. The incident power will cause a thermal bump on the surface of the mirror. The shape of this bump is nearly spherical with a radius of ~10^3 m in sagittal (vertical) direction to ~10^4 m in meridional (horizontal) direction. This increases the meridional beam divergence to 20-25 µrad (RMS) at lower energies. At higher energies, the thermal distortion becomes negligible compared to the effect of surface roughness and the divergence decreases to approximately 17 µrad (RMS). The incident power on the MLM is negligible if used in combination with the hDCM.

Table 3 List of components and estimated distance from the source.

Component	Length (mm)	Center position (mm)
IVU16	3700	0
XBPM 1		12000
XBPM 2		15100
FE Aperture		19200
Ratchet Wall	1400	21800
Trigger Unit	500	22750
Bremsstrahlung collimator	200	23170
Diamond filter	200	23520
Laue Monochromator	400	23890
White beam slit 1	300	24460
BV1	300	24910
hDCM	750	25655
BV2	300	26400
MLM	1000	27270
White beam stop & bremsstrahlung collimator	400	28190
Monochromatic slit 1	100	28440
BV3 + future BPM	500	30550
CRL 1	600	31100
Monochromatic slit 2	100	31600
Safety shutter	400	32200
OH end wall	200	32500

Table 4. Highest X-ray power at each of the optical components, along with the dissipated power and X-ray spot side. Normal operation value assuming a 0.7×0.7 mm^2 movable front end mask, a 4 mm undulator gap and a 500 mA storage ring current.

Optical component	Max P reaching component (W)*	Max dissipated power in normal operation (W)	Beam size at the component (μm)
Diamond filter #1 (0.6 mm)	152.1	70.1	900×850
Diamond filter #2 (0.4 mm)	82.0	10.9	
BPM#1 (0.3 mm diamond)	71.1	5.03	
DCM crystal #1	71.1	70.45	960×960
DCM crystal #2	0.65	0.52	
BPM#2 (0.3 mm diamond)	71.1	0.29	
ML mirror #1	71.1	64.91	1040×1040
ML mirror #2	6.19	1.92	
BPM#3 (0.3 mm diamond)	4.27	0.29	
CRL guard aperture	4.27	1.65	1050x1120
CRL (first lens)	4.27	0.06	circular, d=900
CRL (full set, 50 lenses)	4.27	1.52	
Safety shutter	4.27	4.03	Variable, between 1130 and 550

*for the 4 mm gap and 0.8×0.8 mm^2 FE mask

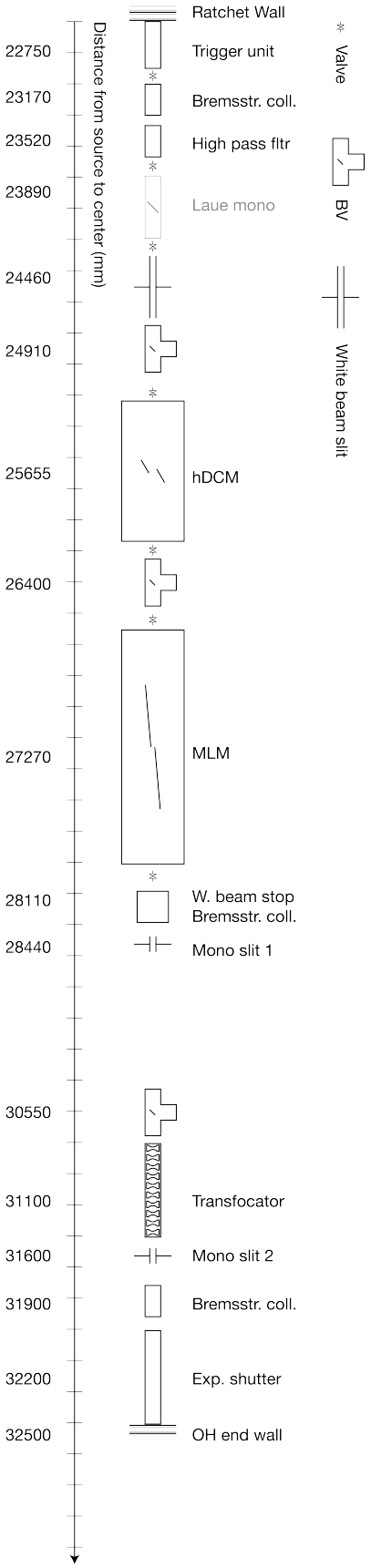

Figure 7.1 Block diagram of the proposed optical layout of DanMAX. The distances are in mm and reference the estimated source to center of component distance.

7.4. Higher harmonic rejection

The amount of photons from higher harmonics transmitted by the hDCM when the primary energy is low, i.e. 15-20 keV, is significant (λ_3/λ_1 = 5.4x10^{-4} @ 15 keV) and will affect some accurate experiments. Therefore, additional harmonic rejection is needed at these energies. By utilizing the both DCM and MLM the ratio drops to virtually 0 (λ_3/λ_1 = 1.5x10^{-14} @ 15 keV). Introducing the MLM in the beam will reduce the primary intensity by approximately 50% (@ 15 keV) and thus, the users will have to decide between complete harmonic rejection at the expense of intensity, or higher intensity at the expense of some harmonic contamination.

7.5. Beam transport

The first focusing element of the beamline will be a compound refractive lens transfocator. Compound refractive lenses (CRLs) have become very popular for focusing of hard X-rays due to their stability, relatively large aperture (beam acceptance), compact size and ease of alignment. Focusing CRLs are in-line optical elements that do not deviate or deflect the X-ray beam. The major drawback of the CRLs are their chromatic properties. This is caused by a strong variation of the refractive index with energy, and thus a different number of individual lenses (lenselets) is required at different energies in order to maintain a nearly constant focal distance. A mechanical device, which allows easy changing the number of lenses (a transfocator), will be used in the optical hutch. It is located after the second monochromator, at about 31.1 m from the source. The purpose of this device (CRL1 in Table 3) is either beam collimation or preliminary focusing at the sample position. With the 50 individual lenses grouped in 6 individual groups, this task can be achieved for the whole energy range. X-ray beam size at the sample position can be as small as ~40 x 10 µm with low divergence (~15 µrad RMS).

A smaller focal spot can be produced with the secondary focusing element located in the experiment hutch at a shorter distance to the sample. Such a secondary focusing element can be an additional set of CRLs, a Frensnel zone plate, a pair of Kirkpatrick-Baez mirrors or a multilayer Laue lens. The acceptance apertures of all these possible elements ranges typically from ~50 to ~500 µm, and the first CRL transfocator is capable of filling this aperture sizes with the X-ray beam. The choice and design of the secondary focusing optical element(s) will be done together with the design of the actual end station instruments in collaboration with the DanMAX Consortium.

7.6. Diagnostics

To maximize the usability of the beamline it is important to quickly and easily obtain direct information on the beam position, shape, and intensity at several positions along the beam path. Diagnostic elements (BV1,2,3 in Table 3), with fluorescence imaging and Compton scattering from diamond foils, will be placed after each of the larger optical elements. The diagnostic element downstream of the CRLs will be placed in the experimental hutch. All of these screens will be retractable via pneumatic actuators. They can be used during normal operation at the expense of lower intensity. The detailed design of the diagnostic element will be done by the vendor. A conceptual design of the element is shown in Figure 7.2.

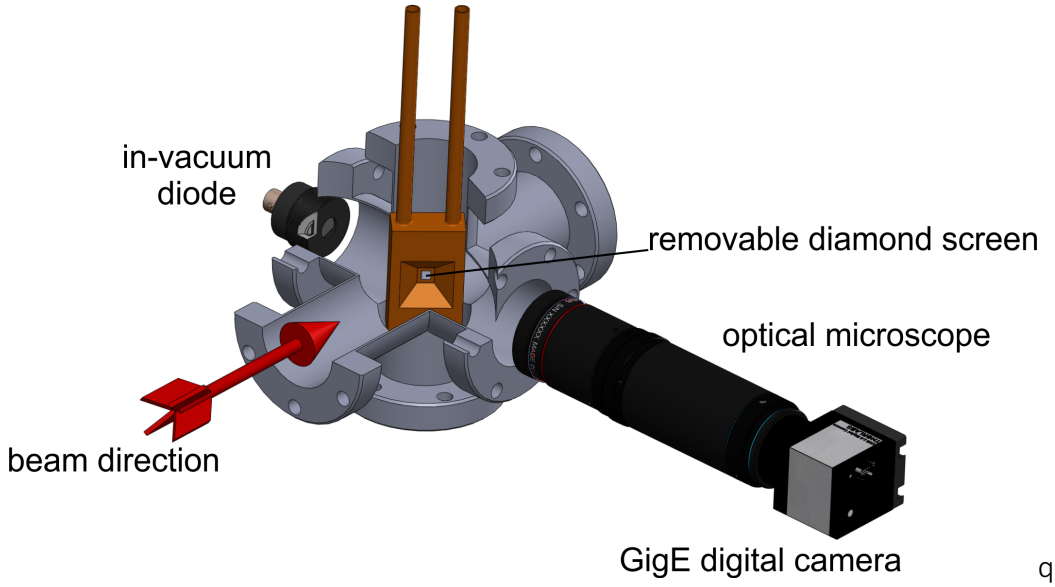

q

Figure 7.2 Conceptual design of the diagnostics element. The beam intensity will be gauged by fluorescence intensity and Compton scattering intensity. The beam shape will be monitored by fluorescence.

In addition to the diagnostics elements the front end contains two beam position monitors separated by ~3 m. These monitors can monitor both the beam position and the angle. The information from these will be used in an orbit correction feedback system.

To monitor the intensity during experiments we have the possibility to install simple ion chambers in the experimental hutch. The ion chambers will complement the intensity measurements from the diodes in the beam stops.

7.7. Radiation Safety

The optical layout of DanMAX has been designed to always have a horizontal beam offset of 10 mm. The 10 mm horizontal offset is also used for the NanoMAX and BioMAX beamlines which use similar, although shorter, IVUs. Thus, we do not foresee major problems with this layout.

The flexibility of the DanMAX optics can lead to the following situations that will be included in the radiation safety assessment.

- Neither DCM nor MLM are in the beam: The beam is not offset and should hit the water-cooled white beam stop placed downstream of the MLM. Parking positions of the DCM and MLM may also be monitored by the PLC to prevent this situation from occurring.
- The 1st ML mirror is in grazing incidence and thus fully reflecting the beam: The ML mirrors are quite short, 200 mm, thus the acceptance of the mirror is very low. In addition, hardware limit switches may be included in the MLM to prevent this situation. If this situation occurs the reflected beam will hit the white beam stop and thus, prevent damage to downstream components.

A full radiation safety calculation and detailed design of bremsstrahlung collimators and white beam stops is pending at this time. But we anticipate the following radiation safety components in the optical hutch:

- Bremsstrahlung collimator at the entrance to the optical hutch
- Combined unit with white beam stop, bremsstrahlung stop, and bremsstrahlung collimator downstream of the 2nd bremsstrahlung collimator
- Potentially a 3rd bremsstrahlung collimator just upstream of the photon shutter.

7.8. Commissioning plan and beamline development

The commissioning of the beamline will happen in a partially sequential way gradually increasing the complexity and the capability. The following stages for the optics are foreseen:

1. Operation using the hDCM at fixed energy and unfocused beam.
2. Operation using the hDCM with tunable energy and unfocused beam.
3. Operation using the MLM only and unfocused beam.
4. Operation using both hDCM and MLM and unfocused beam.
5. Addition of CRLs (CRL1) in the optical hutch.

The commissioning of the experimental hutch will happen in a sequential mode where it is anticipated that commissioning of the PXRD experiments begin first followed by the imaging instrument.

8. Experimental Station

The detailed design of the experiment station is ongoing, and only a brief description is included here. The DanMAX Consortium has been consulted on the needs and wishes for the end station design during the 2nd DanMAX Users Meeting and here the conceptual design discussed below was approved. The detailed design will be completed in the first half of 2018.

To increase the flexibility of the beamline we will develop a common kinematic detector mount to allow (nearly) all detectors at DanMAX to be mounted on all instruments. This will e.g. mean that the large 2D area detector can be mounted at the downstream end of the hutch and could be used for SAXS measurements while using the 1D strip detector for PXRD.

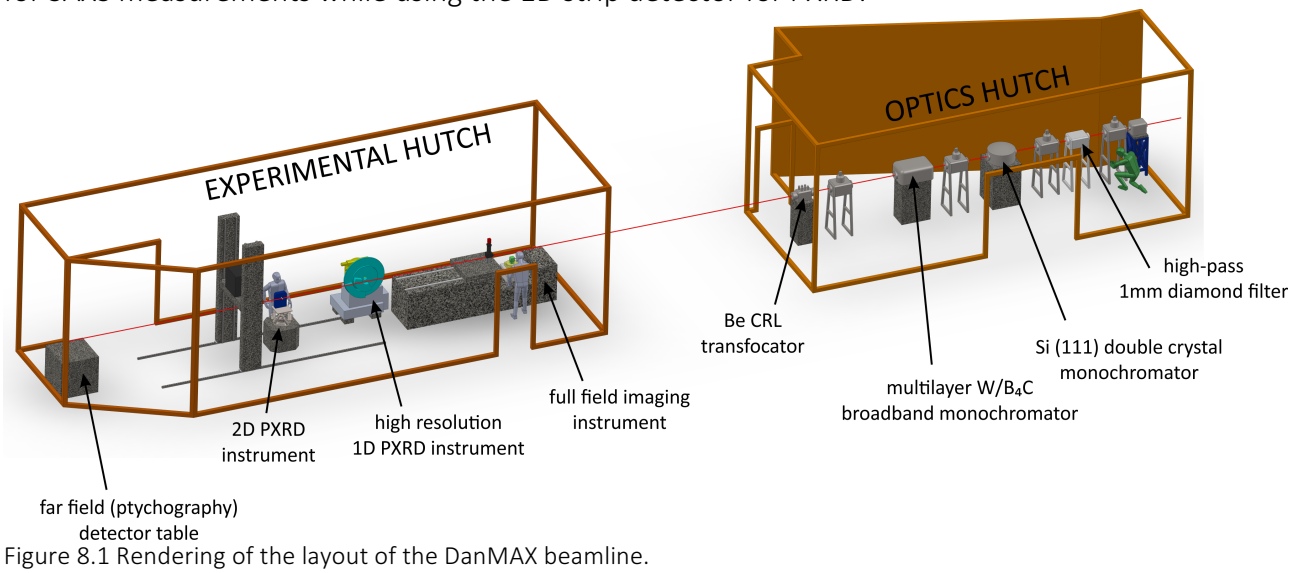

Figure 8.1 Rendering of the layout of the DanMAX beamline.

The design is based around a single large hutch containing both instruments, see Figure 8.1. This choice does have some advantages and disadvantages. The advantages of a single large hutch are the possibility to have a larger sample to detector distance, an overall reduced price (compared to two independent hutches). In addition, it yields more flexibility in the future development of the beamline, and there is higher potential for synergy between the imaging and PXRD communities. The main disadvantage of a single hutch compared to two separate hutches is the limited access to the instruments during experiments. This applies of course only to the downstream instrument in case of two sequential hutches.

The maximal length of the beamline is governed by the radius of the storage ring and the width of the experimental hall. Around the outside of the experimental hall there is a 3 m 'keep clear' path (see Figure 10.1) which restricts the total length of the beamline to approximately 52 m. It is possible to build longer beamlines where the experimental station is located in a separate satellite building, as e.g. NanoMAX. The DanMAX budget, however, does not permit building a long beam line.

The upstream wall of the experimental hutch (EH1 in Figure 10.1) will be at approximately 38.1 m from the source. Inside the hutch the first element will be a vacuum window followed by a beam monitor providing an image of the beam for easy and fast diagnostics. Downstream of this monitor will be a focusing device (or multiple focusing devices), which can tightly focus the beam at the imaging sample position (approx. at 41.2 m). In the future 1D focusing may also be added here to focus the beam further in the horizontal direction at the PXRD sample positions.

8.1. Imaging instrument

The imaging instrument will be placed upstream in the hutch. The instrument consists of a precise tomographic stage rotating on an air bearing. To decrease vibrations, the stage will sit on a large granite support, which will also support the near field detector and the EH focusing device(s). Far field detectors, e.g. for diffraction contrast imaging, will be able to be moved to many locations in the hutch to obtain vary the sample to detector distance and scattering angle. The imaging sample position will be at approximately 41.2 m from the source. The distance from the sample to the far field detector may be up to 8-10 m at certain scattering angles. To facilitate ptychographig imaging it will be possible to position detectors at the downstream end of the hutch. To let the beam to the downstream PXRD instrument the near field detector needs to be removable or moved in/out-board to facilitate installation of an evacuated beam transport tube.

8.2. PXRD instruments

The PXRD setups will be placed between the imaging sample position and the far field detectors. There will be two instruments, one for medium-to-high resolution PXRD and one for experiments with larger sample environments. The medium-to-high resolution instrument consists of a two circle diffractometer with a state-of-the-art 1D strip detector (Dectris Mythen 24K or similar). This setup will be at approx. 44.8 m from the source. A sample changer robot will be installed in connection with this setup. To facilitate small to medium sized sample environments a table with height adjustment will be installed in front of the goniometer.
The large sample environment setup consists of a sample stage, either a conventional table or preferably a hexapod, which can carry heavy sample environments (up to ~250 kg). The diffracted intensity will be recorded on a large state-of-the-art 2D detector (Dectris Pilatus 3X CdTe 2M or

similar). The mount for the area detector will be shared with the far field imaging detector and will be highly flexible. Besides XYZ movement the 2θ angle of the detector will also be adjustable. Additionally, an energy dispersive detector can be mounted to record the fluorescence signal from the sample. The sample position will be approximately 48.2 m from the source. Both setups should have motorized beam stops with the possibility to image the beam or at least record the beam intensity.

9. Virtual Experiments with McXtrace

During the design process the ray tracing software package McXtrace (Knudsen *et al.*, 2013) has been used extensively. The aim is to also build a virtual beamline along with the real beamline, in terms of a computer model. This will facilitate source to detector simulations of the experiments that are considered at DanMAX. There are several reasons to build the model DanMAX in parallel with designing the real beamline:

- Having a complete model will be great help when planning potential upgrades or other changes to the beamline.
- The model is a 1:1 copy of what is actually built. Beamlines evolve over time and sometimes details are lost in the process.
- Given sufficiently rich and user-friendly interface, the model may be used for experiment planning, preparing detailed proposals and/or user teaching. Beam time can be planned and experiments executed more productively if the users are already familiar with the beamline's properties and operation. Ideally the model beamline should be operated from an identical interface as the real beamline.

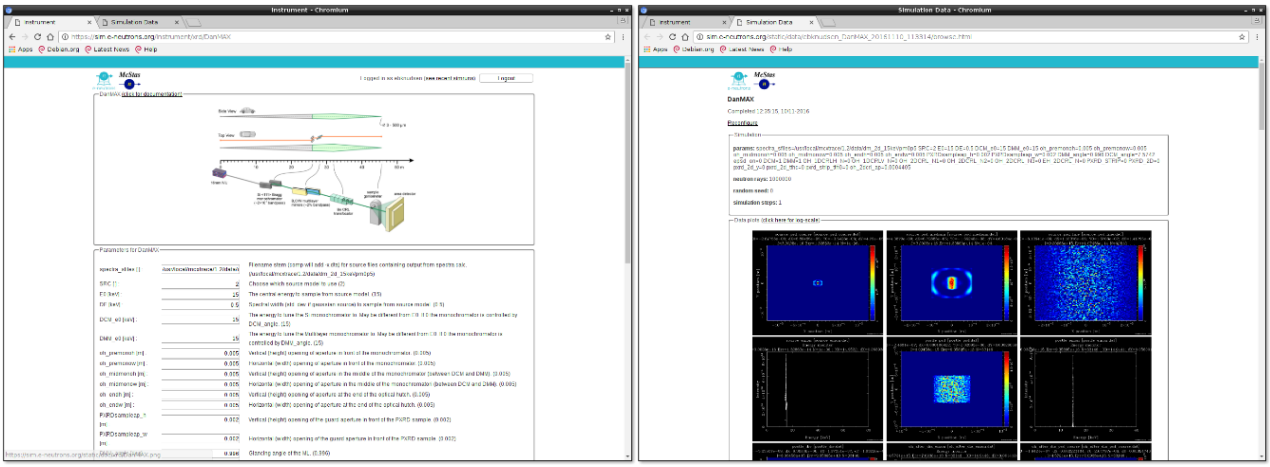

Figure 9.1 Screenshots of the web-service simulation of the DanMAX-beamline. Left: The run configuration-view. Various settings are exposed to the user. Right: Result view of the simulation for a single setting of the simulation.

McXtrace itself is a general, open source, modular software package distributed under the GNU Public License (GPLv2). It is intended for simulating any type of X-ray experiment. The software is multiplatform, runs on hardware ranging from large scale supercomputers (e.g. FERMI) to Raspberry PIs.

To run a beamline simulation a user specifies the beamline settings required, such as the photon energy, monochromator configuration, slit openings etc. A web interface exists for any beamline model built using McXTRACE. Screenshots of the operation and result screens are shown in Figure 9.1. The web-service runs simulations remotely and in addition to the plots shown, also grants the users access to the generated data. It may be preferential to have more than one beamline front end, i.e. a simple interface and an advanced one, where more settings are exposed to the user. The underlying model is the same for the web service as well as for the design project, thus avoiding the problem of keeping separate models updated.

10. Hutches and Infrastructure

Besides creating ample space for the experiment and for future development of the instruments, the DanMAX beamline should provide comfortable areas for the users while they are conducting their experiments. The floor plan for DanMAX can be seen in Figure 10.1. There will, as mentioned above, be build three radiation safety hutches; one for the optics, one for the PXRD and imagning instruments (EH1), and one for a future instrument, EH2.

The optical hutch (OH) will be 9.9 m long and use the ratchet wall as part of the construction. There will be two doors for accessing the outboard side of the optics. Additional access will be possible from backside of the hutch. The main experimental hutch (EH1) will be approximately 13.8 meters long and 4.5 meters wide. Due to the 'keep clear' pathway in the experimental hall, the hutch will have a tapered shape near the downstream end. EH1 will have two doors; a single door for normal access through the sample environment area and a double door on the opposite side for easy access with larger equipment. A number of chicanes will be installed, one of which has direct access to the sample environment area and can be used for user equipment.

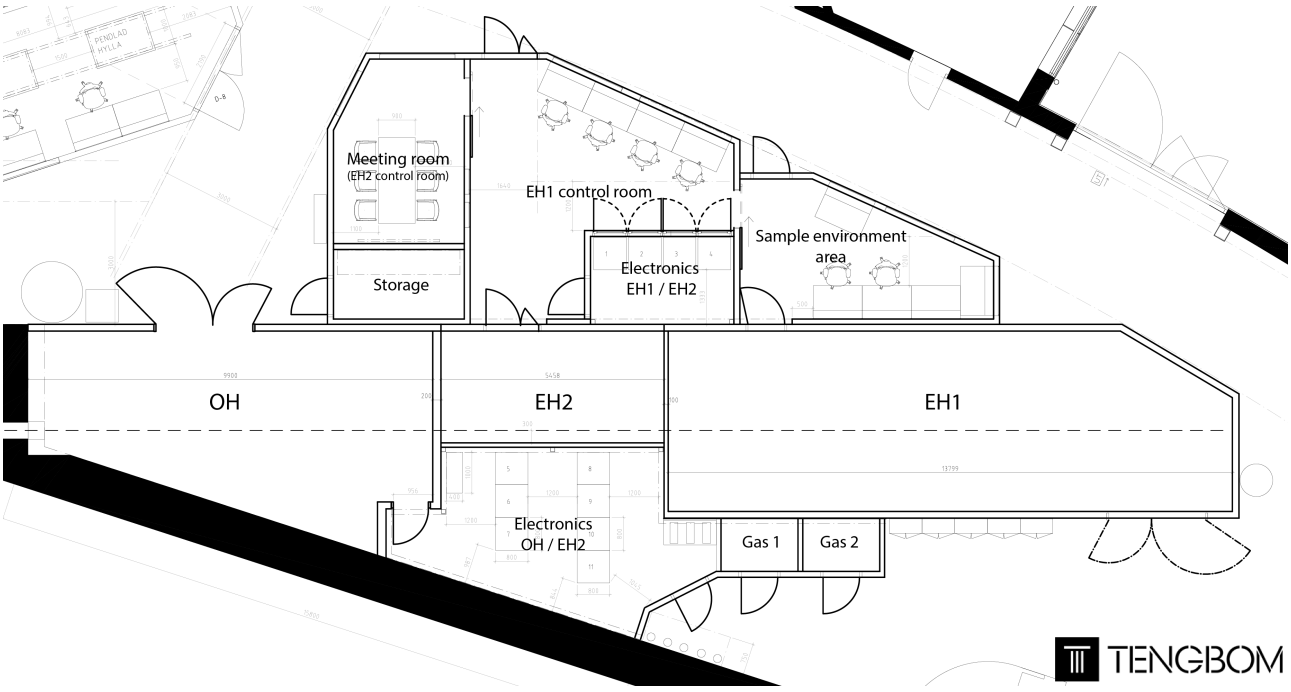

Figure 10.1 Floorplan of the DanMAX beamline at achromat 4. Please observe that the room marked 'Electronics OH/EH2' will not be built as a room but will be left open. The electronics racks will be closed and cooled using small A/C units mounted on the racks. A small pump-room will be built next to the gas rooms.

A gas system will be permanently installed in the EH1. The specification will be decided in collaboration with the user community. A gas system with similar requirements will be installed at the BALDER beamline, and it is likely that much of this design can be reused at DanMAX. To allow experiments with gasses the EH1 will be equipped with process ventilation with fume extraction arms and appropriate gas sensors to facilitate *in situ* gas and chemistry experiments.

EH2 is built between the OH and EH1, and will be 5.5 m long. A one and half door will provide access to the hutch directly from the control room. The beam to EH1 will go through EH2, but the fight tube is shielded and thus the PSS system for this hutch will be large independent of EH2.

The main ventilation and temperature control of all the radiation safety hutches is controlled by one large A/C unit located outside the radiation safety hutches. The temperature stability of the radiation safety hutches has been specified to ±1 °C, with strong emphasis on temporal temperature stability and less emphasis on absolute temperature.

The electronics racks for the equipment in the OH, network, UPS and vacuum will be placed behind EH2 and between the OH and EH1. The racks will be closed and cooled using small A/C units mounted on top of the racks. To accommodate pumps and other noisy equipment to comply with the sound level regulations in the experimental hall we will have a pump room next to the gas rooms.

The control area consists of 4 rooms; the EH1 control room, a meeting room, a sample environment (SE) area, and a room for electronic racks. The racks are placed in a separate room to keep the noise level in the control room low. The four racks can be accessed directly from the control room. This location is convenient for the operators, but also close to both EH1 and EH2, thus, keeping the length of the cables at a minimum. The control room itself will accommodate 4-6 persons.
The control area also encompasses a meeting room with a large screen to analyze and present data etc. This area will be used both by users during experiments, and for the beamline staff during day to day planning and for training of the users. In the future, this room can be converted to a control room for EH2.

The last room is the SE area where sample environments can be assembled and tested before being moved into the EH for subsequent experiments. This will be equipped with workshop tables, a high quality microscope, and a range of tools. Nitrogen gas and pressurized air is available in the room. A fume extraction arm is also installed to facilitate e.g. soldering and gluing etc. There will not be a separate chemistry laboratory at DanMAX. Users will instead use the facility laboratory located right across ‘keep clear’ path between achromat 3 (NanoMAX) and achromat 4.

Besides the rooms described above, there will be an approx. 6 m^2 large storage room. Furthermore, there will be a number of metal cabinets for storage of minor components behind the EH.

11. Beamline Control

The beamline control system will be compliant with the MAX IV standard, namely based on TANGO[**]. The user interface and GUIs will be built on top using SARDANA[††]. The motor control system at MAX IV is the ESRF developed IcePAP[‡‡].

The Control and IT group at MAX IV will provide software solutions for the beamline hardware, enabling control of the hardware over the beamline network. They will also provide a basic user interface for beamline operation. We will need to develop advanced and user friendly solutions for advanced data collections and easy interfacing with sample environments (SE). A detailed analysis of the needs will be carried out in parallel with the planning of the end station and infrastructure.

12. Timeline

DanMAX is among the phase 2 beamlines at MAX IV, and thus the project benefits from a lot of the lessons learned during the construction of the phase 1 beamlines. Nevertheless, the timeline of DanMAX is quite ambitious, see Table 5, and efficient resource management at MAX IV is essential when the phase 1 beamlines are transitioning to user operations and while the phase 2 beamlines are under construction and later on commissioning.

It is anticipated that the first commissioning experiments at DanMAX can start in 2019. During the commissioning of the experimental stations we plan to bring in expert users to test out the setups as soon as they are ready. It is anticipated that DanMAX can transition into the general user program in 2020.

13. Roles and Responsibilities

The DanMAX team currently consist of two persons (2 full-time equivalents, FTE) who are performing the majority of the design and planning of the beamline. Some of the design work is done in collaboration with experts at the MAX IV laboratory.

Innokenty Kantor (IK), Senior Researcher, Technical University of Denmark, is one of the two beamline scientists. IK is responsible for design and development of the imaging instrument.

Mads Ry Vogel Jørgensen (MJ), Project Manager, Aarhus University, is the other beamline scientist. MJ is responsible for the design and development of the PXRD instrument.

IK and MJ are co-responsible for the design and construction of the optics, all shared systems, and infrastructure/installations. In addition, they are working with the user community and will set up collaborations to build sample environments.

[**] http://www.tango-controls.org
[††] http://www.sardana-controls.org
[‡‡] http://www.esrf.eu/Instrumentation/DetectorsAndElectronics/icepap

Erik Bergbäck Knudsen (EK), Research Engineer, Technical University of Denmark, was working part time with IK and MJ on developing the X-ray optics of the beamline using ray tracing in the program McXtrace (Knudsen *et al.*, 2013) during 2016 and 2017.

In 2018 the group should be expanded by a mechanical engineer (0.5-1 FTE). The group may be expanded by a software engineer later in the project.

Several other personnel resources are available at MAX IV for e.g. heat load modeling, insertion device modeling, front end design, radiation protection, survey and alignment, computer hardware and software, technical drawings, etc. The use of MAX IV resources is managed through the beamline project office (BPO).

The DanMAX steering group currently consist of Christoph Quitmann (MAX IV), Yngve Cerenius (MAX IV), NN (MAX IV), Henning Friis Poulsen (DTU), Bo Brummersted Iversen (AU), and Kirsten Marie Ørnsbjerg Jensen (KU). The steering group is the ultimate decision-making body of the DanMAX project.

The Danish user communities have formed the DanMAX consortium, which acts as a reference group securing that the strategic and scientific focus of the user communities is prioritized. The board of the DanMAX consortium currently consists of Dorthe Posselt (RUC), Henning Friis Poulsen (DTU), Bo Brummersted Iversen (AU), and Kirsten Marie Ørnsbjerg Jensen (KU). A member representing the industry will be selected in the future.

In the operations phase there will be 2 beamline scientists and two other FTEs (Postdocs / Technicians) hired by DTU and AU.

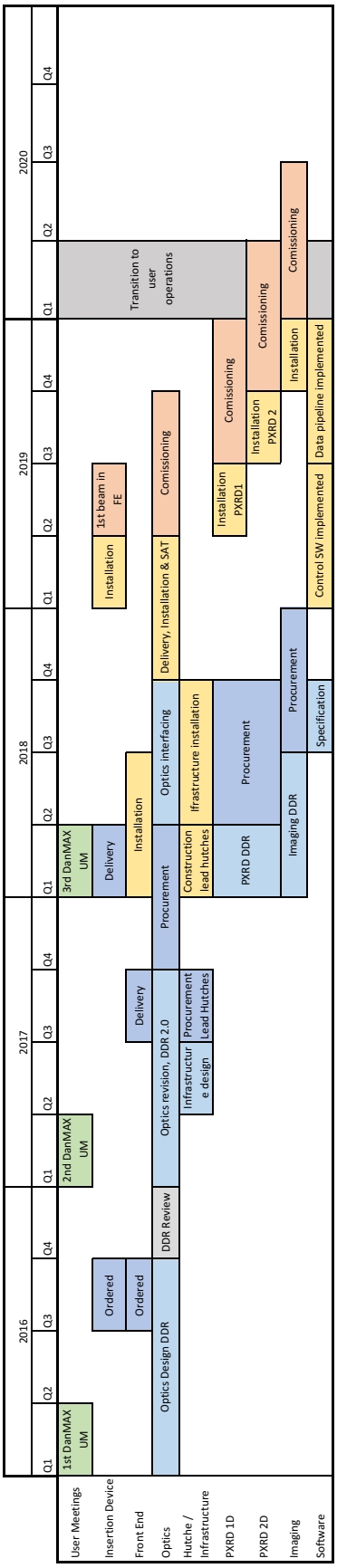

Table 5 Overview of the DanMAX project.

14. Budget

The total budget of the DanMAX is 78 M DKK plus 25 M SEK contributed by the various sources. The contributions are listed in Table 6. The budget for the construction of DanMAX is show in Table 7.

Table 6 Contribution sources to the DanMAX project

Source	M DDK	M €*
Danish Agency for Science, Technology and Innovation	35	4.6
Capital Region of Denmark	12	1.6
Central Denmark Region	6	0.8
MAX IV	18.7 / 25 M SEK	2.5
DTU	9.5	1.3
AU	9.5	1.3
KU	6	0.8
Total	96.9	12.7

* Assuming exchange rates of 100 € = 744.56 DKK and 100 SEK = 75.018 DKK

As the detailed design of the experimental station and the instruments themselves are not yet finalized the budget presented here is not very specific.

Table 7 Preliminary budget for DanMAX

Description	M€
Insertion device	1.23
Front end	0.45
Optics	1.64
End Station	4.31
Diffraction instruments	*2.21*
Imaging instrument	*2.02*
Infrastructure and hutches	2.46
Staff	0.84
Software & Computing hardware	0.70
Contingency	0.82
Total	12.7

15. References

Gundlach, C., Poulsen, H. F., Jørgensen, M. R. V. & Iversen B. B. (2014). "Conceptual Design Report for DANMAX –In situ materials studies in the 10-35 keV range using powder X-ray diffraction and full field imaging", Nov. 2014.

Knudsen, E. B., Prodi, A., Baltser, J., Thomsen, M., Willendrup, P. K., Sanchez del Rio, M., Ferrero, C., Farhi, E., Haldrup, K., Vickery, A., Feidenhans'l, R., Mortensen, K., Nielsen, M. M., Poulsen, H. F., Schmidt, S. & Lefmann, K. (2013). *J. Appl. Cryst.* **46**, 679-696.

Kristiansen, P., Johansson, U., Ursby, T. & Jensen, B. N. (2016). *J. Synchrotron Rad.* **23**, 1076-1081.

Sánchez del Rio, M. & Dejus, R. J. (2011) Proc. SPIE 8141, 814115.

Tanaka, T. & Kitamura, H. (2001). *J. Synchrotron Rad.* **8**, 1221-1228.

Windt, D. L. (1998). *Comput. Phys.* **12**, 360-3.

Appendix A. Insertion Device

A.1. Choice of Undulator Technology A-1
A.1.1. Undulator technologies available A-2
A.1.2. Comparison of IVU and CPMU A-3
A.1.3. Conclusions A-4
A.2. References A-4

A.1. Choice of Undulator Technology

According to the scientific goals of DanMAX, the insertion device should provide the highest possible photon flux in hard X-ray range, i.e. the aim has been to optimize the ID design to yield at the highest possible flux at 35 keV (the highest operation energy). The DanMAX beamline will utilize the achromat 4 straight section at the MAX IV 3 GeV storage ring, which has a length of 4.3 m. Significant dips in the spectrum are acceptable, the beamline will not be used for spectroscopy and a monochromatic beam of ~0.01%-2% bandwidth (FWHM) is required. Additionally, preference was given to a choice of technology that pose a low technical risk and operational costs were considered.

To maximize the flux most of the straight section will be used, leaving room only for essential infrastructure at each end. The maximal feasible magnetic length is approximately 3 m. With a magnetic array length of 3 m the minimal physical gap is 3.8 mm and minimal magnetic gap is 4.0 mm. To increase the peak field, it is necessary to use a small gap, and thus, the device needs to be in vacuum.

The electron energy of MAX IV is 3 GeV and thus 35 keV radiation is only available from the higher harmonics from the undulator (~11^{th}-19^{th} depending on design). For these high harmonic numbers the phase errors reduce the peak brilliance significantly (see Table A.1.1) e.g. for the 11^{th} harmonic the brilliance can be doubled by decreasing the phase error from 5 degrees to 2.5 degrees. Therefore, the phase errors need careful consideration.

Table A.1.1 Expected peak brilliance ratio due to RMS phase errors calculated using the expression, $R = \exp(-n^2\sigma^2)$, where n is the harmonic number and σ is the RMS phase error in radians (Walker, 2013).

Harmonic number	RMS phase error (deg)					
	2	2.5	3	3.5	4	5
1	99.9	99.8	99.7	99.6	99.5	99.2
3	98.9	98.3	97.6	96.7	95.7	93.4
5	97.0	95.4	93.4	91.1	88.5	82.7
7	94.2	91.1	87.4	83.3	78.8	68.9
9	90.6	85.7	80.1	73.9	67.4	54.0
11	86.3	79.4	71.8	63.7	55.4	39.8
13	81.4	72.5	62.9	53.2	43.9	27.6
15	76.0	65.2	54.0	43.2	33.4	18.0
17	70.3	57.7	45.3	34.0	24.5	11.1
19	64.4	50.3	37.2	26.0	17.2	6.4

A.1.1. Undulator technologies available

Three in-vacuum undulator technologies are available at present: permanent magnets at room temperature, permanent magnets at cryogenic temperature and superconducting magnets.

Superconducting undulator (SCU)

Superconducting undulators are a fairly new development, which can deliver higher peak fields compared to other technologies. However, at present the technology is only on a prototype stage and the devices built so far are quite short. If a 3 m long device were to be build the phase error is expected to be quite large. In addition to high technical risk the running cost of a SCU is expected to be high due to the use of liquid helium to keep the superconducting coils at 4.2 K. In addition, there is a risk of quenching the SCU which could damage the device.

In-vacuum permanent magnet undulator (IVU)

An IVU is the least technically complex device in this list, and is a proven technology. It is also the technology used at other MAX IV beamlines, e.g. NanoMAX & BioMAX. Nevertheless, the length of the device (3 m) combined with the short period lengths (16 mm) and the very small gap (4 mm) does pose some significant technical challenges. The designs considered here are of the hybrid type with NdFeB magnets and Vanadium Permendur poles. For a 3 m long device it is estimated that the phase error is ≤ 2.5 degrees.

Cryogenically cooled permanent magnet undulator (CPMU)

For some magnetic materials, e.g. NdFeB and PrFeB, both the remanent field and the coercivity increase as temperature decreases. Therefore, it is possible to increase the peak magnetic field and to decrease the undulator period. Cryogenic cooling of the magnetic arrays also has a positive impact on the radiation resistance of the magnetic material.

Much of the mechanics of the CPMUs are identical to an in-vacuum PMU except for the cooling system which is often comprised of closed cycle refrigerators or pulse tube cryocoolers with copper braids to couple the magnetic array and the cold heads. It is not possible to quench the device. The added complexity of the device does pose an increased technical risk and it does increase the cost of both the device (~130% of the cost of a similar PMU), the running cost (~10.000€/year) in addition to the maintenance of the cryosystem. The designs considered here are similar to the IVUs, i.e. NdFeB magnets and Vanadium Permendur poles, however, the due to the increased coercivity the undulator period is smaller.

The CPMU devices built and installed so far are shorter than the 3 m magnetic length envisioned here. Experience has shown that the phase errors increase when cooling down due to thermal expansion, although in some cases it has been possible to adjust the magnetic array to obtain phase errors as low as the ones expected for room temperature IVUs. For a 3 m long device it is estimated that the phase error is ≥3.0 degrees at low temperature.

In order to avoid the high risks associated with a superconducting device, we restricted the detailed technical to a comparison between a standard in-vacuum undulator and a cryogenic permanent magnets undulator.

A.1.2. Comparison of IVU and CPMU

The following section compares two reference undulator designs. The preliminary design has been made without correct parameters for e.g. maximal roll-off field and good-field width. The brilliance calculations are performed using SRW (Chubar & Elleaume, 1998). The parameters used in the calculations and the resulting brilliance curves are shown in Table A.1.2 and Figure A.1.1. According to these calculations only a small increase in flux is possible using a CPMU instead of a PMU.

Table A.1.2 Expected properties a IVU16 and a CPMU14 undulator.

	IVU16	CPMU14
Magnetic material	NMX-S41EH+Dy Diffusion/VP	PrFeB
Pole material	Vanadium Permendur	
Magnetic length	3.0 m	
# of periods	187	
Stay-clear gap	3.70 mm	
Magnetic gap	4.05 mm	
Min. remanence @ Temperature	1.24 T @ RT	>1.4 T @ RT
K Effective	1.66	1.55
RMS Phase error (degrees)	2.5	3.5

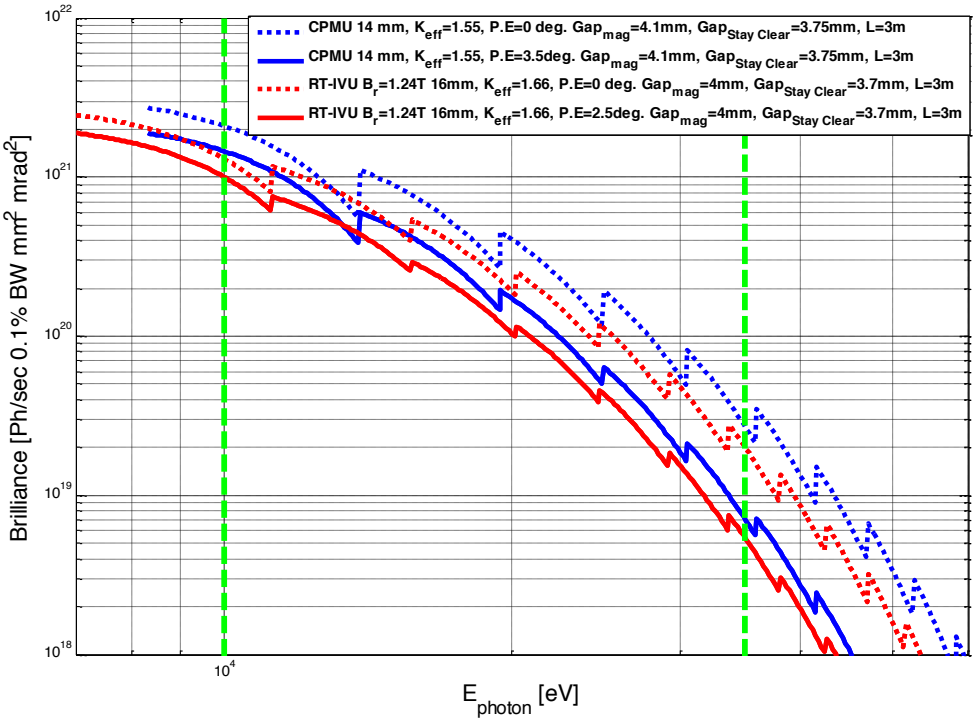

Figure A.1.1 Expected peak brilliance of a IVU16 and a CPMU14 undulator. The values represent the theoretical limit of an ideal device – i.e. without phase errors.

A.1.3. Conclusions

Although CPMUs are becoming more and more common it is still a fairly new technology and thus the technical risk is increased compared to the conservative choice of an IVU. In terms of performance we conclude that the CPMU provides less than a twofold increase in peak brilliance.

Based on the assessment of risk, running costs and peak brilliance at 35 keV it has been decided that DanMAX will utilize an IVU operating at room temperature.

A.2. References

Chubar, O. & Elleaume P. (1998). *Proc. EPAC98 Conf.* 1177-1179.
Walker, R. P. (2013). *Phys. Rev. ST Accel. Beams*, **16**, 01070

Appendix B. Beamline Optics

Contents

B.1. High-pass filter B-1
B.2. Future upgrade: Diamond Laue Monochromator B-4
B.3. Horizontally Deflecting Double Crystal Monochromator B-5
B.3.1. DCM effect on the spectrum B-5
B.3.1. Heat load on the hDCM B-6
B.3.2. Geometrical and mechanical aspects of the hDCM B-7
B.4. Multilayer Monochromator B-9
B.4.1. MLM effect on the spectrum. B-12
B.4.2. MLM effect on beam shape (divergence). B-15
B.4.3. Geometrical and mechanical aspects of MLM. B-17
B.5. Higher Harmonic Contamination B-19
B.5.1. Alternative HH rejections methods B-22
B.6. Transfocator B-22
B.6.1. Beyond the optics hutch transfocator. B-30
B.7. Slits B-33
B.8. McXtrace model used in the simulations B-33
B.9. Alternative optical solutions considered B-35
B.10. References B-39

B.1. High-pass filter

To decrease the heat load on the first optical element a single crystal diamond filter is placed at the upstream end of the optical hutch (OH). To minimize risks to the downstream optics the filter is fixed and not movable. There are no windows between the vacuum of the optical components and the machine vacuum. To handle the heat load, the maximum front end aperture will be limited to 35 x 35 µrad^2 (0.7 x 0.7 mm^2 at 18.7 m from the source). Opening the front end aperture to the maximal aperture of 100 x 100 µrad^2 will likely damage the diamond filter.

Physically two separate windows would be used – first one with the thickness of 0.6 mm and second one with 0.4 mm. The main idea behind it is that during the proposed beamline upgrade the second window will be replaced by a diamond crystal in Laue geometry with the same thickness, so that overall absorption of the direct beam is not affected.

The left panel of Figure B.1.1 shows a total transmission of 1 mm thick diamond window, and the right panel shows photon flux through a 0.7 x 0.7 mm^2 aperture before and after 1 mm of diamond. The flux loss at 15 keV is below 25%.

When the movable FE mask is set to 0.7 x 0.7 mm^2 (normal working conditions), the maximal total power transmitted through this aperture is about 131 W, and more than half of it (68 W) is absorbed in the first 0.6 mm thick window, generating a very high heat stress. A heat transfer finite

element simulation was performed using the COMSOL package in order to simulate the diamond window performance.

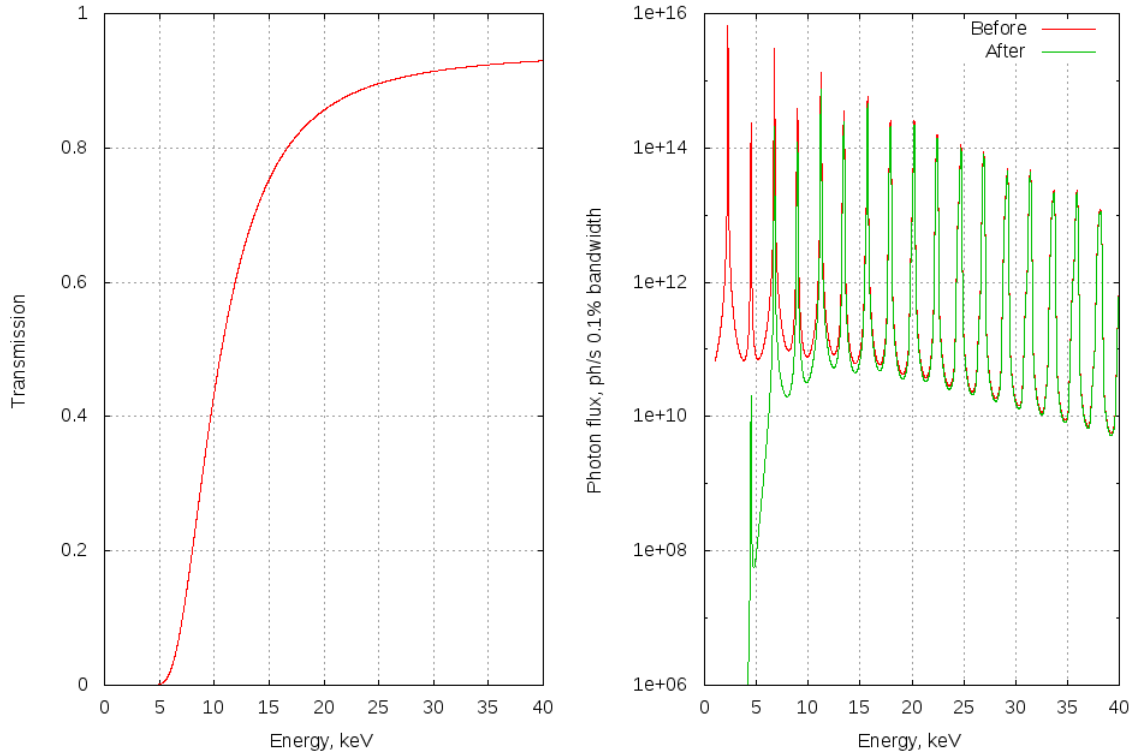

Figure B.1.1. Left – total transmission of a 1 mm thick diamond window. Right – calculated flux before (red) and after (green) 1 mm thick diamond filter.

The non-uniform heat absorption in a window has been simulated as a stack of four cylindrical volumes inside window (with the thicknesses of 10, 30, 180 and 380 µm), each acting as a 17 W power source. The most critical parameter defining the resulting window temperature is the thermal contact between diamond and water-cooled copper frame. We propose to use a 8 x 8 mm^2 diamond window in contact with a copper frame with a 3 x 3mm^2 clear aperture, which will give 55 mm^2 of contact area on a top surface in addition to the 19 mm^2 on the window edges (Figure B.1.2).

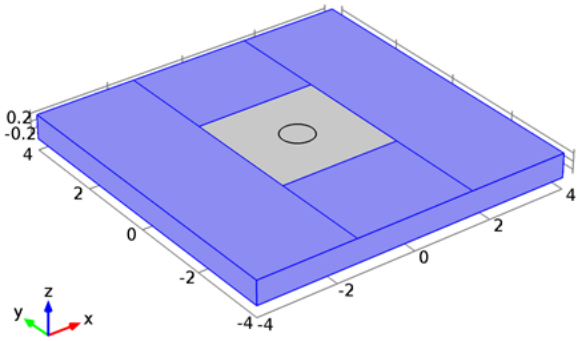

Figure B.1.2. CAD model of the 8 x 8 x 0.6 mm^3 diamond window used in the simulations. Blue color shows contact surfaces to the copper frame.

Figure B.1.3 shows the resulting window temperature, von Mises stress and a heat bump of the first window, assuming a moderate value of 3 $Wcm^{-2}K^{-1}$ for the diamond-copper surface heat transfer coefficient. A thermocouple should be installed on a water-cooled copper frame close to the interface with diamond window in order to monitor the temperature. A simple diode to detect scattered X-rays will be installed close to the window as a simple primary beam presence and intensity diagnostics of the beamline. Heat management of the windows strongly depends on the heat transfer coefficient *h* between diamond and copper frame. For *h* = 3 $Wcm^{-2}K^{-1}$, peak temperature of the diamond window is approximately 380 K; for *h* = 10 $Wcm^{-2}K^{-1}$, diamond window temperature stays below 360 K. The minimal acceptable value of *h* is approximately 0.3 $Wcm^{-2}K^{-1}$, with the corresponding peak temperature of ~660 K.

Although the temperature is relatively high, it is well within safe limits for diamond (Davis & Evans, 1972). Due to very high thermal conductivity in diamond, thermal gradients are very low and the induced heat bump is negligible. It is important that a movable front end mask should never be opened completely with the undulator gap closed. In this situation, the window temperature would rapidly increase to ~3000 K resulting in almost immediate window damage and graphitization. In order to avoid such situation, a hardware PLC interlock with redundant encoders will be installed to prevent undulator gap closure with the movable front end mask open or vice versa.

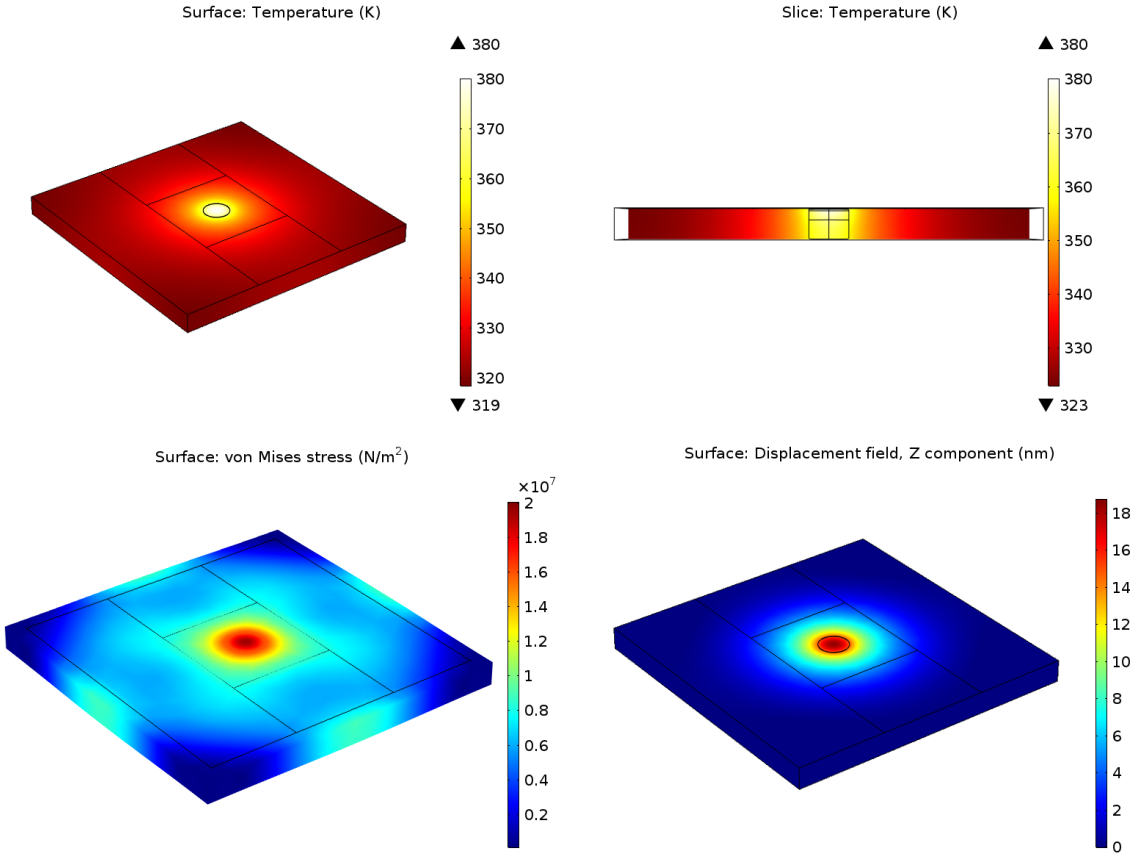

Figure B.1.3. Temperature distribution, von Mises stress and heat bump of the first diamond window with the closed undulator gap and 0.7 x 0.7 mm^2 movable FE mask aperture. Total power absorbed is 70 W.

The second 0.4 mm thick window absorbs only about 10 watts of power, and the resulting temperature increase is around 10 K.

Using a single-crystal diamond window will ensure that no X-ray scattering on grain boundaries occurs, thus the coherence of the beam should be preserved. The diamond window surface distortion due to the thermal expansion is only few nm, so no effect on the beam divergence is expected.

B.2. Future upgrade: Diamond Laue Monochromator

DanMAX has been prepared (see section 10) to be easily upgradable with an instrument in experimental hutch 2 (EH2). The funding for this upgrade has not been secured and the type of instrument to be installed has also not been determined. The preparations for this future instrument mainly consists of the EH2 radiation safety hutch itself including ventilation and utility installations etc., and the installation of the PSS system. Additionally, rack space has been prepared to ensure easy installation of beamline hardware. The meeting room has furthermore been prepared with extra network ports and electrical outlets to be used as the EH2 control room in the future.

The optics for the EH2 will consist of a diamond 111 Laue crystal which replaces the second high-pass filter and a Ge 220 Brag monochromator. The thickness of the crystal will be similar to the filter thickness, thus ensuring that the power load on the EH1 optics are unchanged.

Detailed simulation, FEA nor ray-tracing, has not been performed for this setup, however, geometrical calculations has been performed to illustrate the layout, see Figure B.2.1.

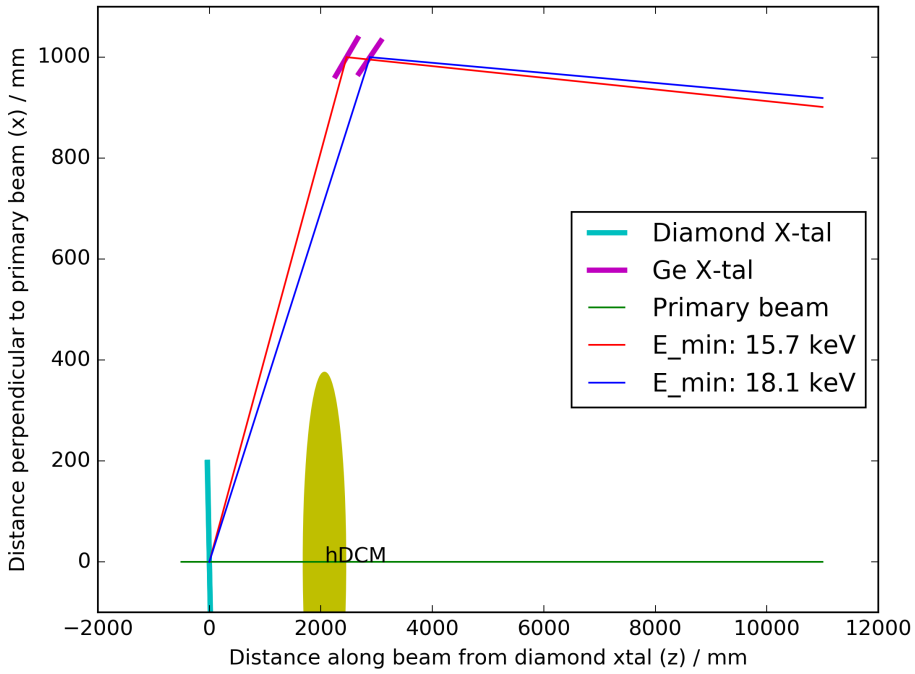

Figure B.2.1. Geometrical representation of the optics and beam path for the EH2. The photon energy, 15.7-18.1 keV corresponds to the 7th harmonic at different undulator gaps. Please note the different scaling of the axis.

The energy difference between the various harmonics of the IVU16 is approximately 2.4 keV and thus the EH2 optics must be able to accept photons in this energy interval to be able to take beam at all undulator gaps. The d-spacing of diamond 111 and Ge 220 is not identical and the mismatch does lead to some challenges as the position of the beam and the incoming angle changes as a function of energy. For a nominal offset of 1000 mm between the beam to EH1 and the beam to EH2 the beam over the 2.4 keV energy interval will shift approximately 17.7 mm in the middle of EH2. The incident angle will change approximately 0.1 degrees. Due to the d-spacing mismatch the real offset between the beams will be decreased to approximately 900 mm. Due to the relatively low photon energy CRLs can efficiently focus the beam. The required beam size will depend on the instrument that will be installed in EH2.

B.3. Horizontally Deflecting Double Crystal Monochromator

At conventional synchrotron sources, double crystal monochromators (DCMs) are typically employing a vertical scattering geometry. The primary reason for this is due to the higher energy resolution in this direction caused by smaller vertical divergence compared to the larger horizontal divergence. The horizontal extent of the MAX IV source is greatly reduced and thus the energy resolution using a horizontal geometry is nearly as high as a vertically deflecting geometry. A horizontally deflecting geometry is especially attractive as it can be made more rigid, thus less prone to vibrations. Additionally, there are no gravitational forces working on the rotation of the crystals. A drawback to this geometry is the loss of reflected intensity due to the P-polarization of the undulator radiation. However, this effect small at the working energy of DanMAX and will only cause a loss of 13% at 15 keV and decreasing to only a 2.5% loss at 35 keV. Both NanoMAX and BioMAX have chosen a similar solution and preliminary tests and results are promising (Kristensen *et al.*, 2016).

B.3.1. DCM effect on the spectrum

Silicon is produced as nearly perfect single crystals. The performance of silicon DCM is thus usually defined by the natural Darwin width of silicon, X-ray beam divergence and monochromator geometry. Due to the small beam divergence of the MAX IV source, virtually no compromise between energy resolution and DCM throughput is required, as well as any pre-condensing of the beam. Figure B.3.1 shows a part of DuMond diagram for Si (111) reflection at 20 keV.

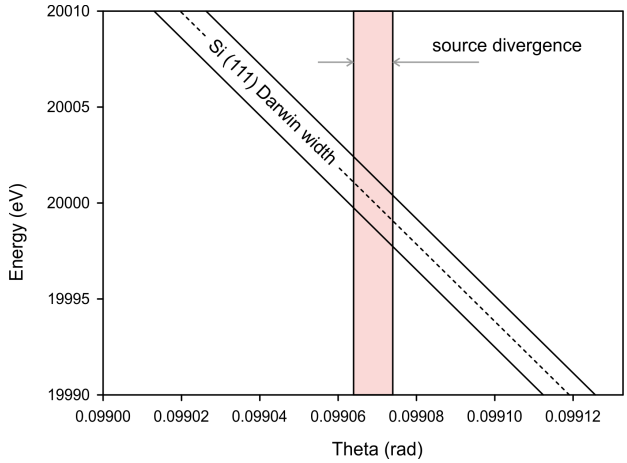

Figure B.3.1. A section of DuMond diagram for the Si (111) reflection around of 20 keV. X-ray beam divergence (RMS) is almost perfect match to the Darwin width of silicon crystal.

The performance of the monochromators has been modeled using MASH (Sondhauss, 2014) a front end for the ray tracing software SHADOW3 (Sanchez del Rio *et al.*, 2011) and the finite element model software COMSOL. The simulation is iterative where the incident photon source is modeled using URGENT (Walker & Diviacco, 1992) and this beam is propagated to the first optical element using Shadow3. The thermal deformation of the first optical element is modeled in COMSOL. The deformed model is used in the subsequent simulations. The three operation modes of DanMAX has been simulated, both with (case #2) and without (case #1) thermal deformation. The details from the simulations have been plotted for 11.25, 15, 25, and 35 keV. The 11.25 keV case is included as this corresponds to the minimum undulator gap (4 mm) and thus, represents a worst case with respect to incident power and thus, thermal deformation. The full details of the simulations can be found in a separate document (Sondhauss, 2016).

The expected energy spread (resolution) obtained with the SHADOW3 ray tracing simulations is shown in Figure B.3.2. This energy resolution obtained with the Si (111) reflection, $\Delta E/E < 10^{-4}$ (RMS), is well suited for the experiments foreseen at DanMAX.

B.3.1. Heat load on the hDCM

The hDCM is the first active element of the beamline and is a high heat load monochromator. Total X-ray beam power received by the DCM is as high as 70 W, and due to a relatively small footprint at low energy, the beam power density can reach 2 kW/cm^2 (Figure B.3.3). At higher energies with more shallow diffraction angles, the beam footprint increases and the power density decreases correspondingly. At 35 keV the power density has decreased to approx. 550 W/cm^2.

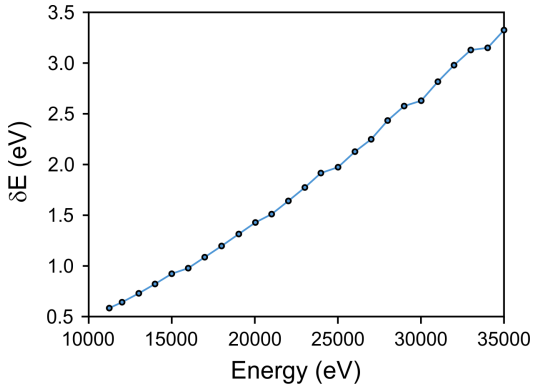

Figure B.3.2. Simulated energy resolution (RMS) of the Si (111) double crystal monochromator.

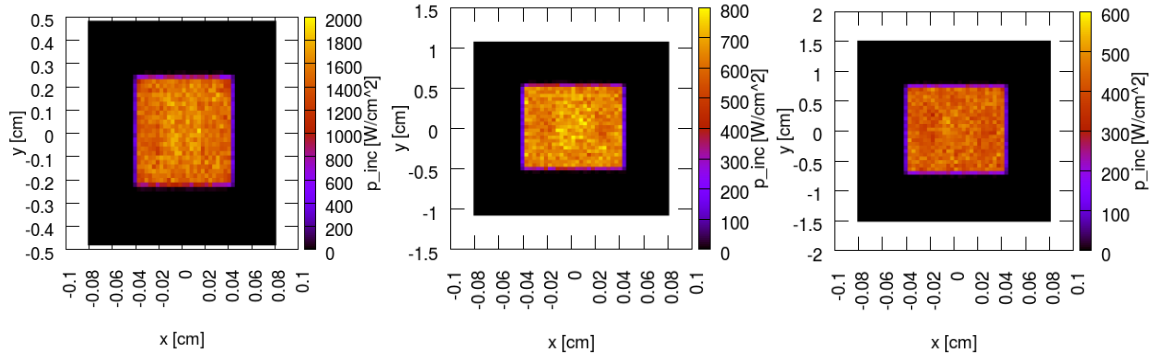

Figure B.3.3. Deposited beam power density on the first monochromator crystal at 11.25 (left), 25 keV (center) and 35 keV (right). Note the difference in vertical scale.

The active liquid nitrogen cooling on the sides of the first crystal should have enough total cooling power, and thanks to the high thermal conductivity of silicon at nitrogen temperature power density is also not a problem. Temperature gradients on the surface of the crystal do not exceed 10 degrees (Figure B.3.4).

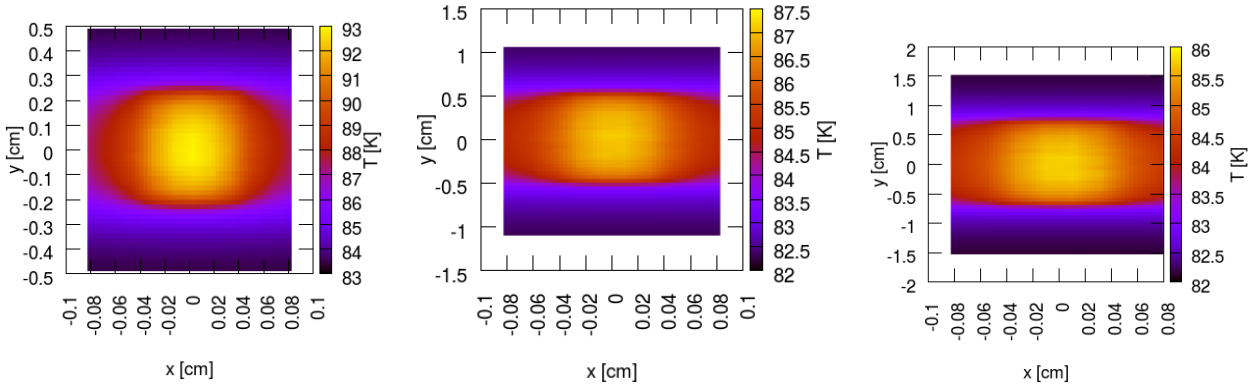

Figure B.3.4. Surface temperature distribution of the first DCM crystal for 11.25 (left), 25 (center) and 35 (right) keV.

Silicon has a negative thermal expansion coefficient around 90K, therefore thermal load of the beam generates a negative (concave) curvature deformation of the first crystal, and DCM performs as a slightly focusing device. The surface curvature error of the first crystal changes from ~1 x 10^{-5} cm^{-1} to about ~1 x 10^{-6} cm^{-1}. The resulting X-ray beam divergence decrease in the sagittal (vertical) direction is negligible, while in the meridional (horizontal) direction is noticeable at energies below ~30 keV (Figure B.3.5).

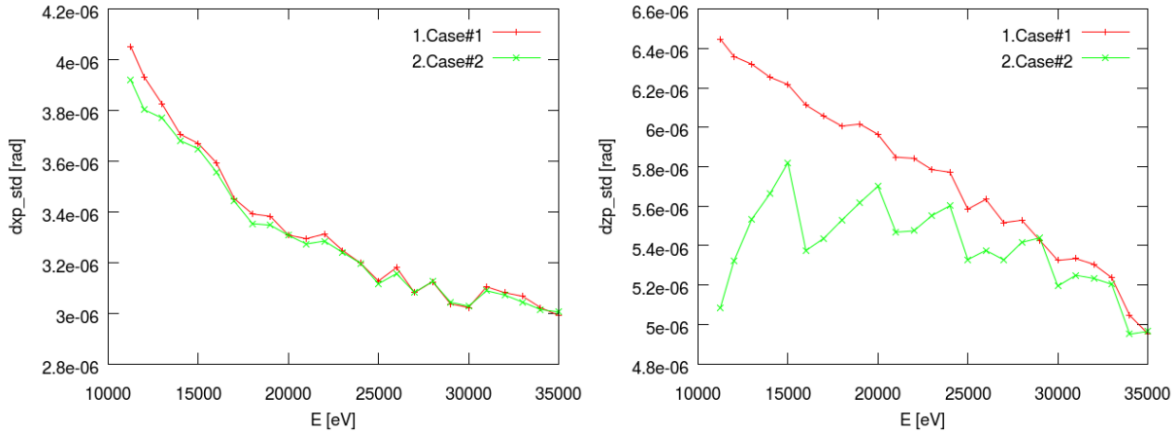

Figure B.3.5. X-ray beam divergence (RMS) after the hDCM with no thermal deformation (case#1, red curves) and with the thermal deformation (case#2, green curves) of the first silicon crystal. Left is for sagittal (vertical) and right is for meridional (horizontal) directions.

B.3.2. Geometrical and mechanical aspects of the hDCM

The monochromator is a Bragg-Bragg horizontal reflection double-bounce device with a (+,-) parallel setting (non dispersive) and symmetrically cut crystals. The hDCM will be a fixed exit monochromator, and the principal mechanical design is very similar to the devices installed on BioMAX and NanoMAX beamlines at MAX IV.

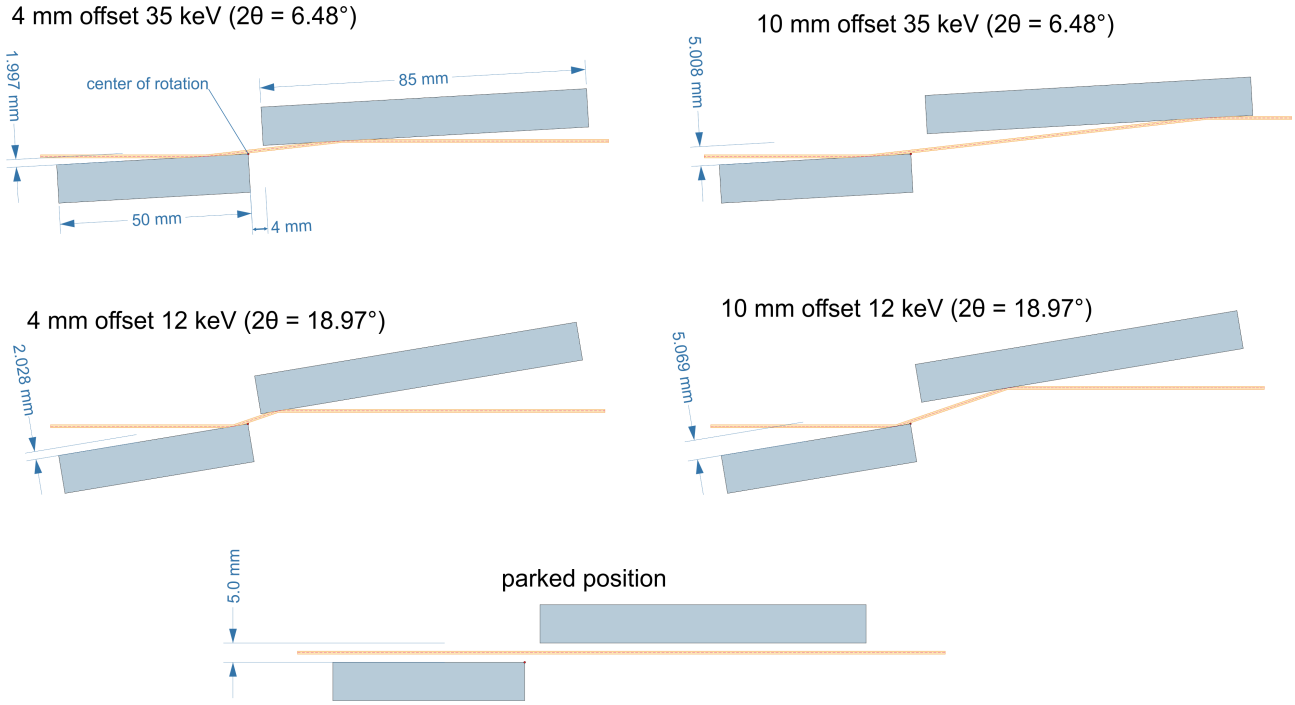

Figure B.3.6. Geometry of the double crystal monochromator at different energies and beam exit offsets. The 2θ value is show in parenthesis. Actual proportions are compliant.

The angular range (~3.2 – 9.5 degrees) of the hDCM is relatively small, however, an additional complication comes from the fact that hDCM should be able to adopt two different fixed offsets; 4 and 10 mm (Figure B.3.6). With the two crystals lengths of 50 and 85 mm no crystals translation along the beam (Z-direction) is required, but as additional horizontal (X-direction) translation of few millimeters for the second crystal should be used in order to accommodate the offsets (see Figure B.3.6). The movement mechanics is virtually similar to that of the regular fixed exit monochromators.

Piezo actuators for fast and fine adjustments of the first crystal roll and the second crystal yaw are required to maintain a perfect parallelism of two crystals within 0.2 µrad and fine tuning of the vertical beam position. The whole device should fully comply with the general MAX IV standards, e.g. for vacuum (UHV, $P < 5 \times 10^{-9}$ mbar), mechanical stability (all eigenfrequences must be kept above 55 Hz, if possible), electrical standards, and alignment requirements. The mechanical design of DCM is left to the vendor, and the required parameters for the motorized movements to be incorporated to the DCM are given in Table B.3.1.

Table B.3.1 Preliminary motion specifications for the hDCM.

Translation	Parameter	Specifications
Yaw (Ry)* main reflection angle (whole cage)	range resolution repeatability	0 – 200 mrad <2 µrad <1 µrad
Yaw (Ry) fine adjustment (second crystal)	range resolution repeatability	150 µrad ≤.01 µrad ≤.05 µrad
Pitch (Rx) whole cage	Range resolution repeatability	±2 mrad <2 µrad <1 µrad
Roll (Rz) coarse adjustment (first crystal)	range resolution repeatability	±10 mrad <8 µrad <2 µrad
Roll (Rz) fine adjustment (first crystal)	range resolution repeatability	150 µrad ≤.01 µrad ≤.05 µrad
Lateral translation (Tx) whole cage	range Resolution repeatability	± 10 mm <1 µm <2.5 µm
Lateral translation (Tx) second crystal*	range resolution repeatability	-0.5 – +6.5 mm <1 µm <2.5 µm

*Second crystal is translated relative to the first one inside vacuum chamber.

B.4. Multilayer Monochromator

Multilayer X-ray mirrors (ML) are widely used for two main reasons. Firstly, when used at a grazing angle geometry, they provide extremely high reflectivity with a sharp high-energy cutoff at much higher incidence angles then a usual total reflection mirror. Therefore, ML can be much shorter for the same beam acceptance, or they can accept much larger beam for the same length. Secondly, the reflectivity curve of ML has a sequence of relatively narrow reflectivity bands caused by their periodic structure. These bands can be used to create a low energy resolution and high throughput X-ray multilayer monochromator (MLM). At DanMAX a double bounce multilayer mirror will perform two tasks: in the high flux mode, mainly demanded by time resolved imaging applications, it will work as a broadband fixed exit monochromator, and in the high resolution mode (when paired to the silicon DCM) it will work as a higher harmonic rejecting device. The ML performance presented in this section has been calculated using the IMD program (Windt, 1998).

Most widely used for hard X-rays ML material pairs are B_4C/Mo, B_4C/W and B_4C/Ni (for manufacturing reasons nickel coating contains 6-7% of vanadium for magnetism suppression). Since the Mo K-edge (20 keV) falls in the DanMAX energy range, tungsten was chosen as the primary high-Z coating material.

The emission spectrum of the DanMAX undulator naturally consists of a relatively sharp (ideal value is around 0.6% ΔE/E (FWHM), the actual value can be up to 1.8% at higher harmonics) peaks, and the MM period was optimized to match this value (Figure B.4.1), so that one and only one undulator peak will be transmitted by MLM. Upon the factory acceptance test of the undulator the

actual magnetic field profile has been measured. The expected undulator peak bandwidth is approximately 6×10^{-3} at 15 keV and it increases up to 9×10^{-3} at 35 keV.

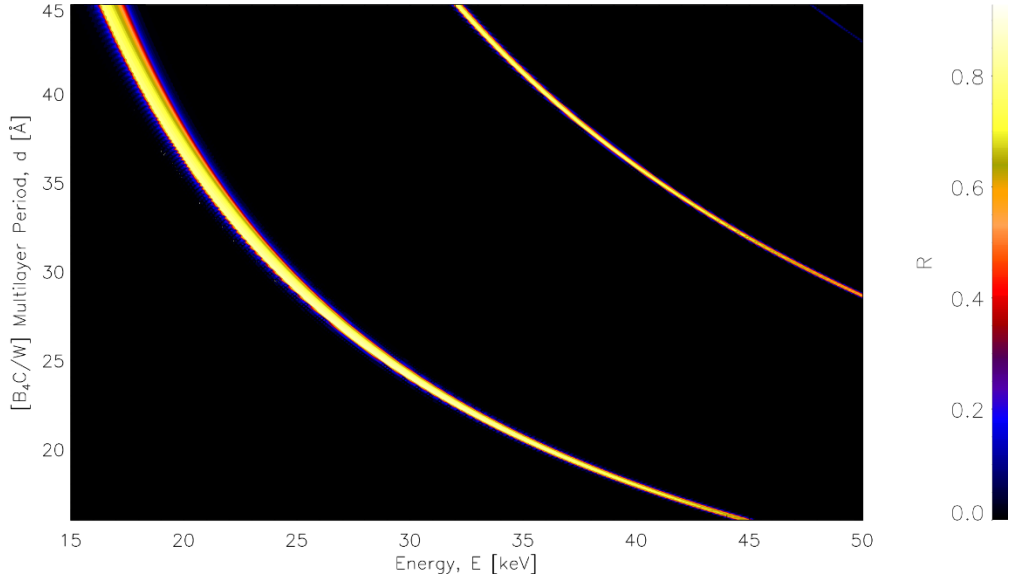

Figure B.4.1 B_4C/W mirror reflectivity at a function of energy and multilayer period (at a fixed incidence angle of 0.5 degrees).

The best match between ML reflectivity and undulator peaks is around 15-18 Å. However, such layer thickness is challenging to manufacture. A reasonable compromise between reflectivity, reflectance angles and the manufacturing process, is a period of 25 Å. This will give a 1.9 – 2.1% ΔE/E (FWHM) transmission.

For some of the experiments at both, imaging and powder diffraction instrument, an intermediate energy resolution would be beneficial, even on the cost of somewhat lower flux. This can be obtained using a second multilayer coating with smaller period. $B_4C/Ni_{0.93}V_{0.07}$ coatings with a 20 Å period is successfully used for similar purpose at the ESRF ID01.

An optimized (for the intermediate photon energy of 25 keV) layers thickness ratio was found to be 0.8 for W and 0.65 for Ni coatings (Figure B.4.2). The number of periods affects the ML efficiency as well, and the optimal number of bilayers is around 200 for W coating, while Ni coating with smaller period requires 400 bilayers (Figure B.4.3). The resulting optimized ML reflectivity functions for the whole range of energies and incidence angles are shown in (Figure B.4.4).

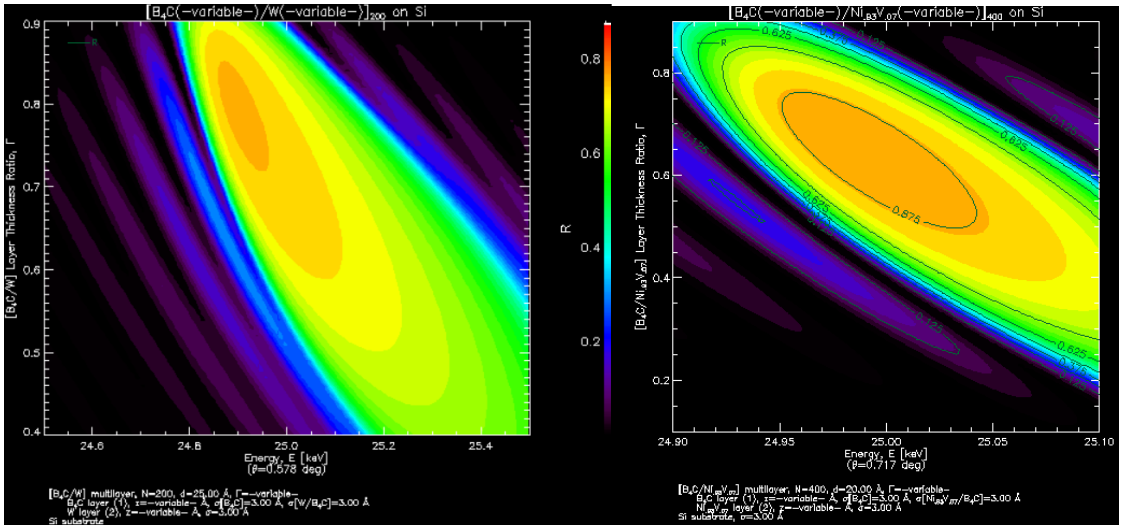

Figure B.4.2 Optimization of the layers thickness ratio for B_4C/W (left) and $B_4C/Ni_{0.93}V_{0.07}$ (right) coatings for *E*=25 keV.

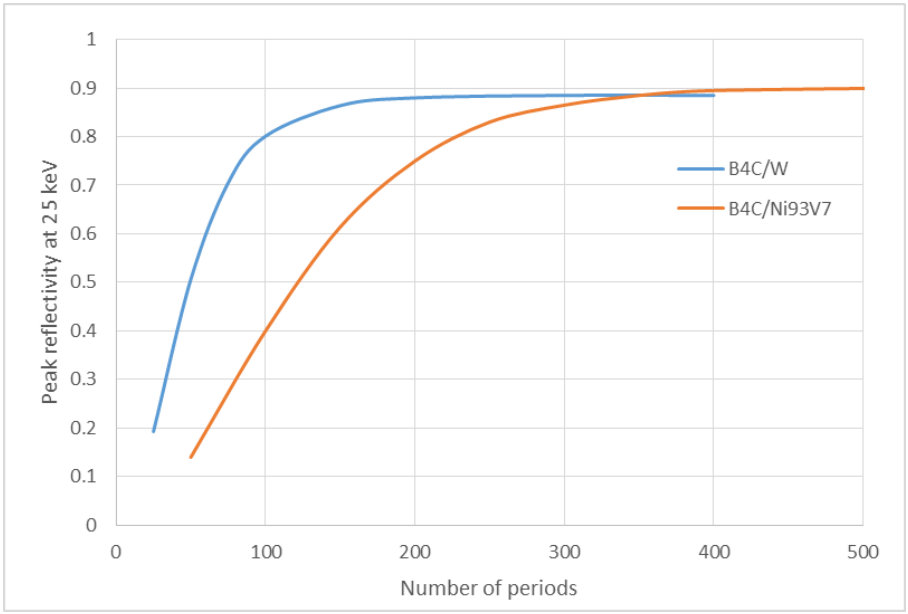

Figure B.4.3 Peak ML reflectivity at 25 keV for two different ML coatings as a function of number of bilayers. Blue is for B_4C/W, and orange is for $B_4C/Ni_{0.93}V_{0.07}$.

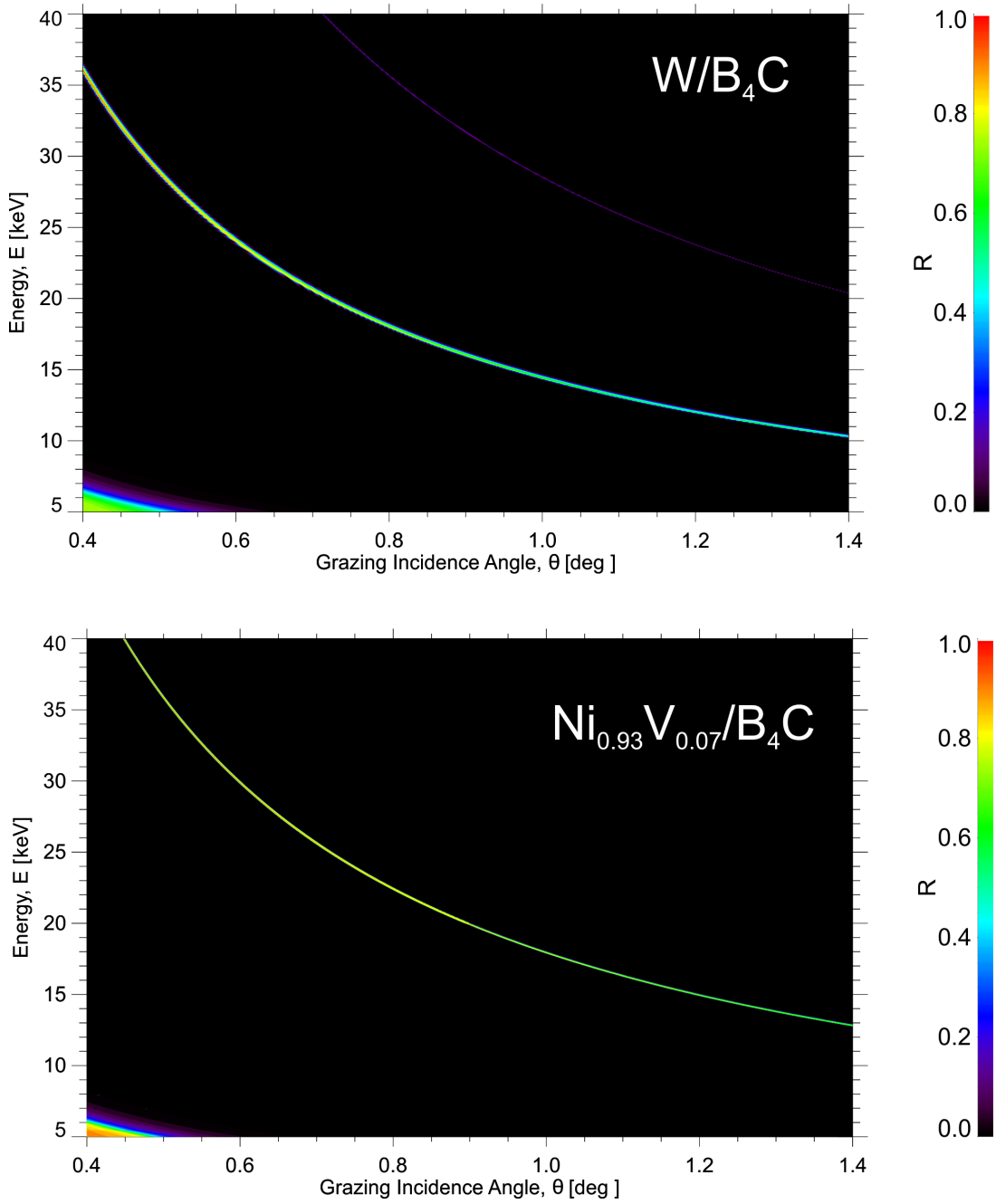

Figure B.4.4. Multilayer reflectivity for two different coatings proposed here.

B.4.1. MLM effect on the spectrum.

Since the rocking curve of the ML is significantly larger than the X-ray beam divergence, the effect of the double mirror system on the X-ray spectrum depends solely on its reflectivity. Figure B.4.5 shows the simulated X-ray spectrum for different incidence angles, optimized for the 5^{th}, 7^{th}, 9^{th}, 11^{th} and 13^{th} undulator harmonic with the smallest (4 mm) undulator gap. The reflectivity curves were calculated assuming 3 Å RMS mirror roughness and 3 Å RMS layer interdiffusion value.

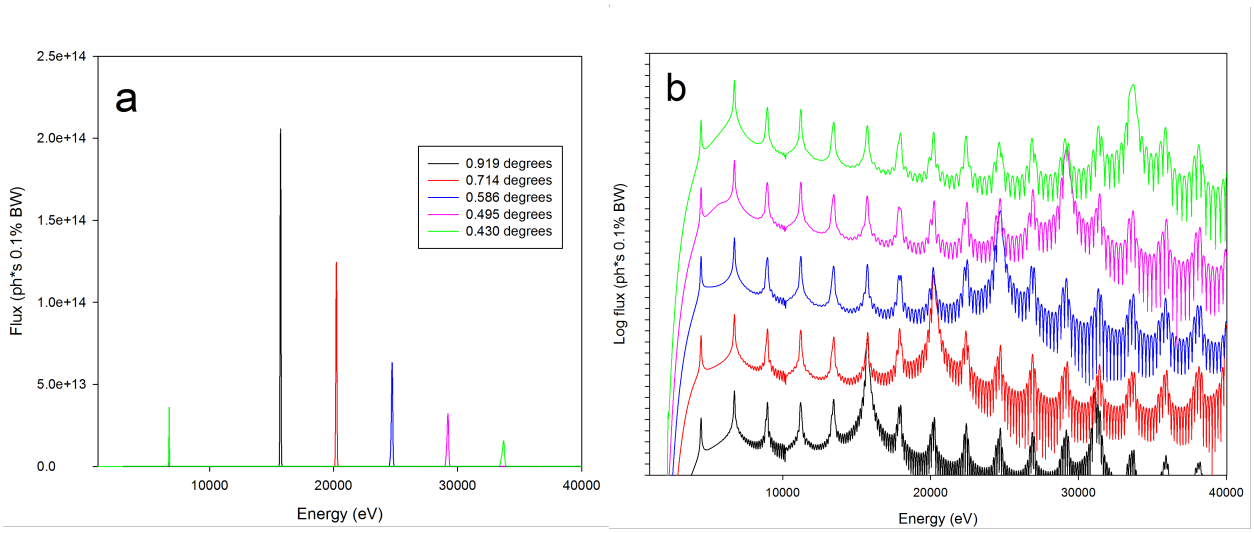

Figure B.4.5 Simulated X-ray spectra after a double-bounce MLM (B_4C/W), set to different incident angles. Left: linear scale. Right: logarithmic scale. Spectra are shifted vertically on the right plot, one tick on vertical scale is one order of magnitude.

As can be seen from Figure B.4.5, the MLM clearly selects a single undulator peak in a full energy range of DanMAX. All unwanted photons are in general suppressed by four to five orders of magnitude (Figure B.4.5b). As the incidence angle falls below ~0.5 degree, a lower energy peak around 6.7 keV becomes more pronounced, and at 34 keV it becomes more intense than a main peak. Under normal experimental conditions these low-energy photons would be completely filtered out by focusing optics and absorbed by the air in the experimental hutch and by the sample. However, they can be potentially preserved all the way to the detector (using vacuum/helium flight tubes in the experimental hutch and avoid CRLs), potentially allowing some special dual energy experiments.

Figure B.4.6 shows the squared reflectivity (to represent reflection from both mirrors) of two ML coatings at different energies (left columns) and the corresponding energy transmission (right columns). The normalized source spectrum is shown as dashed orange curves for comparison, too.

At lower energies, the resulting energy distribution is defined primarily by the source and is very close to a Gaussian. For the high energy part of the spectrum, the undulator harmonic becomes broader and less symmetric with a low energy tail, and the resulting energy profile depends on the selected coating. The spectral X-ray beam characteristics provided by MLM are given in Table B.4.1.

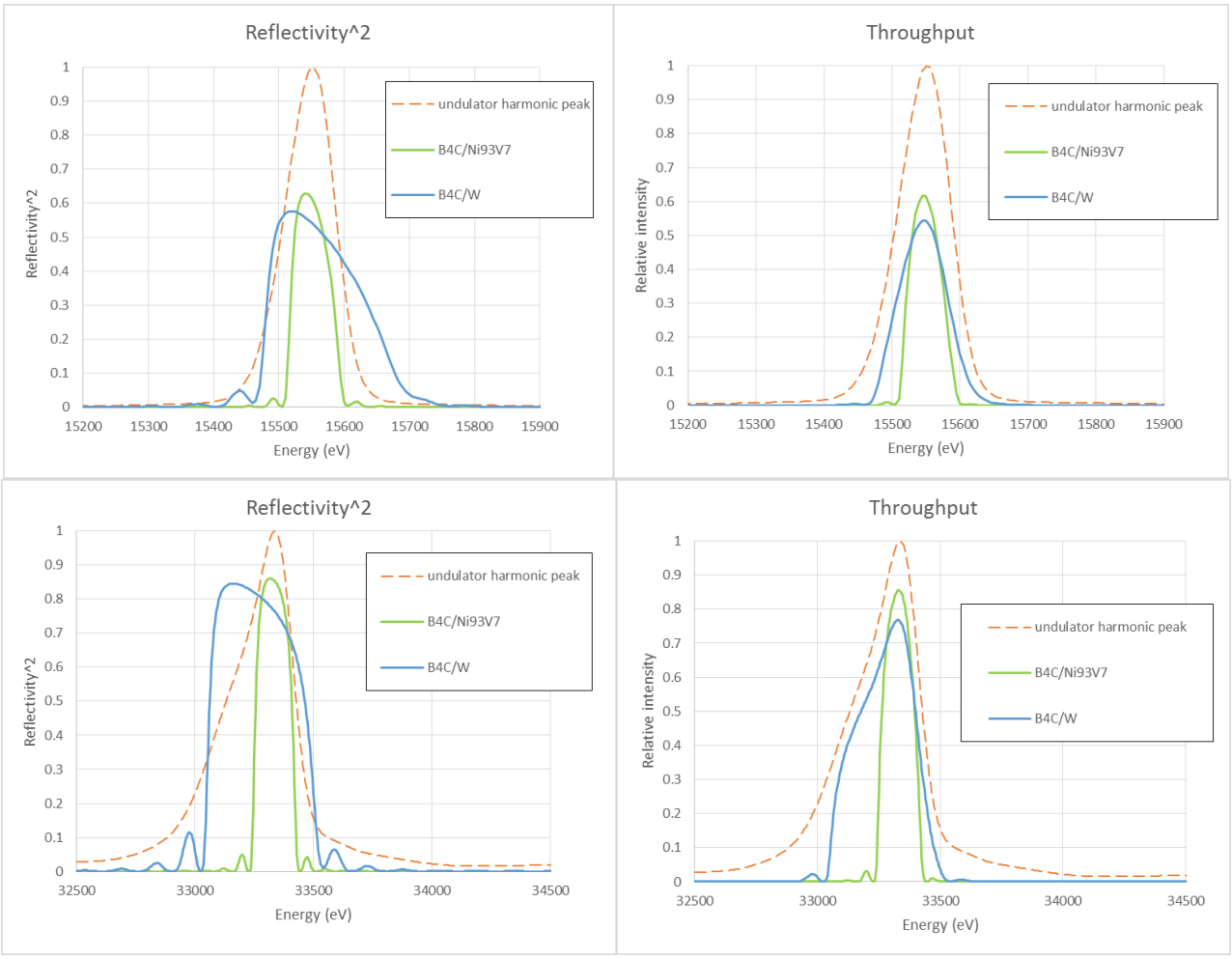

Figure B.4.6. Squared reflectivity of two ML coatings (left) and their resulting throughput spectra (right). Top row corresponds to 15.5 keV, and the bottom to 33.3 keV photon energy.

Table B.4.1. X-ray photons energy band delivered by the multilayer monochromator. Throughput values are given relative to the full undulator harmonic.

Energy (keV)	Harmonic order	Source ΔE (eV)	Source ΔE/E	B_4C/W ΔE (eV)	B_4C/W ΔE/E	B_4C/W Throughput	$B_4C/Ni_{0.93}V_{0.07}$ ΔE (eV)	$B_4C/Ni_{0.93}V_{0.07}$ ΔE/E	$B_4C/Ni_{0.93}V_{0.07}$ Throughput
15.3	7	94	6.1×10^{-3}	81	5.2×10^{-3}	46%	50	3.2×10^{-3}	33%
33.3	15	300	9.1×10^{-3}	304	9.1×10^{-3}	58%	121	3.6×10^{-3}	31%

The second potential use of the MLM is as a high harmonic suppressor for the PXRD experiments. Due to the spectral characteristics of the DanMAX source, the DCM third harmonic (Si (333)) reflection at 47.1 keV has approximately 5 x 10^4 times less photons then the first harmonic (Si (111); 15.7 keV) even without any additional optical elements and monochromator detuning. However, if a better harmonic suppression is required, the MLM can be moved into the beam after the DCM. Harmonic suppression given by MLM is approximately 2 x 10^{-14}, well above any reasonable demands. However, useful photon flux will be reduced by approximately 50% due to the non-ideal ML reflectivity. More details are given in section B.5.

B.4.2. MLM effect on beam shape (divergence).

A perfectly flat X-ray mirror does not affect the X-ray beam divergence. However, the MLM cannot be considered a perfect mirror due to the surface roughness and the thermal expansion bump on the surface caused by the heat load of the beam. The MLM will operate in a horizontal deflection mode and at room temperature (using water cooling at 300 K). The first mirror will be directly water-cooled via side mounted copper blocks, while the second mirror is cooled indirectly via either solid copper heat conductors immersed in a GaIn bath (Figure B.4.7) or flexible copper braids.

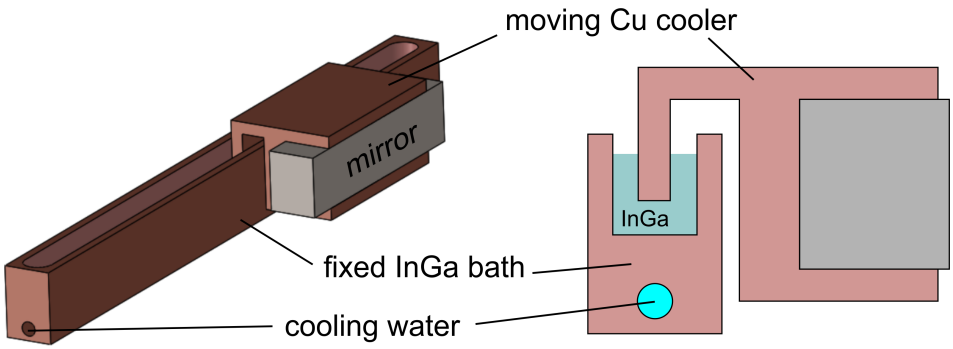

Figure B.4.7 Schematics of the second ML mirror cooling scheme: a long InGa liquid metal alloy bath is water cooled and fixed, while the second mirror with a long horizontal translation is cooled by immersing copper cooler into the bath, without any mechanical coupling.

In a high flux mode MLM is a high heat load optical element. The peak temperature of the first ML is expected to be below 318 K (Figure B.4.8 left), while the second mirror surface should not heat up above 309 K (Figure B.4.8 right). The resulting heat bump of the first mirror is nearly toroidal with a radius equal to about ~1.2 x 10^3 m in sagittal direction and ~1.5 x 10^4 m in meridional direction. As the result, the beam divergence approximately doubles for low energies (up to 20-25 µrad) while at higher energies thermal distortion effect becomes negligible compared to the surface roughness, and at 35 keV beam divergence after MLM is about 17 µrad (Figure B.4.9). For comparison, the intrinsic beam divergence of the undulator at 35 keV is about 10 µrad. The peak mechanical Von Mises stresses in the first mirror are below 3 MPa, i.e. completely safe for the silicon substrate.

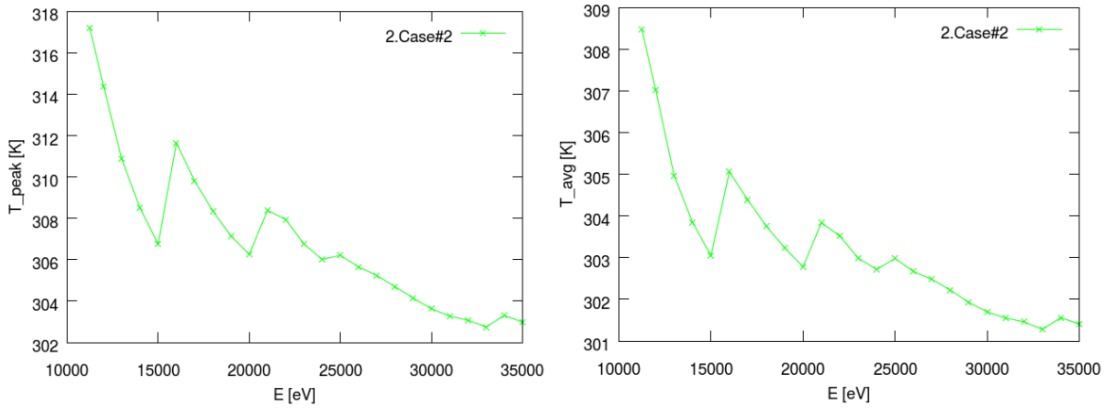

Figure B.4.8 Peak surface temperature of the first (left) and second (right) multilayer mirrors at different energies under high heat load (high-flux mode).

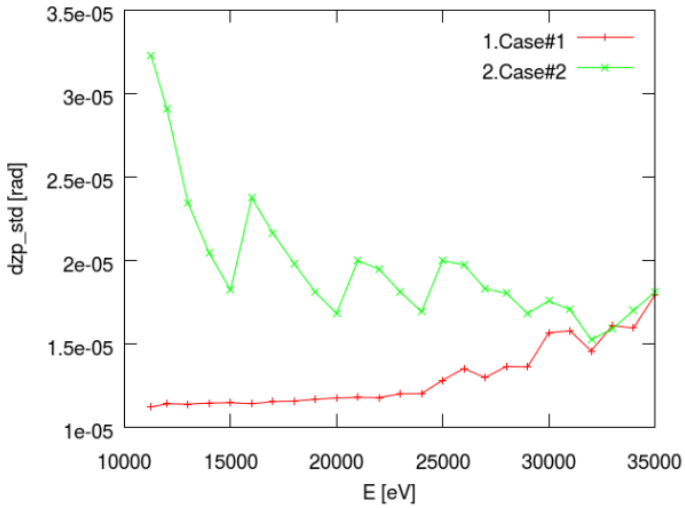

Figure B.4.9 Simulated meridional X-ray beam divergence (RMS) after the MLM in a high-flux mode. Case#1 (red line) is for flat mirror surface, while case#2 (green line) includes thermal bump effect.

Thermal heat bump on the mirror surface, generated by the X-ray beam, can be significantly decreased by optimizing the cooling geometry. The above-mentioned results (as well as the ray tracing simulations in section B.3.1) were obtained for the non-optimized cooling geometry. This is illustrated in the top row in Figure B.4.10. As was demonstrated by Zhang *et al.* (2015), by choosing cooling blocks profiles to match the beam footprint, the resulting thermal deformations are dramatically improved.

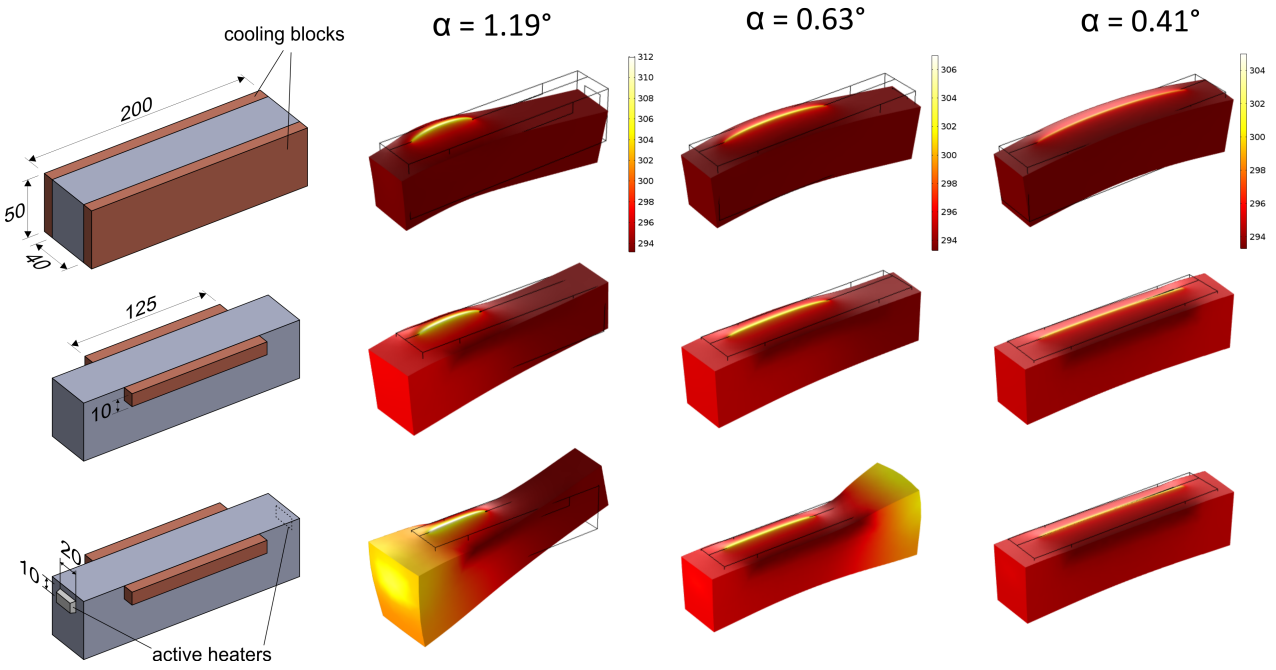

Figure B.4.10 Optimization of the first ML mirror cooling geometry. Top row corresponds to non-optimized cooling, central row – to profile-matching side cooling and bottom row – with the additional active heating. Left column demonstrates the schematic geometry, while other columns show the resulting temperature distribution (shown by the color) and thermal substrate deformation (exaggerated for clarity) for different beam incidence angles, from the highest ($Ni_{0.93}V_{0.07}/B_4C$ @ 15 keV) to the lowest (W/B_4C @ 35 keV).

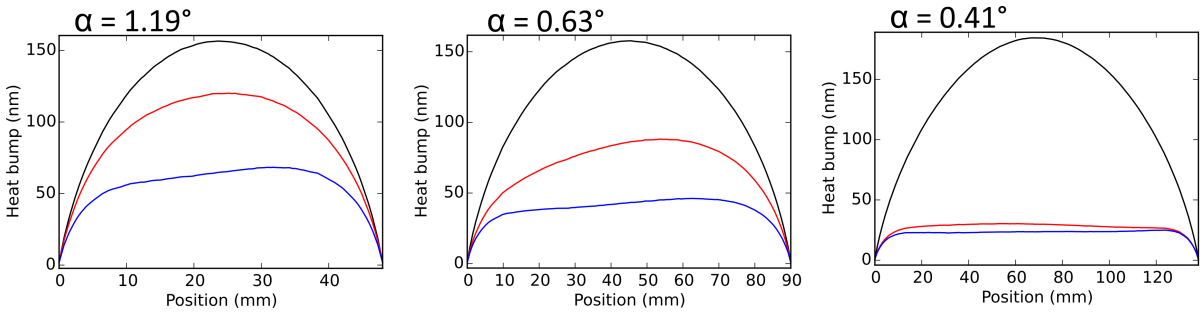

Figure B.4.11 First ML mirror surface Heat bump profiles along the beam for the cases shown in Figure B.4.10. Black curve – non-optimized cooling, red – with the profile-matching cooling, blue – with the additional active heaters.

However, such optimization is possible for a fixed beam footprint, while for lower energies (and thus higher angles and shorter footprints) the distortion is only reduced partially, see middle row in Figure B.4.10.
We propose to add two small (~10x20 mm^2) resistive heaters to the ends of the first ML mirror. By varying the amount of heat, dissipated by these heaters (up to ~25 W) it is possible to control the mirror reflecting surface shape and further reduce thermal bump, at least for the central part. The deformation is illustrated in Figure B.4.10 and plotted in Figure B.4.11.

When used in a high monochromatic mode downstream of the DCM, the heat load on the MLM is negligible, and so is the effect on the beam divergence due to the heat load. The only small increase in divergence results from the mirrors surface roughness.

B.4.3. Geometrical and mechanical aspects of MLM.

The multilayer monochromator would operate in a horizontal deflection geometry, since it provides better mechanical and vibrational stability compared to the vertical beam deflection.
The mechanical design of the MLM is complicated by two factors: firstly, the incidence angles are relatively shallow, and secondly, it needs to operate in fixed offset mode with two discrete offsets (6 and 10 mm). Due to a small X-ray beam size and divergence, the length (along the beam) of each mirror can be as short as 200 mm. At the same time, in order to change the offset from 6 to 10 mm for all energies, the second mirror requires a linear translation of over 500 mm along the beam (Z-direction) in addition to the 4-mm horizontal translation along X. In order to be able to choose between two types of coating, sufficiently long range vertical (Y-direction) translation of the whole monocromator is also required (Figure B.4.12).

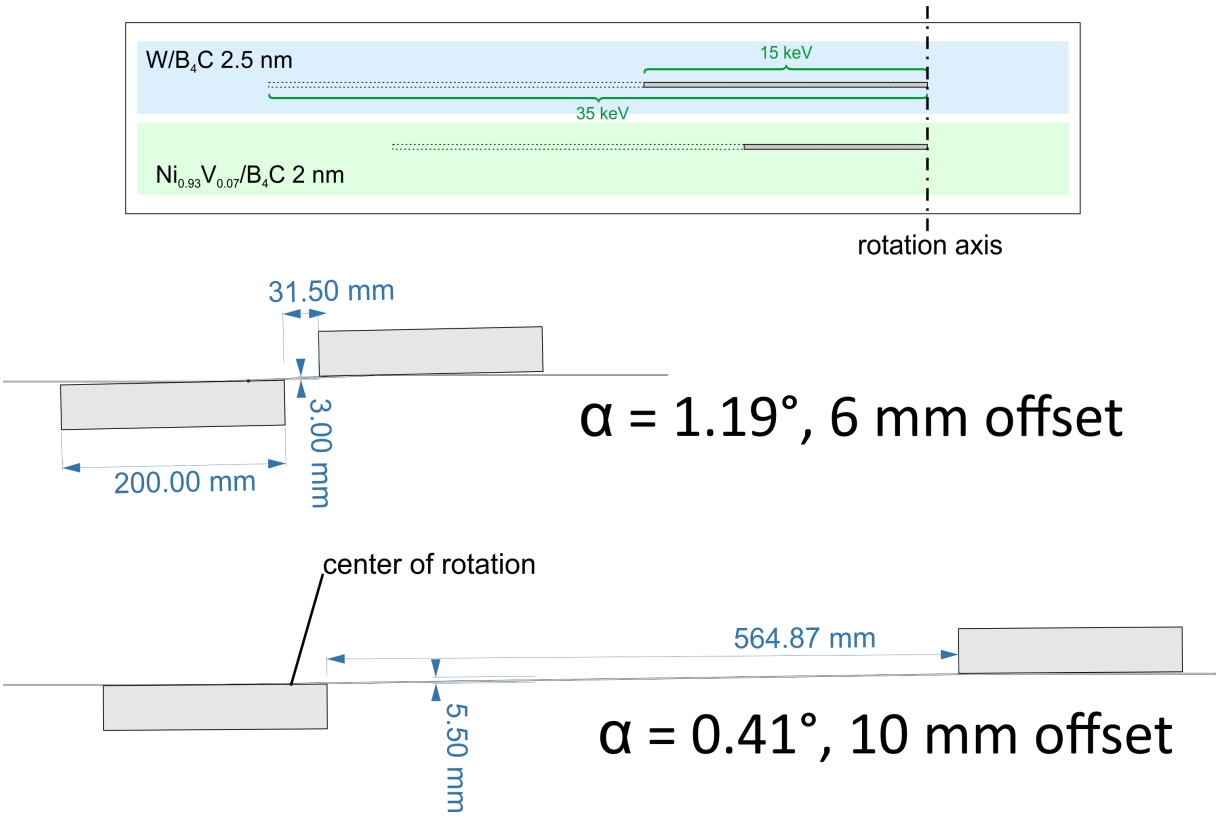

Figure B.4.12 Top: the location of two different coatings at a 200x40 mm^2 mirror front surface, and the corresponding beam footprints for two extreme energies. Bottom: relative position of two mirrors for two extreme cases: 15 keV and $Ni_{0.93}V_{0.07}/B_4C$ coating with a 6 mm offset, and 35 keV and W/B_4C coating with a 10 mm offset. The figure is to scale.

The active (direct) water cooling blocks would be installed on the first mirror, while the second mirror can be cooled either via flexible copper braids or via solid copper heat conductors immersed in a cooled bath of GaIn alloy (Figure B.4.7). The latter option is preferable, since flexible copper braids would bend a lot due to the long mirror translation, and could become brittle due to the effect of work-hardening. Due to the broad rocking curve of the ML, slow thermal drifts of the second mirror would not affect the MLM performance nor the beam position. The detailed mechanical design of the MLM is left to the vendor with the specifications are given in Table B.4.2. The whole MLM assembly is expected to fit into an approximately 1 meter long vacuum chamber. The total beam power received by the MLM will be up to 70 W.

The whole device should fully comply with the general MAX IV standards, e.g. for vacuum (UHV, P < 5 x 10^{-9} mbar), mechanical stability (all eigenfrequences must be above 60 Hz), electrical standards, and alignment requirements.

Table B.4.2 Preliminary motion specifications for the MLM

Translation	Parameter	Specifications
Yaw (Ry)* main reflection angle	range	0 – 45 mrad
	resolution	<8 µrad
	repeatability	<2 µrad
Pitch (Rx)	range	±2 mrad
	resolution	<8 µrad
	repeatability	<2 µrad
Roll (Rz)*	range	±2 mrad
	resolution	<8 µrad
	repeatability	<2 µrad
Lateral translation (Tx) chamber	range	± 5 mm
	resolution	<1 µm
	repeatability	<2.5 µm
Lateral translation (Tx) second mirror**	range	-0.5 – +4.5 mm
	resolution	<1 µm
	repeatability	<2.5 µm
Horizontal translation (Tz) second mirror**	range	-5 – +530 mm
	resolution	<2 µm
	repeatability	<5 µm
Vertical translation (Ty) chamber	range	± 25 mm
	resolution	<5 µm
	repeatability	<10 µm

* Yaw and roll rotations should be independent for two mirrors. A possible solution would be an in-air rotation of the whole chamber and fine in-vacuum adjustment on one of the mirrors.
**Second mirror is translated relative to the first one inside vacuum chamber.

B.5. Higher Harmonic Contamination

The proposed optical scheme with both a hDCM and a MLM requires quite complex mechanics in both the monochromators to enable fixed exit operation at both 10 mm and 4/6 mm offsets. The combined use is foreseen only in the case where higher harmonic (HH) contamination could cause problems. If the degree of contamination is very low this mode may not be needed and both monochromators could have a 10 mm fixed offset only, thus, simplifying the mechanics greatly.

Contamination by HH is apparent in the PXRD data if the ratio of intensity from HH to intensity at the primary energy is too high and if the detector cannot discriminate based on photon energy. The signal from the HH can in principle be added to the model, however, this adds a number of variables, which complicates the modeling, and it is thus better to minimize the contamination to obtain the best data possible.

Intensity from the contaminant will appear at lower scattering angles than the primary intensity. Overlap of the two signals will not significantly change the observed intensity of the intense peaks, but accidental overlap of a contaminant peak with a weak primary peak will significantly change the observed intensity of said peak. Contaminant peaks that do not overlap with primary peaks may also cause problems, as identification of minor phases among the contaminant peaks will be difficult.

Double crystal monochromators in a nondispersive setting will transmit not only the primary energy but also higher harmonics. For Si (111) crystals these are Si (222), Si (333), etc. Fortunately, the Si (222) intensity is negligible and does not cause a problem. Si (333) does have a significant intensity ($I_{Si\ (333)}/I_{Si\ (111)}$ ~ 1/20) and the degree of contamination necessitates further study. The following calculations do not include thermal deformation of the crystals nor divergence of the beam.

The intensity from the IVU16 decreases rapidly above the working energy range. I.e. HH contamination is most severe at the lowest working energy, 15 keV. Without including divergence and deformation of the Si crystal, the hDCM transmits 5.2x10^{13} photons/s at 15 keV from the 111 reflections and 2.8x10^{10} photons/s from the 333 reflections. The ratio is thus 5.4x10^{-4}, see Figure B.5.2.

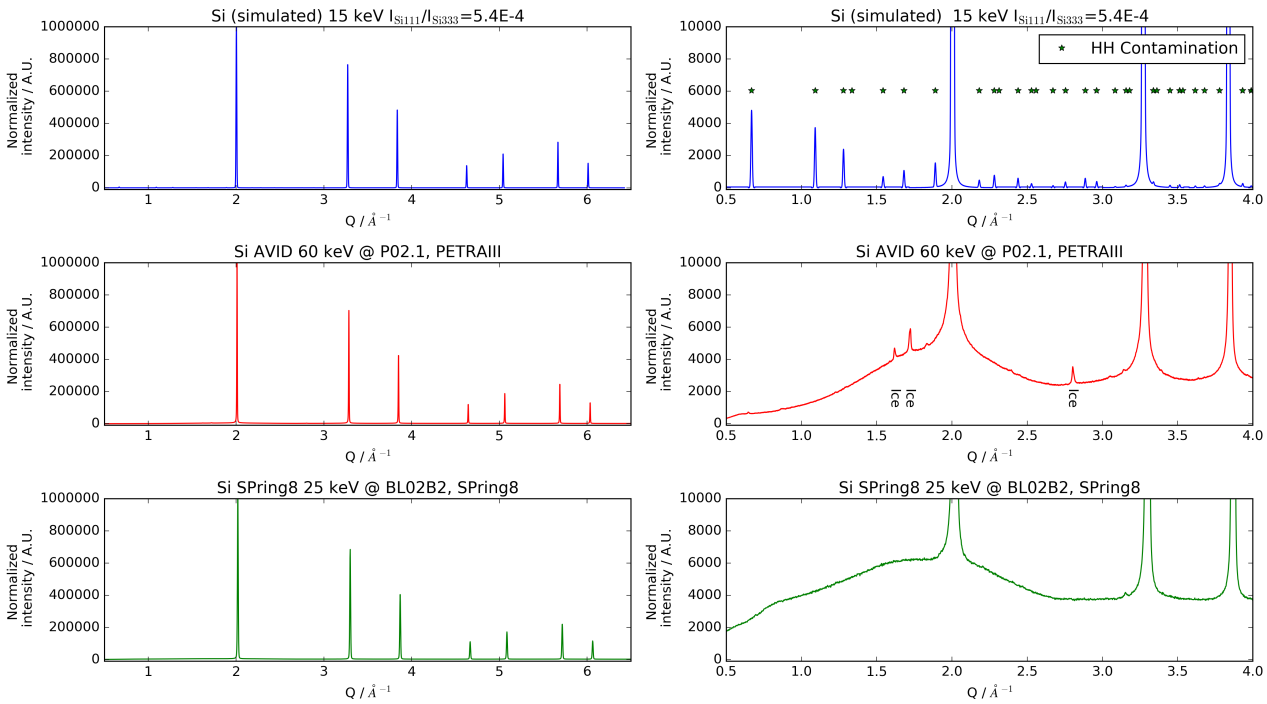

Figure B.5.1 Comparison of simulated and raw PXRD data from Si (NIST 640d). The intensity has been normalized (maximal count) to 1e6 counts and plotted against $Q = 4\pi \sin\theta\ /\lambda$. Top: Simulated data (no background and no noise) from Fullprof includes HH contamination (5.4x10^{-4}). Middle: Raw data from the Aarhus Vacuum Image Plate diffractometer collected at P02.1 at PETRAIII collected with 60 keV X-rays. Bottom: Raw data from the BL02B2 instrument at SPring8 collected with 24.8 keV X-rays.

To simulate the effect of HH a PXRD pattern of Si was simulated in Fullprof (Rdoriguez-Carvajal, 1993) with a ratio of 15 keV to 45 keV set to 5.4x10^{-4}. The result is shown in Figure B.5.1 where it is compared to raw normalized data, NIST Si 640d, from the low background Aarhus Vacuum Imaging plate Diffractometer (measured at P02.1 at PETRA III) and the Debye-Scherer camera at BL02B2 at SPring8. It is clearly seen that the contamination peaks have much higher intensity than the noise level in the other data sets and would be significant in a measurement. The simulation does not include the detection efficiency which for most detector technologies would be lower for the 45 keV X-rays than the 15 keV X-rays.

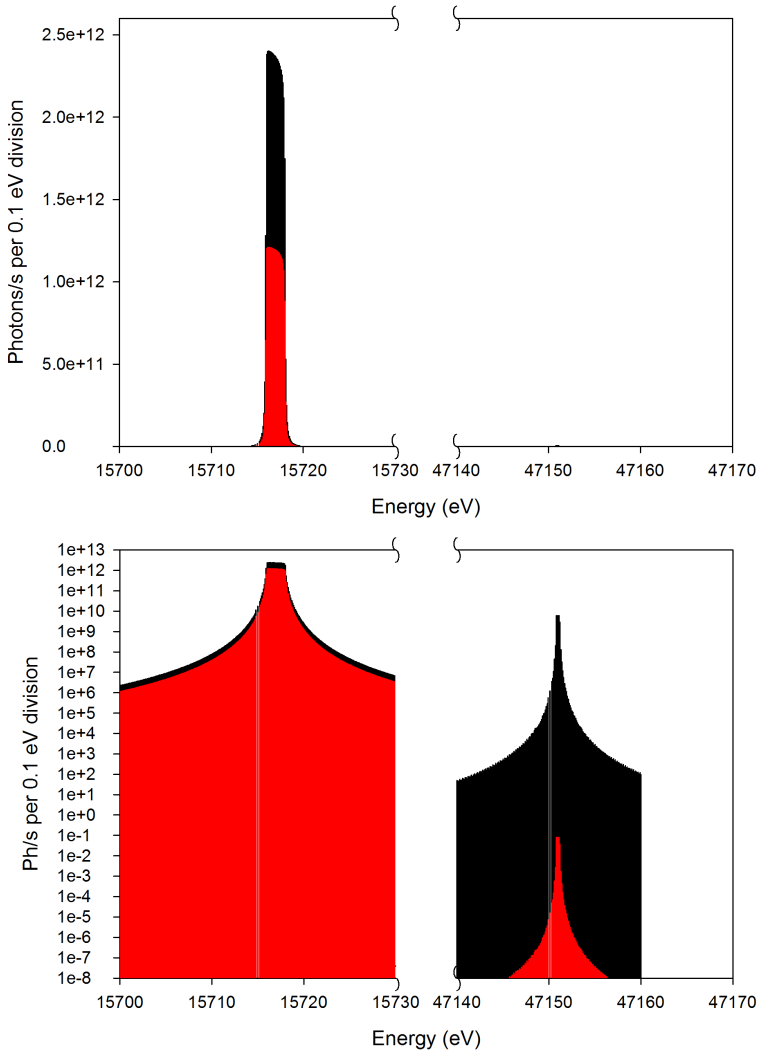

Figure B.5.2 Spectral flux at 15 and 45 keV using only hDCM (black) and combination of hDCM and MLM (red). Data plotted on linear and logarithmic scale on the top and bottom panel, respectively.

In other words, HH contamination is a problem for accurate work at 15 keV and other means of rejection is necessary. Similar simulations indicate that $1x10^{-5}$ is the upper limit and the optics preferably should be designed to reduce the HH contamination to this or even lower values.

The combined use of both hDCM and MLM, neglecting the beam divergence and crystal deformation, transmits $2.6x10^{13}$ photons/s at 15 keV (Si (111)) and only 0.4 photons/s at 45 keV (Si (333)), i.e. a ratio of $1.5x10^{-14}$. His level of HH rejection is much better than the minimum requirement. The sacrifice for this option is the loss in the multilayers which each has a reflectivity of approximately 0.7 (at 15 keV) leading to an intensity reduction of 52%, an increase in beam divergence, and the increased complexity of the mechanics in the monochromators.
At 20 keV the hDCM transmits around $2.58x10^{13}$ photons/s from the (111) reflection and around $3.41x10^{8}$ photons/s from the (333) reflection. The ratio is thus $1.3x10^{-5}$, close to the acceptable limit. Therefore, taking into account significantly lower detectors efficiency and scattering cross-section for high-energy photons, for most experiments at E > 20 keV no additional harmonic suppression is foreseen to be required.

B.5.1. Alternative HH rejections methods

At many beamlines HH contamination is rejected using grazing incidence mirrors. The mirrors are often, besides HH rejection, used to focus the beam. The small divergence at DanMAX means that focusing in many cases is not necessary. Furthermore, the incidence angle, often around 3 mrad, leads to significantly movement of the beam at the sample position (~20 m downstream of the mirrors) in cases where the mirror is removed, unless a second mirror is used. Therefore, we propose to avoid flat or focusing mirrors.

Another commonly used way of minimizing the amount of HH contamination is by detuning the monochromator, i.e. slightly rotating one of the crystals. Either the first of the second crystal is rotated by an amount smaller than the Darwin width from exact parallel orientation. This has the effect of reducing the intensity from the (333) reflection much more than the intensity from the (111) reflection. The highest rejection happens at a detuning angle of approximately half the Si (111) Darwin width (Hou, 2005). At this point the HH intensity is reduced by a factor of approximately $1x10^{-3}$ while the primary intensity is reduced to approximately half. It is possible to use smaller detuning angles at the expense of the efficiency of the HH rejection.

On conventional 3rd generation storage rings this option is convenient as the deflection of the beam (approximately 5 µrad) is much smaller than the natural divergence of the beam. Therefore, downstream optics, slits, and other equipment do not necessarily need to be adjusted. At DanMAX the deflection is approximately equal to the natural divergence and thus the downstream components will need to be realigned. It is possible to use a constant detuning angle at various energies. This ensures that the beam position is not changing as a function of energy, however, the intensity of the primary intensity is slightly reduced.

A third way to minimize HH is to use the chromatic nature of compound refractive lenses. The focal length of these lenses is dependent on energy and thus the focal position of the HH is located far behind the focus of the primary energy. Due to the small divergence of the beam focusing is many cases not necessary and thus a rejection scheme relying on focusing in not possible.

It is expected that next generation detectors may be able to record energy resolved data and thus harmonic contamination would no longer be a problem for PXRD. While this is an exciting development we do not want to rely on this unavailable technology. In addition users may be interest in bringing other detectors, without this capability, to DanMAX.

B.6. Transfocator

The compound refractive lenses for X-rays are using the same principle as the lenses for visible light. The major difference for X-rays is that the refractive indexes of different materials are very close to, but smaller than, unity ($n = 1 - \delta$, where δ is approximately 10^{-6} in the energy range of DanMAX). Thus, a focusing lens will have a concave shape and will inevitably have a low focusing power even with a very small curvature radius. Several lenses need to be stacked together to decrease the focal length (Figure B.6.1). In a thin lens approximation, the focal distance of such lens stack is defined as $f=R/(2*\delta*N)$, where R is the radius of curvature at the apex of the individual lenses, and N is the number of lenses. The detailed formalism regarding various parameters of thick CRLs can be found in a recent publication of Simons *et al.* (2016). For very high ratio of focal distance to CRL thickness found here, a thin lens approximation is quite accurate. After the exact

positions of transfocator and experimental stations are fixed, calculations that are more accurate would be performed. For the energy range of interest, the most convenient material for CRLs is beryllium.

CRLs can be manufactured in both, one- and two-dimensional lenses, and commonly a parabolic shape is used in order to avoid spherical aberrations. With the parabolic surface shape, a numerical aperture of the lens can be significantly higher than its curvature radius R, however, certain limitations still exist from the absorption (lens thickness increases as radius squared) and in the manufacturing process as well.

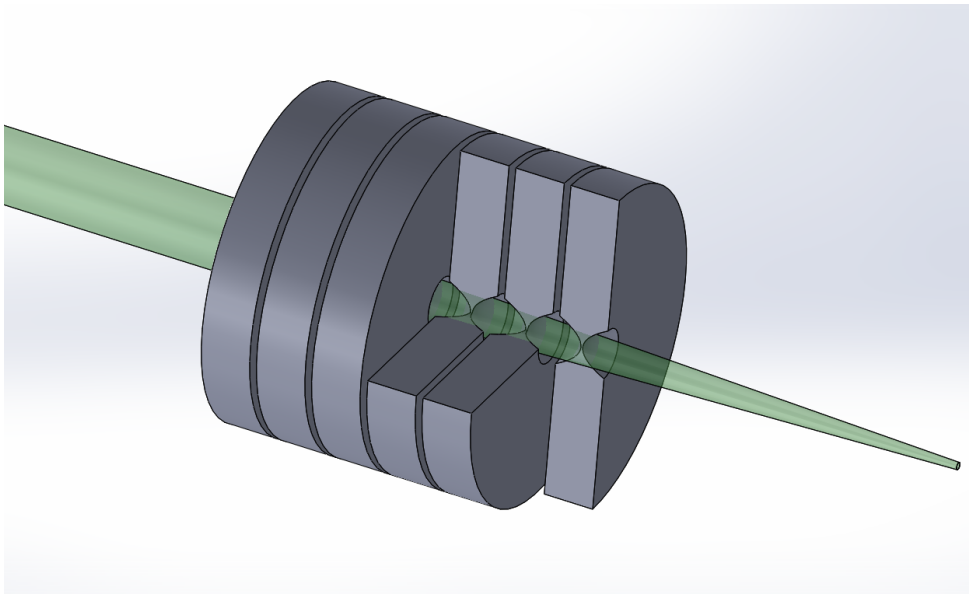

Figure B.6.1 Schematic view of the focusing CRLs.

The design of the transfocator includes a compromise between the minimal R (and thus minimal number of lenses) and overall transmission, including the geometrical effect of the limited aperture and X-ray absorption. RXOPTICS[§§] offers a range of different 2D Be CRL geometries, and five are of an interest for DanMAX: with R = 50, 100, 200, 300 and 500 µm, having effective apertures of 0.44, 0.62, 0.88, 1.08 and 1.39 mm, respectively. In the McXtrace simulations (see Appendix B.8) performed, the main limitation comes from geometrical aperture, not from the absorption. Figure B.6.2 shows the transmission as a function of aperture. Here we find that the best compromise is using R = 200 µm CRLs with a geometrical aperture of 0.88 mm.

[§§] http://www.rxoptics.de/

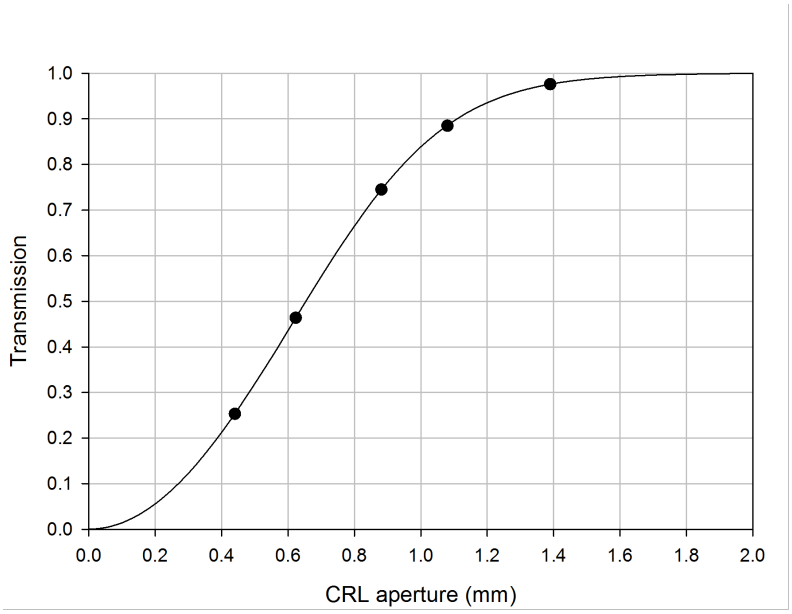

Figure B.6.2 Transmission though different apertures at the CRL transfocator position at DanMAX. Solid circles show the different 2D CRL apertures available from RXOPTICS. The front end aperture limit is at about 1.1 mm.

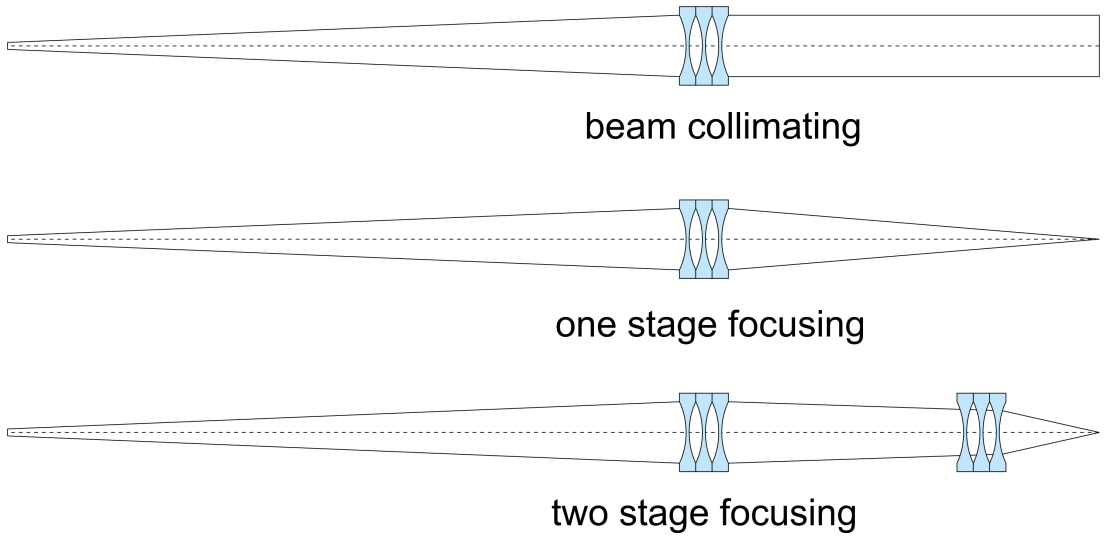

Figure B.6.3 DanMAX focusing schemes with the CRL transfocator(s).

Three possible focusing schemes are proposed for the DanMAX beamline (Figure B.6.3). First, the CRL transfocator can be used for beam collimation to produce a nearly parallel beam. For the 15-35 keV energy range this will require 2 to 12 lenses. The second possible scheme is a direct beam focusing on the sample or detector position. A total number of 6 to 50 (depending on energy and the sample position – imaging or PXRD instruments) are required for this scheme. Finally, a two stage focusing scheme can be utilized for very small spot sizes. The second focusing element(s) will be placed in the experimental hutch.

The 50 lenses will be grouped into six cassettes, holding 1, 2, 4, 8, 16 and 19 lenses, respectively. An in-vacuum transfocator will allow quick and easy selection of any number of lenses from 0 to 50. Due to the discrete number of lenses, an exact focal distance cannot be achieved for any energy.

For example, for beam collimation (target f = 30.9 m) the exact focusing power is achievable for nine different energies (Figure B.6.4).

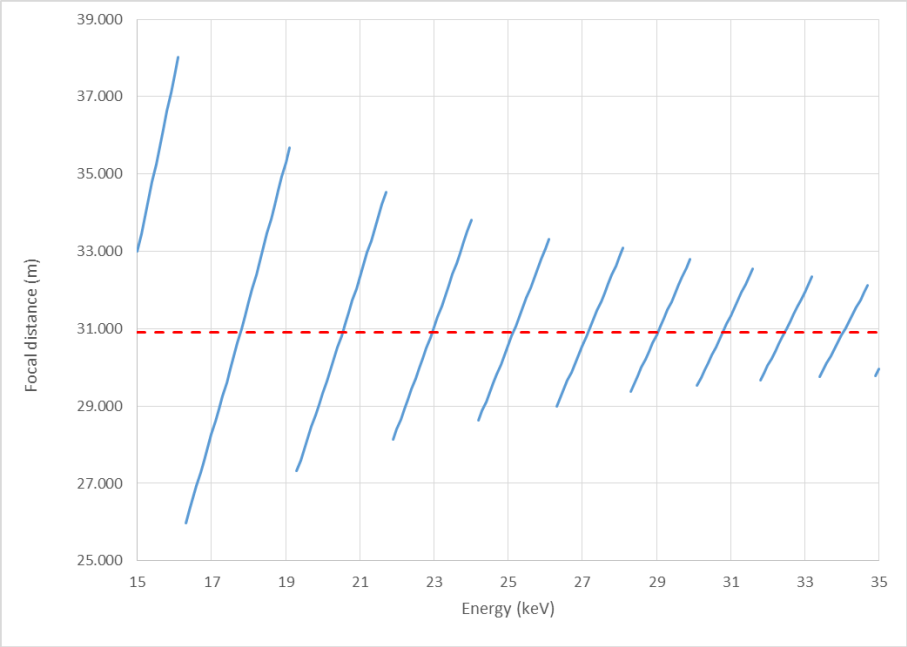

Figure B.6.4 Possible focal distances closest to 30.9 m (collimated beam) achievable with the CRL transfocator.

For focusing at the powder diffraction instrument sample position approximately 15 meters from the CRLs (target f = 10.45 m) a perfect focusing conditions can be achieved approximately every 0.5 keV (Figure B.6.5).

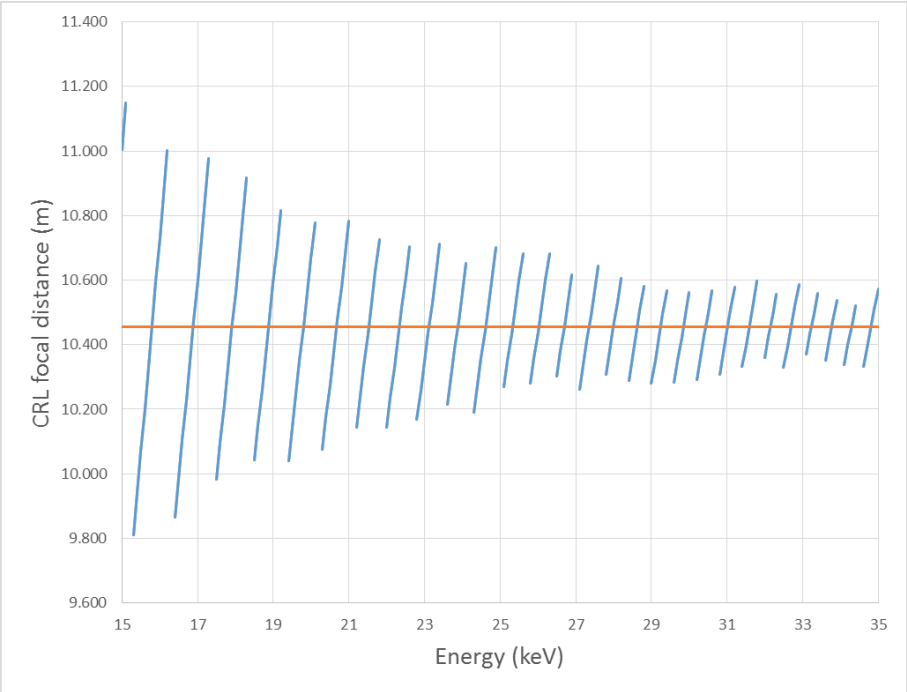

Figure B.6.5 Focal distances closest to 10.45 (focus @15.8 m) achievable with the CRL transfocator.

Although CRLs have strong chromatic aberrations, they are virtually achromatic for the energy range transmitted by DCM and MLM. However, if only the MLM is used (high flux mode), the horizontal focusing is decreased by the increased horizontal divergence caused by the thermal deformation of the first multilayer mirror. As a result, the 2D CRL transfocator has different focal distances in horizontal and vertical direction, and the focused beam is asymmetric in the focal plane. If deemed necessarily, it can be corrected with additional sets of 1D lenses in the experimental hutch.

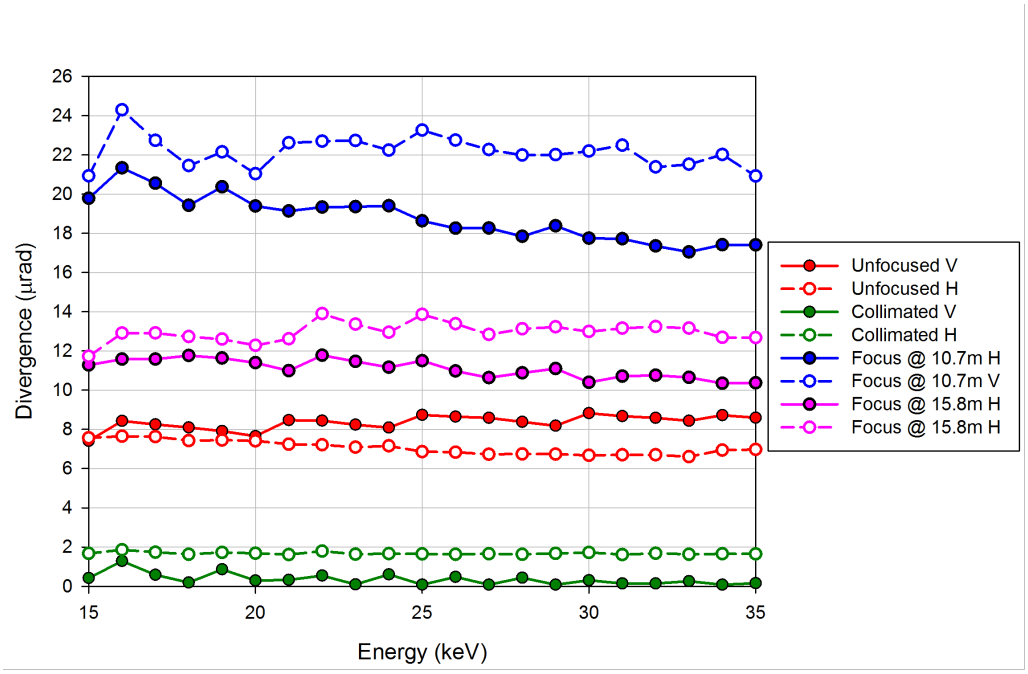

Figure B.6.6 X-ray beam divergence in the experimental hutch for different focusing schemes when the DCM is used.

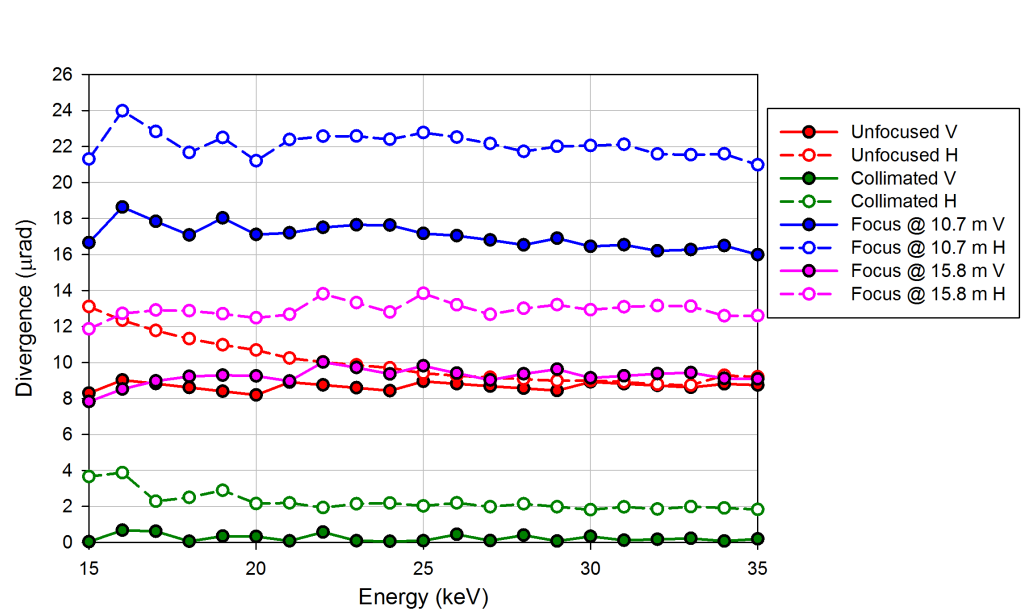

Figure B.6.7 X-ray beam divergence in the experimental hutch for different focusing schemes when only the MLM is used. Note the difference between horizontal and vertical divergence.

Figure B.6.6 and Figure B.6.7 show the resulting beam divergence at the sample position for different energies and focusing schemes with only DCM or MLM monochromators. For some energies, the RMS divergence can be below 0.2 µrad (RMS).

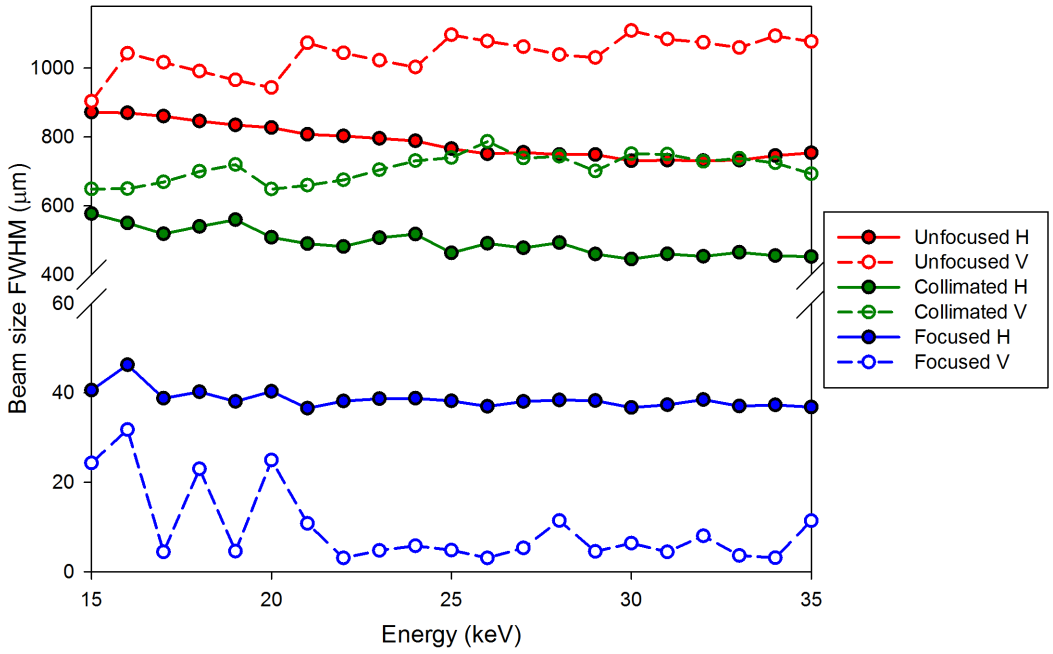

Figure B.6.8 X-ray spot size (FWHM) at the imaging sample position (10.7 m from the CRLs) for different focusing modes when the DCM is used.

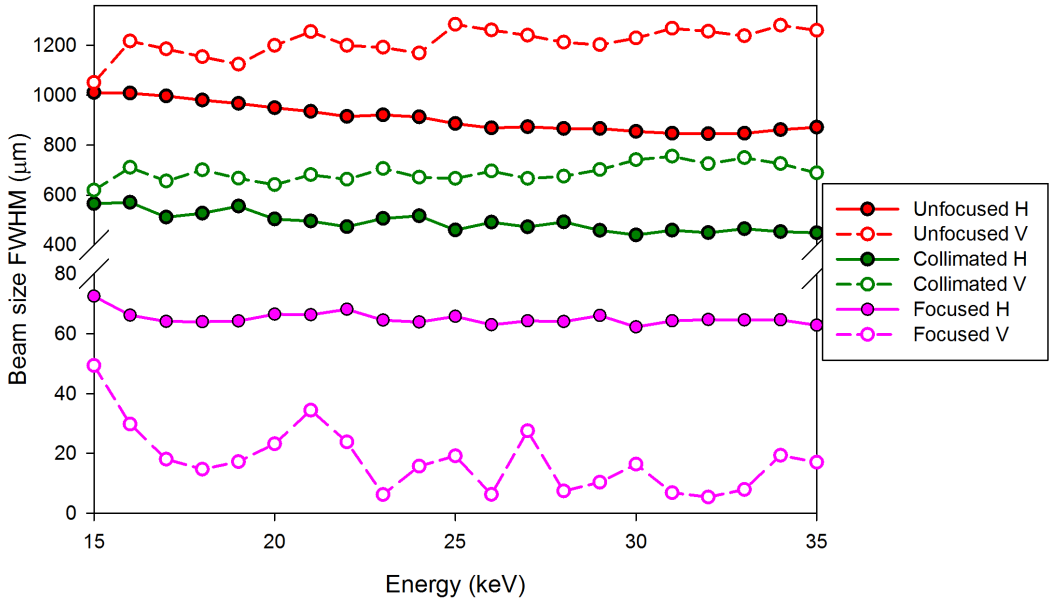

Figure B.6.9 X-ray spot size (FWHM) at the downstream PXRD sample position (15.8 m from the CRLs) for different focusing modes when the DCM is used.

The resulting X-ray focal spot sizes at the imaging and downstream PXRD instrument positions are shown in Figure B.6.8 and Figure B.6.9. The size of the X-ray spot can easily be tuned from several

microns for fully focused to about one millimeter for the unfocussed beam over the whole energy range. A typical shape of the focused monochromatic spot (~ 40 x 10 µm^2 FWHM) is shown in Figure B.6.10.

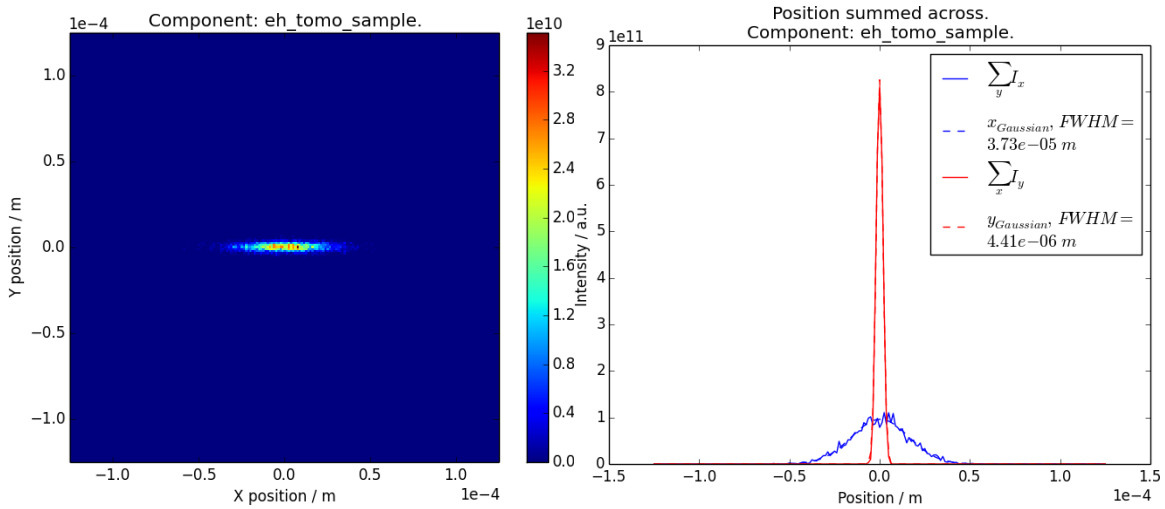

Figure B.6.10. A typical shape of the focused spot at the imaging sample position when the DCM is used (E = 31 keV, 40 lenses). Spot size is 37.3×4.4 µm^2.

For the high flux mode, as mentioned above, the focused spot is not symmetrical and is significantly larger in horizontal dimension for the best vertical focusing (Figure B.6.11 and Figure B.6.12).

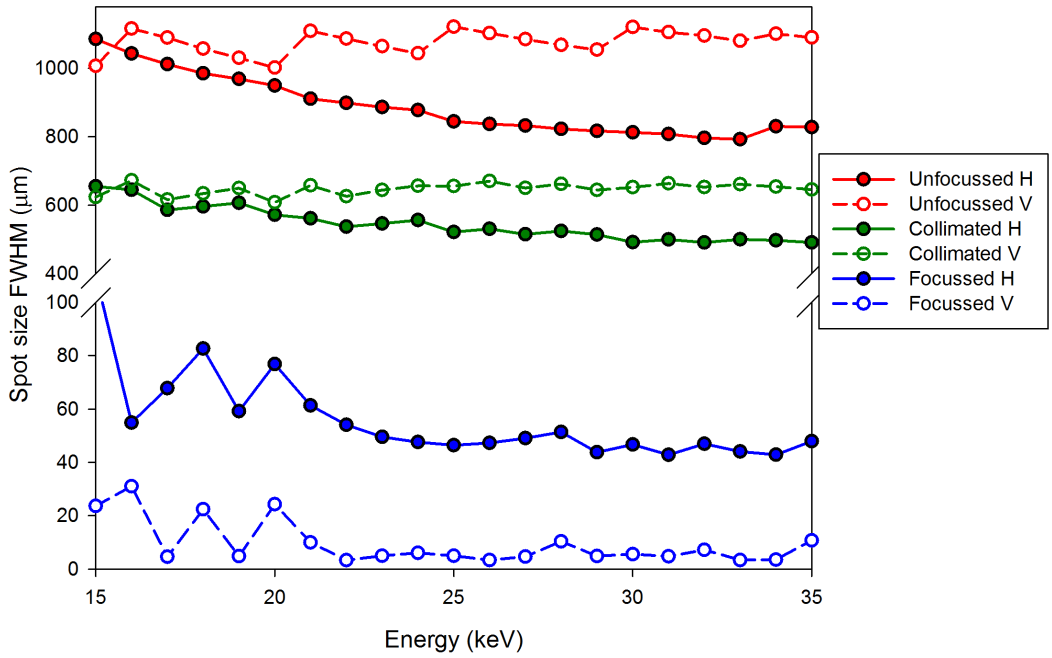

Figure B.6.11 X-ray spot size (FWHM) at the imaging sample position (10.35 m from the CRLs) for different focusing modes when only the MLM is used.

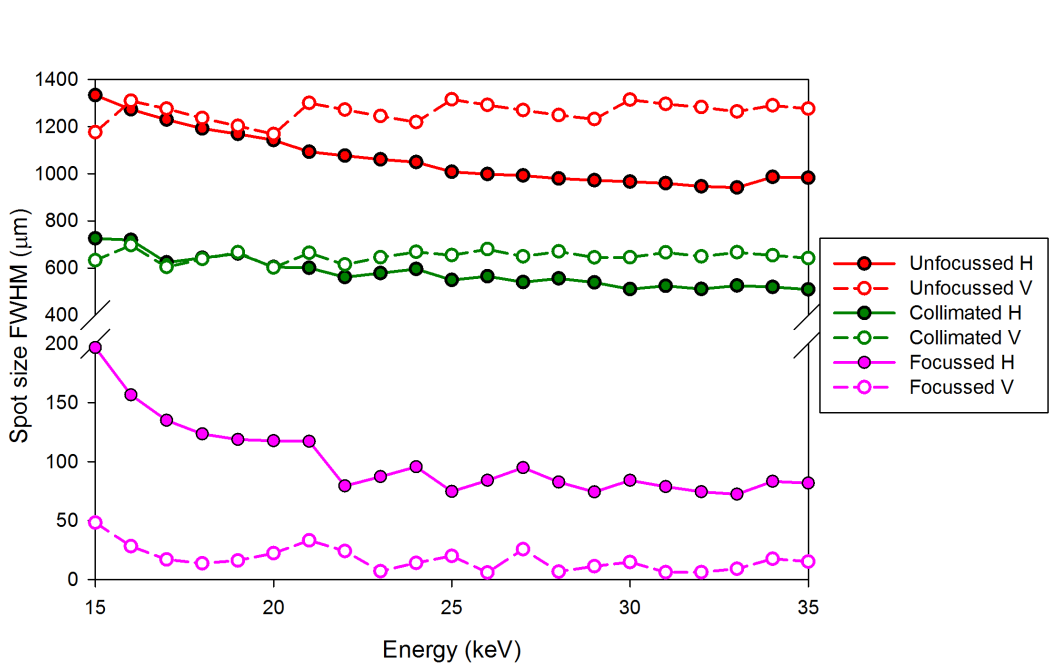

Figure B.6.12 X-ray spot size at the downstream PXRD sample position (15.2 m from the CRLs) for different focusing modes when only the MLM is used.

This strong focusing astigmatism allows some more advanced beam shaping. By adding extra lenses to the transfocator, a better horizontal focus can be achieved, but the beam becomes elongated vertically. Intermediate focusing power, i.e. intermediate number of CRLs, would give a more symmetric beam on the cost of larger spot size. Figure B.6.13 shows a variation of the focused beam shape at the imaging instrument sample position at 24 keV when the number of lenses is varied. The smallest vertical focus of 5 µm can be achieved for N = 26, while the most isometric beam (36.8×34.1 µm^2) is achieved for N = 27.

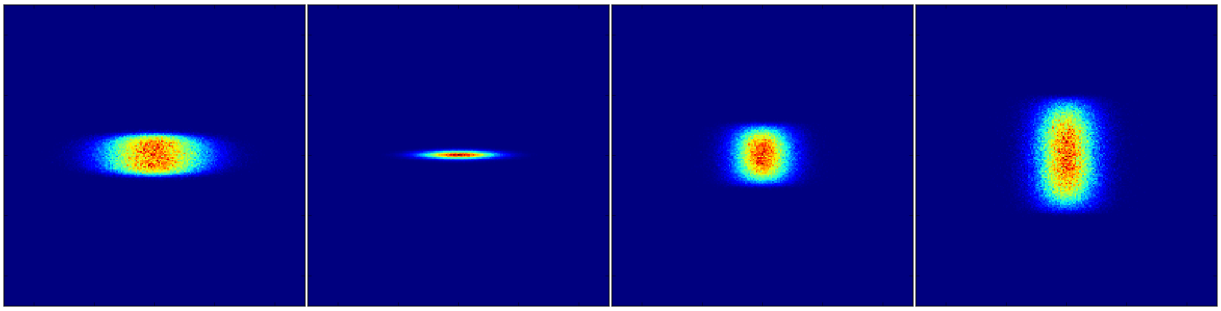

Figure B.6.13 Focused X-ray spot shape variation with the number of lenses when only the MLM is used. Field of view is 0.25 x 0.25 mm^2, E = 24 keV. The number of lenses from left to right: 25, 26, 27 and 28.

The total flux at the sample position for different focusing schemes and different monochromators is shown in Figure B.6.14. The maximal flux is approximately ~8 x 10^{14} ph/s for the unfocussed beam in a high flux mode, and is around ~5 x 10^{13} ph/s for the monochromatic beam.

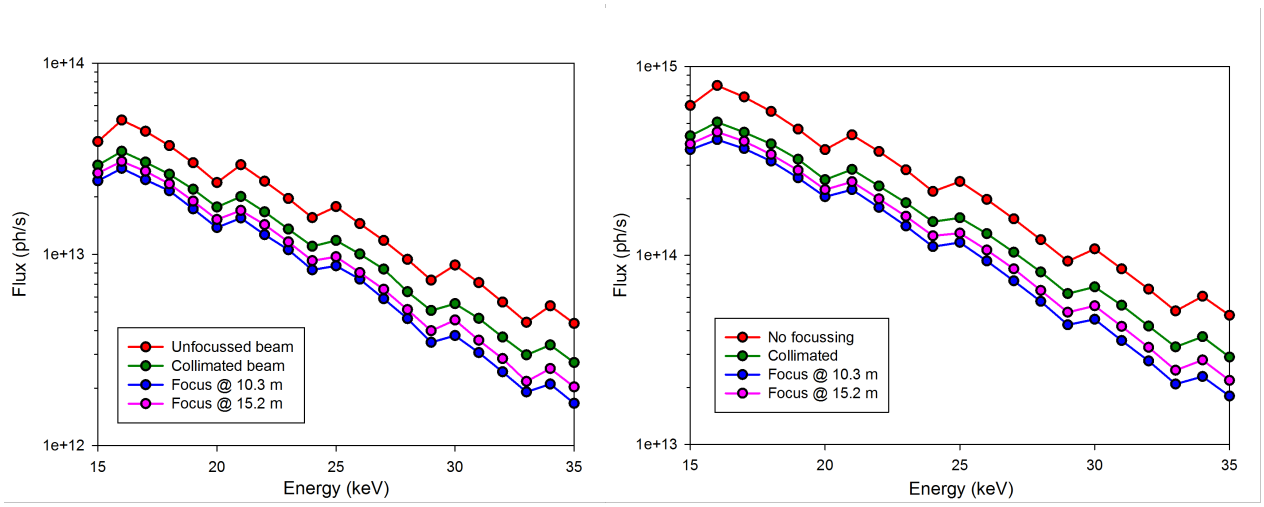

Figure B.6.14 Total photon flux (photons/s) on the sample for DCM (left) and MLM (right).

The maximum flux density at the sample position with the unfocused beam and using a one-stage focusing scheme is shown in Figure B.6.15.

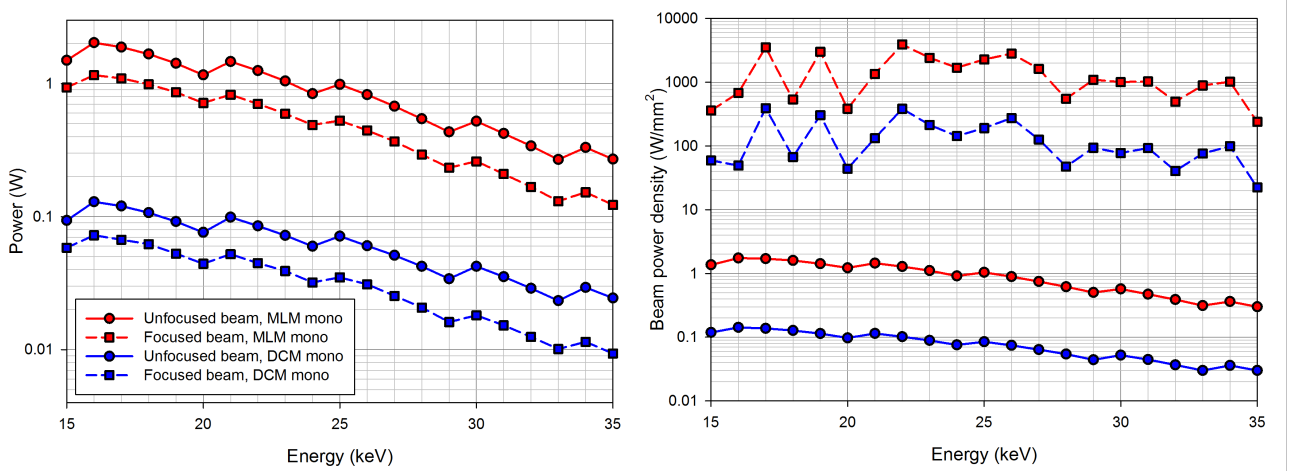

Figure B.6.15 Total power dissipated on a sample by X-ray beam (W) for the focused (using the CRL transfocator) and unfocused beam at the imaging sample position for a monochromatic beam and high flux beam (left), and the corresponding power density (W/mm^2) (right). The proposed focusing scheme provides a gain of ~×1000.

B.6.1. Beyond the optics hutch transfocator.

The CRL transfocator described above allow varying focal spot at the sample position from ~10 microns to 1 mm FWHM. However, the science cases requirements spot sizes both below and above these limits. Some experiments might require focal spot size of 50 nm, while the others might be interested in 5 to 10 mm illumination fields. Although the design of the experimental hutch optics will be discussed in a future document and only the overall layout has been chosen, a few comments on the secondary focusing device(s) are made here.

Creating smaller spots with the optics hutch transfocator is impossible due to maximal demagnification ratio, $m = -q/p$. With the CRLs located at approx. 32 m from the source, and first experimental station about 10 meters further downstream, a maximum source demagnification factor of 3.2 is achievable. Taking into account the source size of ~ 127 x 14 µm^2 FWHM, a focal spot of ~40 x 4 µm^2 is the theoretical limit. Further focusing would require an additional focusing device(s) in the experimental hutch closer to the sample position. Different focusing options include

additional CRLs, Kirkpatrick-Baez focusing mirrors, Fresnel zone plates and multilayer Laue lenses. Depending on the choice of device, a spot ranging from tens of nanometers to few microns can be achieved with various divergence and working distances. The optics hutch transfocator will be used to pre-focus/collimate the beam for the required aperture.

An example could be adding a secondary CRL focusing unit with 46 R=50 µm Be 2D lenses at 2 m from the PXRD instrument would produce a focal spot as small as 10.9 x 1.7 µm^2 (h x v, FWHM) at 35 keV (Figure B.6.16) while still maintain a reasonably low divergence of 44 x 46 µrad (RMS). For the imaging instrument multilayer Laue lenses is a very interesting alternative, both as condenser and objective.

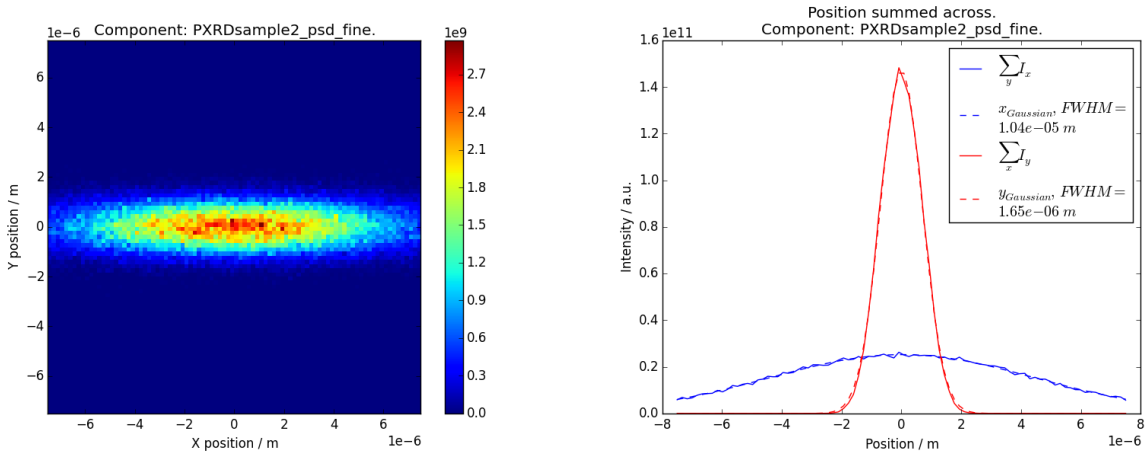

Figure B.6.16 An example of a monochromatic spot produced at the sample position using a two stage focusing geometry and Be CRLs

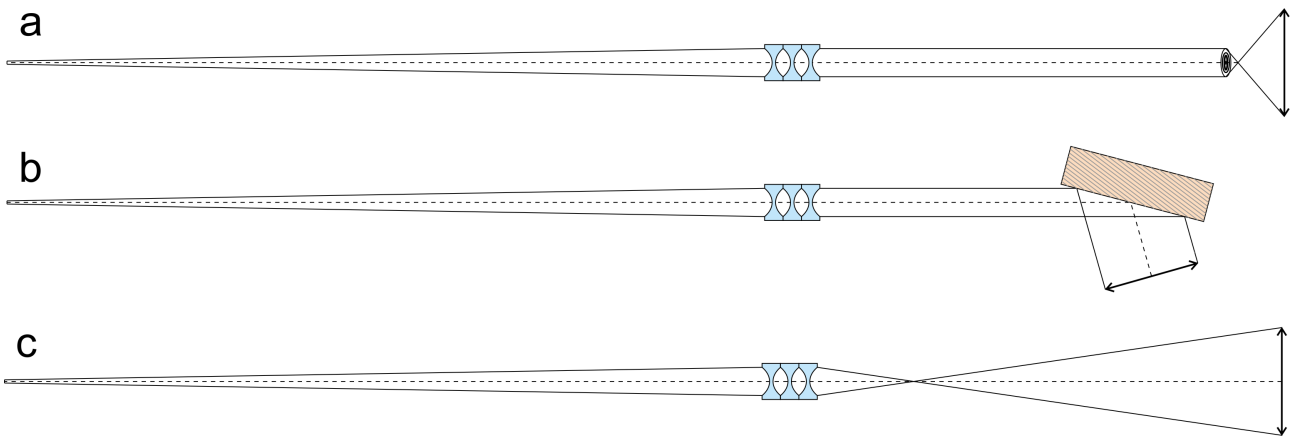

Figure B.6.17 Potential optical scheme for beam enlarging. a) – overfocusing with a zone plate, b) – using asymmetric Bragg crystal, c) – using a secondary source from the transfocator.

Generating large beams is not a trivial task. One option would be to use an over focusing optics with very high divergence (like a multilayer Laue lens or a zone plate) and thus varying the spot size by moving the experiment along the beam axis (Figure B.6.17a). Another option is an asymmetric Bragg crystal magnifier, with can produce very large (cm size) beams with very high throughput and coherence preservation (Figure B.6.17b). This solution is deflecting the X-ray beam, and the

deflection angle as well as the beam size become energy correlated. A third option is generating a secondary source using a CRL transfocator (Figure B.6.17c).

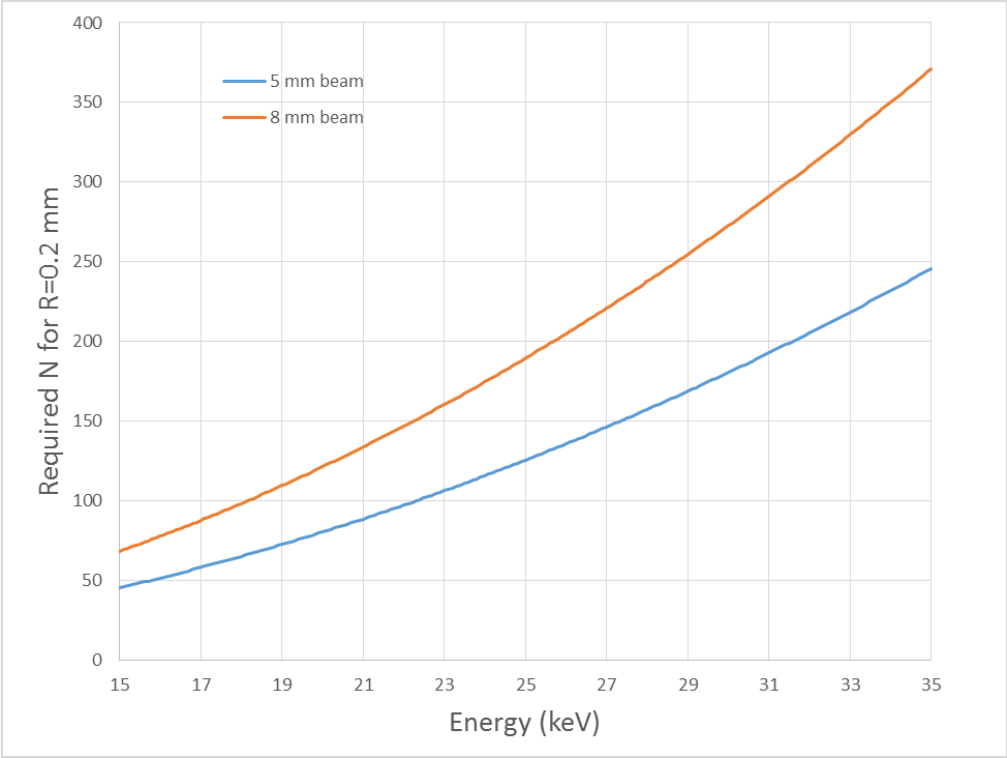

Figure B.6.18 A number of R=0.2mm CRLs required for secondary source generation in order to achieve 5 mm (blue) and 8 mm (orange) beam size at the sample position.

Although DanMAX is a relatively short beamline, the latter option is theoretically possible. Considering CRLs to sample distance of 10.4 m, and 0.88 mm beam aperture size at the CRL, a numerical aperture (N.A.) of 1.05 x 10^{-3} is required on order to achieve a 10 mm beam. Theoretical limit for N.A. is defined by material refraction as $\sqrt{2\delta}$. A maximum possible beam size in the present configuration at 15 keV is 22 mm, while at 35 keV it is around 8.9 mm. However, the total number of lenslets required is very high (Figure B.6.18). The overall transmission through these sets of lenses ranges from 24% at 15 keV to about 8% at 35 keV for an 8 mm beam.

Among these options, the most feasible is an asymmetric Bragg magnifier located at the beginning of the experimental hutch. Such a device can be relative compact, provide relatively high magnification ration with a high throughput of a monochromatic beam and without increasing beam divergence. Asymmetric Bragg diffraction magnifying devices have been successfully used before at synchrotron radiation sources (Christensen *at al.*, 1992; Spiga *et al.*, 2016). Germanium (220) crystal with the asymmetry angle of 5.55° would provide an 8-fold magnification at 25 keV (Figure B.6.19). Such a magnifier will be used in a monochromatic beam mode, so heat dissipation on it is miniscule. Together with a relatively wide rocking curve of germanium, a 1D magnifier can be manufactured as a double-bounce channel cut crystal with a total length under 50 mm. Two such crystals could generate an X-ray beam of 4.8×4.8 mm^2, sufficient for covering large FOV demands of full-field imaging studies. The expanded beam offset is just 5 mm in both, horizontal and vertical dimensions, and can be easily accommodated by the tomography sample stage and imaging detectors. The only disadvantage of such a solution is that the magnifying crystals are optimized for a specific energy with only minor energy tuning would be possible.

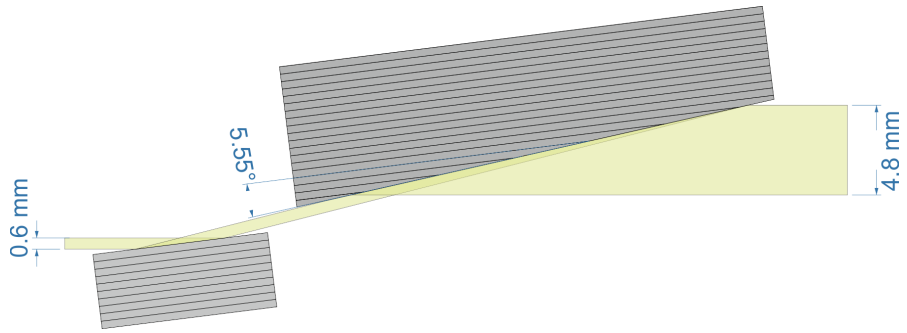

Figure B.6.19 Geometry of a Ge (220) Bragg crystal magnifier at 25 keV (θ is 7.12 degrees). Asymmetry angle of 5.55 degrees would generate a 4.8 mm exit beam.

B.7. Slits

Slits will be used to clean up and shape the beam at various place along the beam path. The first slits are placed immediately before the monochromators. These slits are exposed to the white beam and thus must be water-cooled. The center of the aperture of the slits are always on the undulator axis.

Two monochromatic slit sets will be placed behind the white beam stop and behind the transfocator near the downstream end of the optical hutch. The upstream slit will be the beam defining aperture in experiments with unfocused or collimated beams. In the experimental hutch each instrument will have dedicated slit systems to either clean up or define the beam shape. All of these will be monochromatic slit systems. Both slit sets will be commercially available solutions with encoders. The resolution should be around 1 µm and the repeatability of ± 5 µm. All of the slits must be vacuum compatible.

Additional circular guard aperture, matching the geometrical aperture of the CRLs, will be used in the transfocator.

B.8. McXtrace model used in the simulations

During the design phase an undulator source model as added to McXtrace and is now available in McXtrace v. 1.4. With the proper electron beam and DanMAX IVU16 parameters the generated output is in a perfect agreement with SPECTRA outputs (Tanaka & Kitamura, 2001).

The model automatically calculates the offset of both the monochromators based on the requested configuration. In general, the virtual beamline has the beamline aligned perfectly. The angles of the monochromator crystal and multilayers can be specified or automatically calculated based on the supplied energy. The hDCM is modeled using perfect crystals without absorption. The thermal dent is not modeled and thus the resulting divergence in the model is overestimated by up to approx. 1 µrad.

To model the ML reflectivity we use the IMD code (Windt, 1998) to generate a reflectivity file. The thermal deformation of the first ML if used in the high intensity mode is included as a spherical deformation with meridional and sagittal radii depending on the incident energy. I.e. assuming no resistive heaters on the substrates.

The Be CRLs in the transfocator in the optical hutch are traced as actual thick objects with perfect parabolic surfaces. For simplicity, the lenslets are set in a *single* cassette with a variable number of lenses in it. Given the long focal length of the individual lenses this departure from the real physical implementation with a number of tightly spaced lenslets cassettes is expected to be a minor effect.

Apertures/slits are considered perfectly absorbing infinitely thin planes. Further studies may be performed to study the effect of e.g. slit scattering.

Models of samples may be added to the simulations. A LaB_6 powder diffraction sample exposed to the unfocused 35 keV beam with both DCM and DMM active. The sample slit is 1 x 1 mm^2 and the sample diameter is 0.3 mm. Scattered intensity is collected on detectors resembling the Dectris Pilatus 2M (Figure B.8.1, SDD = 150 mm) and the Mythen 24K system (Figure B.8.2, SDD = 760 mm).

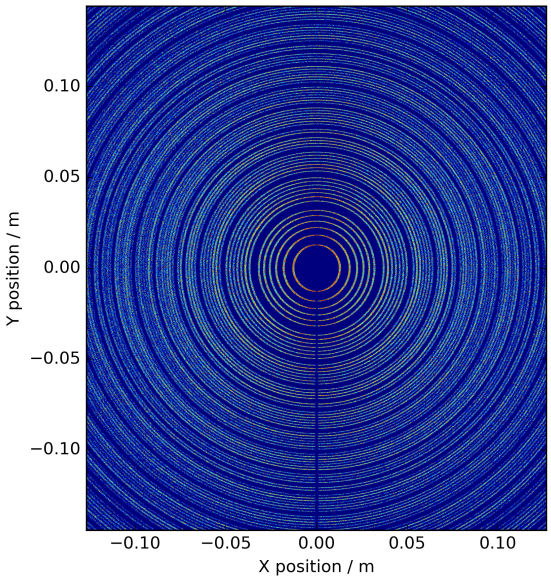

Figure B.8.1 Simulated PXRD pattern from a LaB6 sample on a 2D detector. The photon energy is 35 keV and the sample to detector distance is 150 mm. Intensity shown on a logarithmic scale.

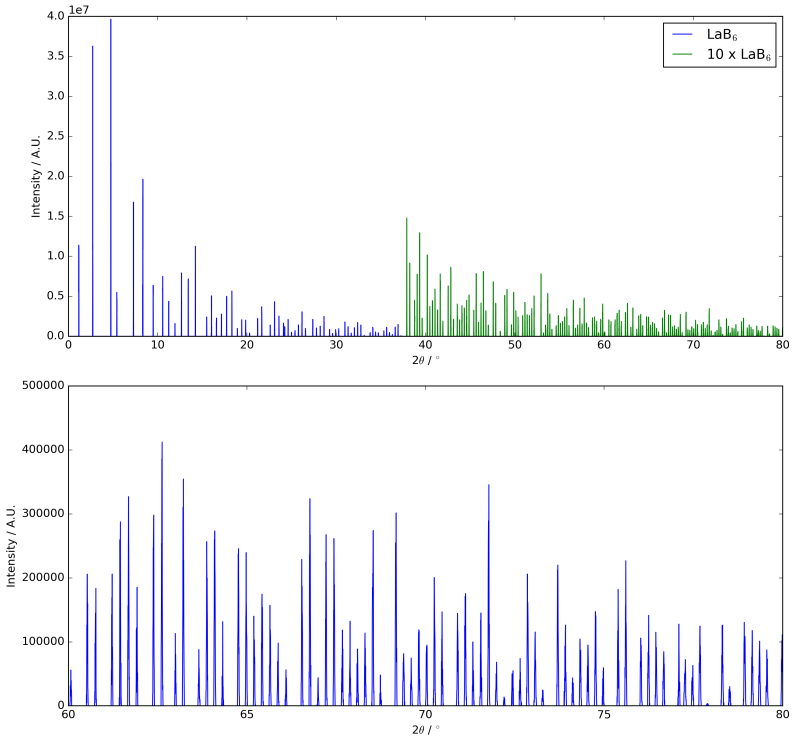

Figure B.8.2 Simulated PXRD pattern from a LaB6 sample on a 1D detector. The photon energy is 35 keV and the sample to detector distance is 150 mm.

It is also possible to simulate imaging samples, here the simulated projection of a model object with the unfocused beam is shown in Figure B.8.3.

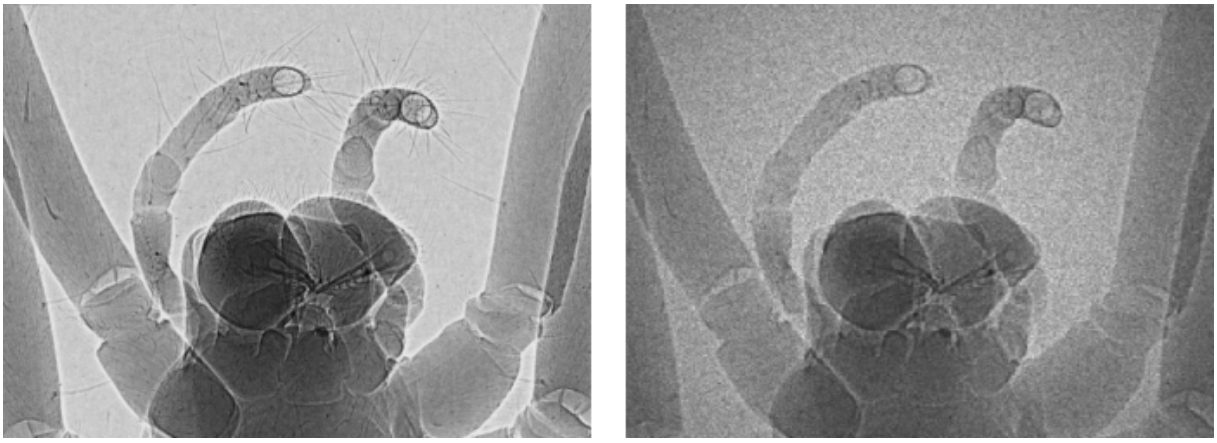

Figure B.8.3. Simulated projection of the model object (a part of a spider head) with the unfocused beam at 15 keV. On the left is the model absorption mask (phase-contrast image, courtesy of Excillum AB), on the right is the simulated detector image. Field of view is 340x250 μm^2, pixel size is 1 x 1 μm^2.

B.9. Alternative optical solutions considered

A disadvantage of the DCM + MLM layout presented above is that it is only possible to perform one experiment at a time. By using a beam splitter in the DanMAX beamline it would be possible to perform both imaging and diffraction experiments in parallel. In this way, the effective beam time would be doubled. Besides doubling the available time on DanMAX two separate branches would additionally lead to more freedom in designing the optical solutions, as there would be little or no

interdependency. Using a beam splitter is therefore a highly desirable option, however, it is essential that the functionality of either branch will not be negatively affected compared to an in-line design.

Due to the relatively short length of the straight sections (~4 m) it is not possible to use canted undulators. In addition, obtaining a usable separation of the two beams would require a beamline longer than 50 m. The narrow and highly collimated undulator beam does not permit using different parts of the beam for the two experiments. Therefore, the only viable option is to use a diffracting crystal in the beam.

Two geometry options are available: Laue or Bragg using either Si or diamond crystals. In both cases the crystal has to be thin, this is especially the case for Si due to the relative low photon energy. To maximize the intensity of the monochromatic beam the reflection used should be the (111) in both cases. The beam for the PXRD branch needs to be monochromatic and thus, the PXRD instrument would be placed on the diffracted beam branch. By using perfect single crystals, the wave-front should be preserved, i.e. the coherence of the primary beam should not be affected.
In both Laue and Bragg geometry the crystal is the first optical element and thus must withstand the high heat load of the beam. The total heat load will be somewhat reduced by placing the monochromator crystal behind a set of diamond high pass energy filters. In this case with 1 mm diamond in the beam path the total incident power on the crystal is approximately 55 W. As the beam splitter/monochromator would have to be placed far up stream (~24 m), to allow space for the optics for the imaging instrument, the beam size is quite small (~400 x 600 μm^2 FWHM) and thus, the power density is significant. The lower thermal conduction of Si combined with the higher absorption strongly favors diamond as the monochromating crystal.

Whereas diamond crystals have been used in Laue geometry on several beamlines the Bragg case has to our knowledge only been used at LCLS (Stoupin *et al.*, 2014). At LCLS the heat load is significantly smaller and it is unlikely that this geometry is applicable with the high power density at DanMAX (Stoupin, personal communication). In addition, the quality of diamond with (111) faces, suitable for Bragg geometry, are lower than crystals with (100) faces used in the Laue geometry. It seems therefore that Laue geometry is the only feasible option.

A detailed FEM study would be required to investigate if it is feasible to cool the crystal at DanMAX to avoid a large thermal bump without introducing significant vibrations. The thermal bump would mainly affect the monochromatic branch, which would see a larger divergence, but it is also possible that the thermal bump would disturb the wave front and thus, decrease coherence in the direct imaging branch.

A downside of using the Laue geometry is the lower resulting intensity in the diffracted beam compared to the Bragg case, and additionally an increased divergence leading to a lower brilliance (Brauer *et al.*, 1995). The brilliance can be regained by using an asymmetrically cut second crystal. The asymmetry can only be matched at one particular energy, thus the brilliance can only be fully recovered at this energy

A possible geometrical scheme would be to deflect back the diffracted monochromatic beam to be parallel with the primary beam. This can be done using a second diamond crystal (111) in Bragg geometry. As the Darwin widths of the two crystals are identical small instabilities in both will affect both the energy and the intensity. An alternative is to use a Ge (220), which has a wider Darwin width and thus reflects the full beam from the diamond (111) reflection. The *d* spacing of Ge (220) is not identical to the *d* spacing of diamond (111), thus, the monochromatic and direct beam will not be exactly parallel, but this can be corrected with a double mirror, also serving as a high harmonic suppressor (Figure B.9.1). The angle and position of the mirrors would have to be tuned when the energy is tuned.

For a practical use of both beams a separation of at least 1.0 m between the beams is necessary. It is *not* an option to fix the energy of the PXRD instrument as various experiments require photon energies in the full 15-35 keV range. To keep a fixed offset of 1 m using two diamond (111) reflections from 15-35 keV the second crystal needs to move approximately 3.5 m along the beam. Both crystal needs to be in UHV and should be kept at the same temperature. The temperature requirement can be relaxed if a Ge (220) crystal is used as a 2nd crystal.

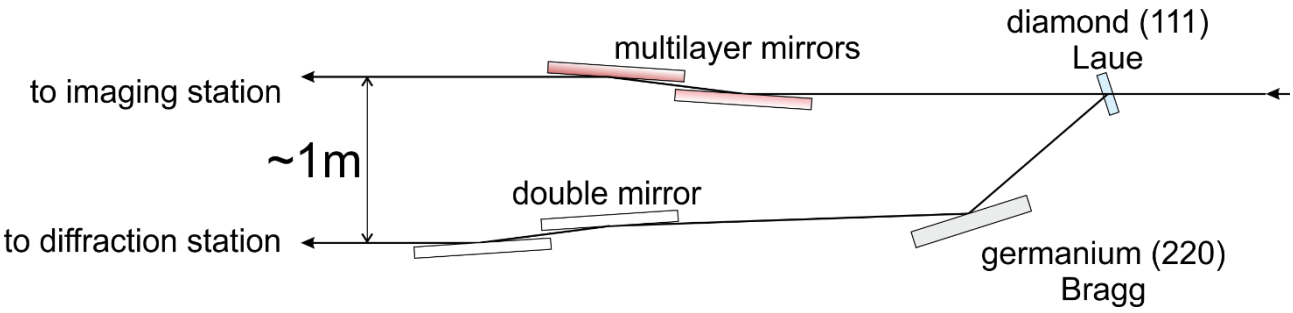

Figure B.9.1 Layout of DanMAX using a beam splitter with parallel beams geometry.

An alternative geometrical scheme for beam splitting would be using a single diamond Laue reflection and place the whole XRD branch on a movable 2θ arm. This moving arm should adopt angular change of a diffracted beam between 9.8 to 23 degrees to cover a target 15-35 keV energy range (Figure B.9.2). Such a scheme would have a great advantage of significantly larger separation between the beams.

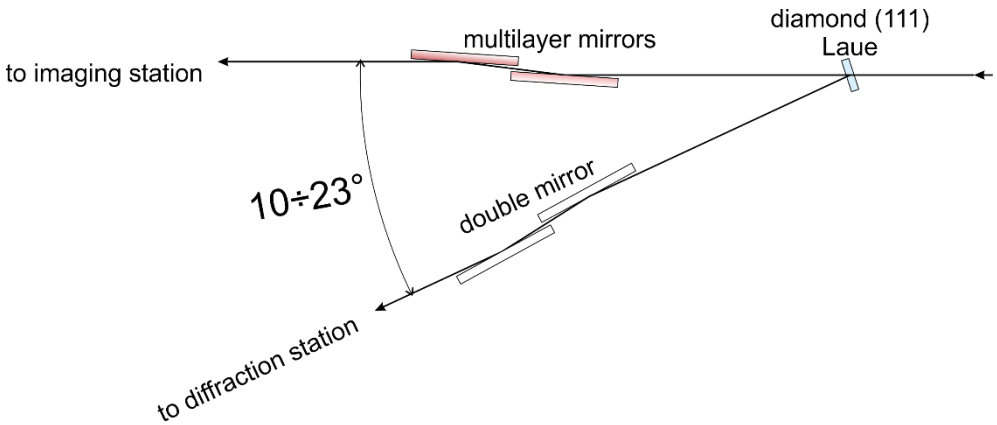

Figure B.9.2 Layout of DanMAX using a beam splitter with 2θ geometry.

Floor space in the MAX IV 3 GeV ring experimental hall should be sufficient to accommodate two experimental hutches (for the diffraction and imaging end-stations) almost without any geometrical compromises. Figure B.9.3 shows an possible layout of two branches using a diamond (111) Laue crystal as a beam splitter.

The major inconvenience of this optical scheme is the necessity of a massive 2θ arm at the diffraction end-station, which must carry all the beam focusing and profiling optics, the sample goniometer and detector(s) in addition to sample environments. Although mechanically challenging, it is nevertheless possible. A somewhat similar moving 2θ arms has been successfully used before on several beamlines, e.g. ID28 or ID24 at the ESRF. In any case, changing of working energy for the diffraction station user is much more complicated compared to a double-crystal fixed-exit monochromator.

For both geometries proposed, in addition to the geometrical/mechanical challenges this poses, the spectrum (and the intensity profile) seen at the imaging instrument will change slightly when changing the energy in the monochromatic branch. It is not clear if this would pose a problem in practice. The imaging end-station should not see any X-ray beam disturbance from the diffraction station if two different undulator harmonics are used. For example, if XRD experiment is performed at 33 keV (11th harmonic), it should not affect imaging experiments at 15, 18, 21, 24, 27 or even 30 keV. However, if users of one of the branches would need to change the undulator gap in order to fine tune the photon energy (for example, adjusting energy close to an absorption edge), the parallel experiment should be stopped, and all X-ray optics should be realigned, and experiment should be recalibrated.

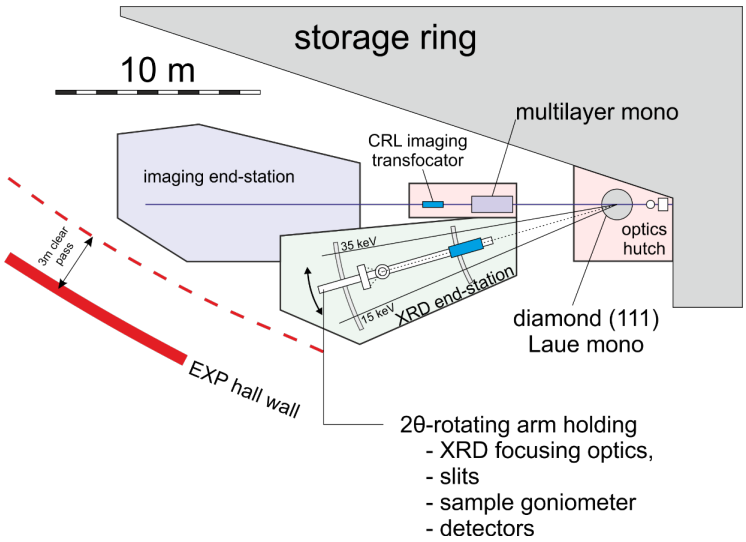

Figure B.9.3 Schematic layout of the hutches in the experimental hall in case of a 2θ-type beam splitter.

The imaging branch is thus largely unaffected by a beam splitter. The only effect is interdependency is the energy used in the two experiments and changes in the energy. The PXRD branch is adversely affected by the solutions presented above. In both cases the change of energy requires much more effort compared to an in-line solution with fixed exit monochromators. It is likely that the users alone cannot perform an energy change, but requires the assistance of the beamline staff. In

addition, the intensity and the brilliance of the beam will be lower due to the lower reflectivity and induced divergence from the Laue monochromator.

Besides the technical details outlined above the choice does have some practical and economical influences as well. The first is the increased cost of building two experimental hutches, each equipped with separate infrastructure installations. In addition, both branches would need separate optics whereas most of the optics in a single branch solution would serve a purpose for both techniques.

Another consequence of splitting the beamline in two is, as mentioned in the beginning, an effective doubling of the available beamtime. The personnel of the beamline, however, are not similarly increased. Thus the 4 persons (2 scientists and 2 other FTEs) need to facilitate 2 experiments 24 hours a day - 210 days a year. This is possible, but will likely strain the personnel and adversely affect the continuous development of the beamline.

B.10. References

Brauer, S., Stephenson, G. B., Mochrie, S. G. J., Dierker, S. B., Fleming, R. M., Pindak, R., Robinson, I. K., Grubel, G., Als-Nielsen, J. & Abernathy, D. L. (1995). *Rev. Sci. Instrum.* **66**, 1506–1509.

Christensen, F. E., Hornstrup, A., Frederiksen, P., Nilsson, C., Grundsøe, P., Ørup, P., Jacobsen, E., Schnopper, H. W., Lewis, R., Hall, C (1992). *Rev. Sci. Instr.* **63**, 1168-1171.

Davies, G. & Evans, T. (1972). *Proc. R. Soc. A*, **328**, 413-427.

Hou, Z., (2005). *Rev. Sci. Instrum.* **76**, 013305.

Kristiansen, P., Johansson, U., Ursby, T. & Jensen, B. N. (2016). *J. Synchrotron Rad.* **23**, 1076-1081.

Rodriguez-Carvajal, J. (1993). *Physica B,* **192**, 55-69.

Sanchez del Rio, M., Canestrari, N., Jiang F., & Cerrina, F. (2011). *J. Synchrotron Rad.* **18**, 708-716.

Simons, H., Ahl, S.R., Poulsen, H.F. & Detlefs, C., arXiv:1602.02703v1

Sondhauss, P. (2014). Proc. SPIE, **9209**, doi:10.1117/12.2061007.

Spiga, D., Pelliciari, C., Salmaso, B., Arcangeli, L., Bianucci, G., Ferrari, C., Ghigo, M. (2016) *Proc. of SPIE* **9963**, 996304.

G. Pareschi1, M. Rossi2, G. Tagliaferri1, G. Valsecchi2, G. Vecchi1, A. Zappettini3

Sondhauss, P. (2016). "Heat load on multilayer and crystal monochromator for the DanMAX beamline v. 2.1", Nov. 7th.

Stoupin, S., Terentyev, S. A., Blank, V. D., Shvyd'ko, Y. V., Goetze, K., Assoufid, L., Polyakov, S. N., Kuznetsov, M. S., Kornilov, N. V., Katsoudas, J., Alonso-Mori, R., Chollet, M., Feng, Y., Glownia, J. M., Lemke, H. Robert, A., Sikorski, M., Song, S. & Zhu, D. (2014). *J. Appl. Cryst.* **47**, 1329-1336.

Tanaka, T. & Kitamura, H. (2001). *J. Synchrotron Rad.* **8**, 1221-1228.

Walker, R.P. & Diviacco. B. (1992). *Rev. Sci. Instrum.*, **63**, 392-395.

Windt, D. L. (1998). *Comput. Phys.* **12**, 360-3.

Zhang, L., Cocco, D., Kelez, N., Morton, D. S., Srinivasana, V., and Stefan, P. M. (2015). *J. Synchrotron Rad.* **22**,1170-1181.